

FLORIDA INTERNATIONAL UNIVERSITY

Miami, Florida

DOLOMITE DISSOLUTION AND CONTAMINANT ADSORPTION IN THE
PRESENCE OF ETHYLENEDIAMINETETRAACETIC ACID (EDTA) IN
DIFFERENT IONIC STRENGTH SOLUTIONS
RELEVANT TO THE WASTE ISOLATION PILOT PLANT (WIPP)

A thesis submitted in partial fulfillment of

the requirements of the degree of

MASTER OF SCIENCE

in

ENVIRONMENTAL ENGINEERING

by

Alexis Vento

2021

To: Dean John Volakis
College of Engineering and Computing

This thesis, written by Alexis Vento, and entitled
Dolomite Dissolution and Contaminant Adsorption in the Presence of
Ethylenediaminetetraacetic Acid (EDTA) in Different Ionic Strength Systems Relevant
to the Waste Isolation Pilot Plant (WIPP), having been approved in respect to style and
intellectual content, is referred to you for judgment.

We have read this thesis and recommend that it be approved.

Yelena Katsenovich

Berrin Tansel

Shonali Laha, Major Professor

Date of Defense: June 26, 2021

The thesis of Alexis Vento is approved.

Dean John Volakis
College of Engineering and Computing

Andrés G. Gil
Vice President for Research and Economic Development
and Dean of the University Graduate School

Florida International University, 2021

ACKNOWLEDGMENTS

I would like to dedicate this manuscript to my family and friends who have always supported me in my decision for chasing my dream education. A thank you for my mom and dad for giving the childhood that inspired me to make the world a better place. I want to thank my grandma for the adoration she always given me which made me feel special all my life. A special thank you to my girlfriend, Yami, for supporting me through thick and thin and always being a bright light in my darkest of days. To my close friends who have stuck with me since the beginning. I want to thank my mentors Drs. Yelena Katsenovich, Johnbull Dickson, Kirsten Sockwell, and Hilary Emerson for supporting and leaving me the breadcrumbs needed to guide me through the adventure of my research. I thank Florida International University's Applied Research Center and Leonel Lagos first, for giving me my shot, an opportunity given to a select few and for helping me become a better version of myself by providing me with the facilities and equipment to make my research possible, especially with the use of their ICP-OES and ICP-MS. I would also like to thank Dr. Shonali Laha from the FIU department of Civil and Environmental Engineering for her academic and professional mentorship as my major professor during the acquisition of my Master of Science degree, Dr. Anna Bernado-Bricker for teaching me so much and shaping my systematic way of thinking, and Dr. Berrin Tansel for showing me the more practical ways of engineering. Finally, I thank the Department of Energy Office of Environmental Management (DOE-EM) for creating the DOE-FIU Science and Technology Workforce Program and the financial support with funding for this project under [SRNS contract DE-AC09-08SR22470](#). Lastly, for providing me the amazing opportunity to experience an internship in the Sandia National Laboratory at Carlsbad, New Mexico that was an adventure of a lifetime!

ABSTRACT OF THE THESIS

DOLOMITE DISSOLUTION AND CONTAMINANT ADSORPTION IN THE PRESENCE OF ETHYLENEDIAMINETETRAACETIC ACID (EDTA) IN DIFFERENT IONIC STRENGTH SOLUTIONS RELEVANT TO THE WASTE ISOLATION PILOT PLANT (WIPP)

by

Alexis Vento

Florida International University, 2021

Miami, Florida

Professor Shonali Laha Major Professor Advisor

The long-term storage and disposal of radioactive waste is considered a challenging and costly endeavor to the U.S. Department of Energy (DOE) tasked with safe management of radioactive wastes. The search for effective ways to manage radioactive waste has increasingly grown due to large inventory of legacy transuranic wastes (TRU) from defense program in the 1940's and nuclear power plants. The U.S. Department of Energy's (DOE) Waste Isolation Pilot Plant (WIPP) is a unique repository for permanent disposition of the Transuranic Waste (TRU). The WIPP, located near Carlsbad in New Mexico, is sited ~655 m below the surface in a salt formation ~610-meter thick that was formed ~250 million years ago through evaporation cycles of the ancient Permian Sea. These salt beds are found in the Salado Formation which consists mainly of interbedded halite (NaCl) and anhydrite layers considered as an ideal repository for storage of TRU wastes due to the absence of free-flowing water, ease of mining, insignificant permeability, and geological stability.

TABLE OF CONTENTS

CHAPTER	PAGE
Introduction.....	1
Background and Theory.....	5
EDTA – Organic Chelating Ligand.....	8
Colloid formation in conditions relevant to the WIPP.....	11
Objective.....	14
Research Challenges.....	15
Hypothesis.....	16
Materials and Methods.....	16
Materials – Dolomite Dissolution.....	16
Batch reactor and sample preparation procedures – Dolomite Dissolution.....	17
Aqueous Phase Analysis.....	19
Inductively coupled plasma optical emission spectroscopy (ICP-OES) – Dolomite Dissolution.....	19
Materials – Adsorption Experiments.....	20
Batch reactor and sample preparation procedures – Contaminant Adsorption.....	20
Aqueous Phase Analysis.....	23
Inductively coupled plasma mass spectroscopy (ICP-MS) – Contaminant adsorption	23
Results and Discussion.....	23
Rate of Dolomite Dissolution in various ionic strength solution in the absence and presence of EDTA.....	23
Actinide and Lanthanide Adsorption onto Dolomitic Surface under Various Ionic Strength Solution in the Presence and Absence of EDTA.....	49
Conclusion.....	72
References.....	75

LIST OF TABLES

TABLE	PAGE
Table 1: EDTA estimates on WIPP Site found in CRA-2014 report Source (Dittrich 2014)	9
Table 2 : Composition and ionic strength of ERDA-6 and GWB, two simulated WIPP brines (95% initial formation), pH correction factor for each brine.	21
Table 3: Size-dependent particle separation methods and expected particle size remaining in solution after separation.	23

LIST OF FIGURES

FIGURE	PAGE
Figure 1: Culebra Member of Rustler Formation Located Above the WIPP	2
Figure 2 : Intrusion Release Scenario. Source from Dittrich 2017. Source from Dittrich 2017.....	3
Figure 3: Specimen of granular dolomite from Thornwood, New York.	4
Figure 4 EDTA “Clawing Mechanism with Calcium – Chelating effect	10
Figure 5: Am ^{III} /EDTA ⁻⁴ speciation diagram	11
Figure 6: Radioactive contaminants adsorbing onto Colloids	12
Figure 7 Size spectrum of natural colloids and selected particle detection methods	13
Figure 8 Dolomite dissolution as a function of time in a 0.1 M Cesium Chloride solution in basic condition (pH= 8±0.5) with constant 5.0 g/L of Dolomite and 5 mg/L EDTA. Error bars are a standard deviation of triplicate samples. (a) Aqueous Phase Calcium in solution. (b) Aqueous Phase Magnesium in solution.....	25
Figure 9: Dolomite dissolution as a function of time in a 1.0 M Cesium Chloride solution in basic condition (pH= 8±0.5) with constant 5.0 g/L of Dolomite and 5 mg/L EDTA. Error bars are a standard deviation of triplicate samples. (a) Aqueous Phase Calcium in solution. (b) Aqueous Phase Magnesium in solution.....	26
Figure 10: Dolomite dissolution as a function of time in a 5.0 M Cesium Chloride solution in basic condition (pH= 8±0.5) with constant 5.0 g/L of Dolomite and 5 mg/L EDTA. Error bars are a standard deviation of triplicate samples. (a) Calcium Concentration in Aqueous Phase (b) Magnesium Concentration in Aqueous Phase	27
Figure 11 : Dolomite dissolution as a function of time in a 0.1 M Sodium Nitrate solution in basic condition (pH= 8±0.5) with constant 5.0 g/L of Dolomite and 5 mg/L EDTA. Error bars are a standard deviation of triplicate samples. (a) Calcium Concentration in Aqueous Phase (b) Magnesium Concentration in Aqueous Phase	29
Figure 12: Dolomite dissolution as a function of time in a 1.0 M Sodium Nitrate solution in basic condition (pH= 8±0.5) with constant 5.0 g/L of Dolomite and 5 mg/L EDTA. Error bars are a standard deviation of triplicate samples. (a) Calcium Concentration in Aqueous Phase (b) Magnesium Concentration in Aqueous Phase	30
Figure 13 : Dolomite dissolution as a function of time in a 5.0 M Sodium Nitrate solution in basic condition (pH= 8±0.5) with constant 5.0 g/L of Dolomite and 5 mg/L EDTA. Error bars are a standard deviation of triplicate samples. (a) Calcium Concentration in Aqueous Phase (b) Magnesium Concentration in Aqueous Phase	31

Figure 14: Dolomite dissolution as a function of time in a 0.1 M Sodium Chloride solution in basic condition (pH= 8±0.5) with constant 5.0 g/L of Dolomite and 5 mg/L EDTA. Error bars are a standard deviation of triplicate samples. (a) Calcium Concentration in Aqueous Phase (b) Magnesium Concentration in Aqueous Phase 33

Figure 15: Dolomite dissolution as a function of time in a 1.0 M Sodium Chloride solution in basic condition (pH= 8±0.5) with constant 5.0 g/L of Dolomite and 5 mg/L EDTA. Error bars are a standard deviation of triplicate samples. (a) Calcium Concentration in Aqueous Phase (b) Magnesium Concentration in Aqueous Phase 34

Figure 16 : Dolomite dissolution as a function of time in a 0.1 M Sodium Sulfate solution in basic condition (pH= 8±0.5) with constant 5.0 g/L of Dolomite and 5 mg/L EDTA. Error bars are a standard deviation of triplicate samples. (a) Calcium Concentration in Aqueous Phase (b) Magnesium Concentration in Aqueous Phase 35

Figure 17: Dolomite dissolution as a function of time in a 1.0 M Sodium Sulfate solution in basic condition (pH= 8±0.5) with constant 5.0 g/L of Dolomite and 5 mg/L EDTA. Error bars are a standard deviation of triplicate samples. (a) Calcium Concentration in Aqueous Phase (b) Magnesium Concentration in Aqueous Phase 36

Figure 18: Dolomite dissolution as a function of time in a 0.1 M Magnesium Chloride solution (a) and 1.0 M Magnesium Chloride solution (b) in basic condition (pH= 8±0.5) with constant 5.0 g/L of Dolomite and 5 mg/L EDTA. Error bars are a standard deviation of triplicate samples. Calcium Concentration in Aqueous Phase 38

Figure 19: Dolomite dissolution as a function of time in a 0.1 M Sodium Tetraborate solution in basic condition (pH= 8±0.5) with constant 5.0 g/L of Dolomite and 5 mg/L EDTA. Error bars are a standard deviation of triplicate samples. (a) Calcium Concentration in Aqueous Phase (b) Magnesium Concentration in Aqueous Phase 40

Figure 20: Dolomite dissolution as a function of time in a 5.0 M Calcium Chloride solution in basic condition (pH= 8±0.5) with constant 5.0 g/L of Dolomite and 5 mg/L EDTA. Error bars are a standard deviation of triplicate samples. Magnesium Concentration in Aqueous Phase 41

Figure 21: Dissolution trend lines of 0.1 M of studied synthetic brines for centrifuged samples with regards to Aqueous Phase Calcium concentration (µg/L) as a function of time in the presence and absence of EDTA. (a) Borax excluded (b) Borax included 43

Figure 22 : Dissolution trend lines of 0.1 M of studied synthetic brines for Settling samples with regards to Aqueous Phase Calcium concentration (µg/L) as a function of time in the presence and absence of EDTA. (a) Borax excluded (b) Borax included 44

Figure 23: Dissolution trend lines of 1.0 M of studied synthetic brines with regards to Aqueous Phase Calcium concentration ($\mu\text{g/L}$) as a function of time in the presence and absence of EDTA. (a) Settling samples (b) Centrifuged samples	46
Figure 24: Dissolution trend lines of 5.0 M of studied synthetic brines with regards to Aqueous Phase Calcium concentration ($\mu\text{g/L}$) as a function of time in the presence and absence of EDTA. (a) Settling samples (b) Centrifuged samples	48
Figure 25: Actinide and Lanthanide concentrations ($\mu\text{g/L}$) as a function of time in a 0.1 M NaCl solution in basic conditions ($\text{pH}= 8\pm 0.5$) with constant 5.0 g/L of Dolomite, 5 mg/L EDTA and 10 $\mu\text{g/L}$ (under-saturated) of contaminants. Error bars are a standard deviation of triplicate samples. (a) Aqueous Phase Uranium Concentrations (b) Aqueous Phase Thorium Concentrations (c) Aqueous Phase Neodymium Concentrations	50
Figure 26: Actinide and Lanthanide concentrations ($\mu\text{g/L}$) as a function of time in a 0.1 M NaCl solution in basic conditions ($\text{pH}= 8\pm 0.5$) with constant 5.0 g/L of Dolomite, 5 mg/L EDTA and 1000 $\mu\text{g/L}$ (over-saturated) of contaminants. Error bars are a standard deviation of triplicate samples. (a) Aqueous Phase Uranium (b) Aqueous Phase Thorium (c) Aqueous Phase Neodymium.....	53
Figure 27: Ternary Systems of $\text{UO}_2^{2+}/\text{CO}_3^{2-}/\text{H}_2\text{O}$ with open system (left) and closed system (right)	55
Figure 28: Actinide and Lanthanide concentrations ($\mu\text{g/L}$) as a function of time in a 1.0 M NaCl solution in basic conditions ($\text{pH}= 8\pm 0.5$) with constant 5.0 g/L of Dolomite, 5 mg/L EDTA and 10 $\mu\text{g/L}$ (under-saturated) of contaminants. Error bars are a standard deviation of triplicate samples. (a) Aqueous Phase Uranium (b) Aqueous Phase Thorium (c) Aqueous Phase Neodymium.....	57
Figure 29: Actinide and Lanthanide concentrations ($\mu\text{g/L}$) as a function of time in a 1.0 M NaCl solution in basic conditions ($\text{pH}= 8\pm 0.5$) with constant 5.0 g/L of Dolomite, 5 mg/L EDTA and 1000 $\mu\text{g/L}$ (under-saturated) of contaminants. Error bars are a standard deviation of triplicate samples. (a) Aqueous Phase Uranium (b) Aqueous Phase Thorium (c) Aqueous Phase Neodymium.....	59
Figure 30: Actinide and Lanthanide concentrations ($\mu\text{g/L}$) as a function of time in a 5.0 M NaCl solution in basic conditions ($\text{pH}= 8\pm 0.5$) with constant 5.0 g/L of Dolomite, 5 mg/L EDTA and 10 $\mu\text{g/L}$ (under-saturated) of contaminants. Error bars are a standard deviation of triplicate samples. (a) Aqueous Phase Uranium (b) Aqueous Phase Thorium (c) Aqueous Phase Neodymium.....	61
Figure 31: Actinide and Lanthanide concentrations ($\mu\text{g/L}$) as a function of time in a 5.0 M NaCl solution in basic conditions ($\text{pH}= 8\pm 0.5$) with constant 5.0 g/L of Dolomite, 5 mg/L EDTA and 1000 $\mu\text{g/L}$ (under-saturated) of contaminants. Error bars are a standard	

deviation of triplicate samples. (a) Aqueous Phase Uranium (b) Aqueous Phase Thorium (c) Aqueous Phase Neodymium..... 63

Figure 32 : Actinide and Lanthanide concentrations ($\mu\text{g/L}$) as a function of time in a GWB (Generic Weep Brine) in basic conditions ($\text{pH} = 8 \pm 0.5$) with constant 5.0 g/L of Dolomite, 5 mg/L EDTA and 10 $\mu\text{g/L}$ (under-saturated) of contaminants. Error bars are a standard deviation of triplicate samples. (a) Aqueous Phase Uranium (b) Aqueous Phase Thorium (c) Aqueous Phase Neodymium.....65

Figure 33: Actinide and Lanthanide concentrations ($\mu\text{g/L}$) as a function of time in a GWB (Generic Weep Brine) solution in basic conditions ($\text{pH} = 8 \pm 0.5$) with constant 5.0 g/L of Dolomite, 5 mg/L EDTA and 1000 $\mu\text{g/L}$ (under-saturated) of contaminants. Error bars are a standard deviation of triplicate samples. (a) Aqueous Phase Uranium (b) Aqueous Phase Thorium (c) Aqueous Phase Neodymium 67

Figure 34: Actinide and Lanthanide concentrations ($\mu\text{g/L}$) as a function of time in a ERDA -6 (Energy Research and Development Administration Well 6) in basic conditions ($\text{pH} = 8 \pm 0.5$) with constant 5.0 g/L of Dolomite, 5 mg/L EDTA and 10 $\mu\text{g/L}$ (under-saturated) of contaminants. Error bars are a standard deviation of triplicate samples. (a) Aqueous Phase Uranium (b) Aqueous Phase Thorium (c) Aqueous Phase Neodymium..... 69

Figure 35: Actinide and Lanthanide concentrations ($\mu\text{g/L}$) as a function of time in a ERDA -6 (Energy Research and Development Administration Well 6) in basic conditions ($\text{pH} = 8 \pm 0.5$) with constant 5.0 g/L of Dolomite, 5 mg/L EDTA and 1000 $\mu\text{g/L}$ (under-saturated) of contaminants. Error bars are a standard deviation of triplicate samples. (a) Aqueous Phase Uranium in solution. (b) Aqueous Phase Thorium in solution. (c) Aqueous Phase Neodymium in solution.71

Introduction

The nation's nuclear defense program in the 1940's resulted in the accumulation of significant amount of radioactive waste. The Waste Isolation Pilot Plant (WIPP) opened in 1999 as a solution to the long-term disposal of the nation's nuclear transuranic (TRU) waste and is the nation's only deep geologic long-lived radioactive waste repository.

Located approximately 26 miles southeast of Sandia National Laboratories the WIPP is sited 2150 feet below the surface in a salt formation approximately 2000 feet-thick that was formed 250 million years ago through evaporation cycles of the ancient Permian Sea. These salt beds found in the Salado Formation mainly consist of halite (NaCl) mineral and are considered as an ideal repository due to the absence of free-flowing fresh water, ease of mining, high impermeability, and geological stability. Moreover, these salt formations are characterized by the unique regenerative ability to seal back up due to their high plasticity.

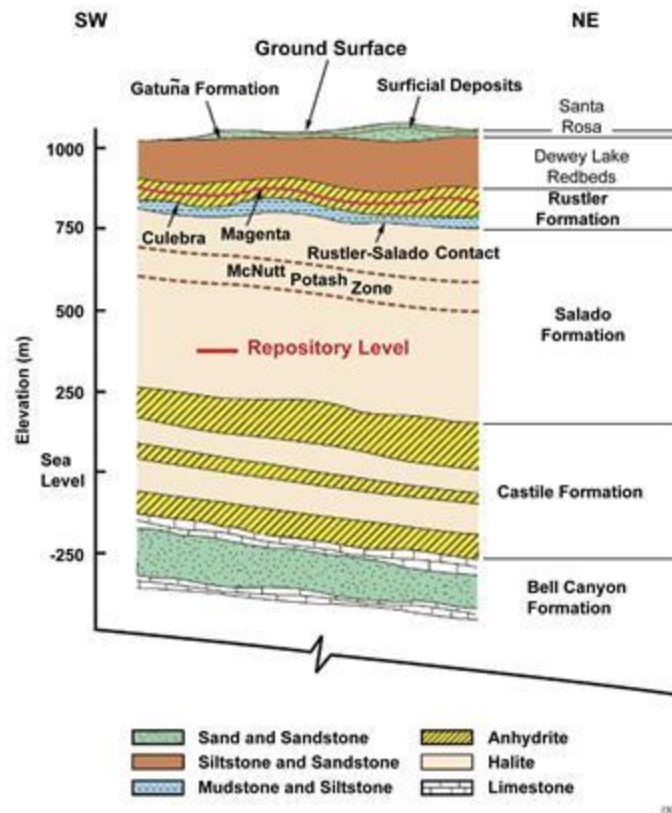


Figure 1: Culebra Member of Rustler Formation Located Above the WIPP. Source from Harry 2015¹

There are the regulatory needs to understand how radioactive waste can be best managed to mitigate risks to human health and the environment. Safety assessment models need a comprehensive understanding not only of the wastes, but also knowledge about the interaction between the TRU waste and the subsurface environment surrounding the WIPP in the case of a potential release scenario. The Permian Basin region is rich in geologic resources such as potash, salt, oil, and gas, making it highly prone to intensive drilling of boreholes that could lead to the release of radionuclides from the WIPP environment due to drill intrusions. Drilling has been on the rise since the 1990's and continues to increase exponentially over the years. For example, the drill rate in 1996 was at about 46.8

boreholes/km² which increased to 67.3 boreholes/km² in 2014. This amounts to about a 40% increase with about 5 intrusion events over the projected 10,000-year post-closure period for the WIPP site (Tracy 2019²). With inadvertent or intentional intrusions, there is the potential for the nuclear wastes to react with brine pockets and lead to an increase in mobility of radionuclides. Thus, there is a critical need to understand the mechanisms governing the behaviors of actinides in the environment and protective measures that could be leveraged to mitigate their exposure risk to humans and the environment. In a low-probability TRU release scenario americium (Am), neptunium (Np) and plutonium (Pu) are considered the most important actinides species to be released from the WIPP environment.

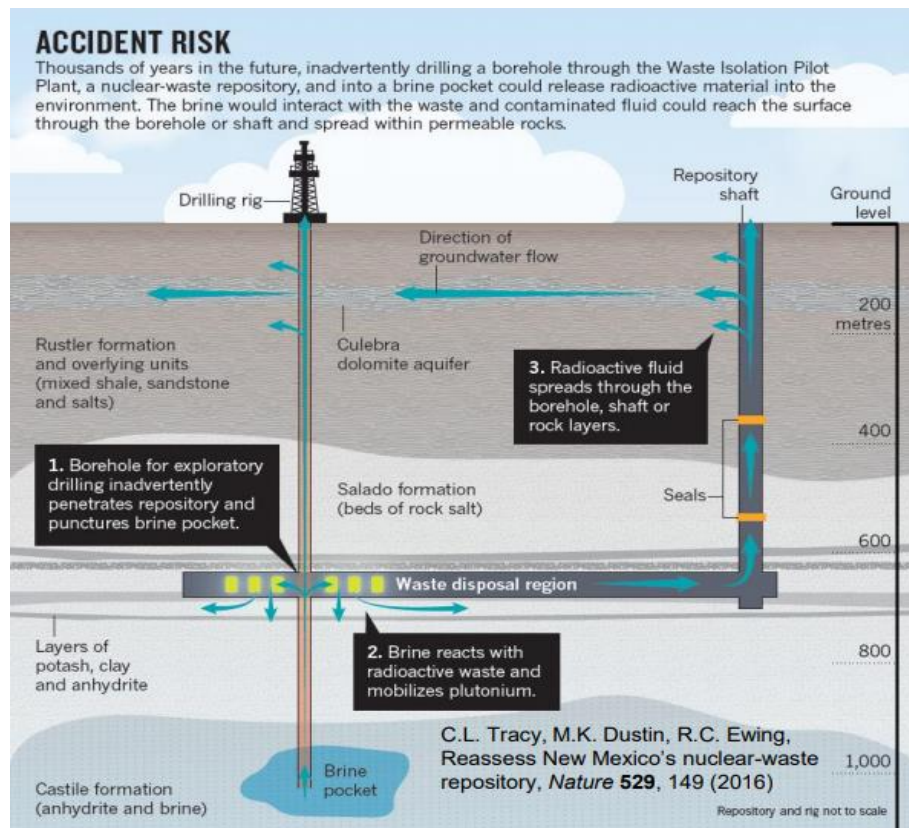


Figure 2 : Intrusion Release Scenario. Source from Dittrich 2017. Source from Dittrich 2017

The Culebra member' located in the Rustler Formation which overlies WIPP is a top priority due to its relatively high transmissivity in many portions of the aquifer. The Culebra consists primarily of dolomite ($\text{CaMg}[\text{CO}_3]_2$), an anhydrous carbonate mineral that is abundant in nature (Figure 3).



Figure 3: Specimen of granular dolomite from Thornwood, New York.

Picture courtesy of geology.com

The Culebra exhibits a heterogenous, complex geology due to the occurrence of many conduits, fissures, cracks, and fractures that increase its hydraulic conductivity. Consequently, as water moves freely through this formation, an increase in dissolution is to be expected. Therefore, in a potential human intrusion scenario where the WIPP is breached dissolution pathways in the carbonate mineral dolomite will pose a potential threat due to actinide release to the subsurface.

This research focuses on dolomite mineral dissolution and actinide in high ionic strength conditions in the WIPP subsurface. It has been demonstrated that dolomite plays a significant role in the biogeochemical cycles of many environmentally important elements, but its reactivity and surface properties are not well understood in comparison to other important carbonate minerals, oxides, and silicates (Stumm 1992³).

Additionally, this research investigated the fate of Uranium (U), Thorium (Th), and Neodymium (Nd) in the WIPP environment. Thorium and neodymium were used as stable analogue for plutonium (Pu) and Americium (Am). The slurry-sludge mixture for TRU waste contains EDTA as high as 3×10^{-4} M (Leigh 2004⁴), which can form complexes with

contaminants of concern (Nd, Th, U) in an intrusion release scenario. Hence, the effect of ethylenediaminetetraacetic acid (EDTA), an organic chelating ligand on Nd, Th, U, was also investigated.

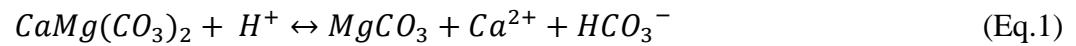
Background and Theory

Dolomite dissolution (DD) has been investigated to a limited extent, but few studies have shown that dolomite's fast dissolution rates and high solubility make it rather difficult to quantify, especially in high ionic strength solutions. Some early work to effectively characterize surface speciation of carbonates minerals rhodochrosite, siderite (Cappelen 1993⁵) and magnesite (Pokrovsky 1999⁶), which share similar geochemical properties with dolomite, became instrumental in establishing the groundwork necessary for understanding the dissolution process. Based on these studies, a new surface complexation model was developed that hypothesized the existence of three key hydration sites: $>\text{CO}_3\text{H}^\circ$, $>\text{CaOH}^\circ$, and $>\text{MgOH}^\circ$. In the majority of natural aquatic environments dolomite surface speciation is modeled as: $>\text{CO}_3^-$, $>\text{CO}_3\text{Z}^+$, $>\text{ZOH}_2^+$, $>\text{ZHCO}_3^\circ$, and $>\text{ZCO}_3^-$, where Z = Ca or Mg. The speciation model led to an improved understanding of the mechanism governing dolomite dissolution/crystallization in aqueous solutions. An important finding is that dolomite dissolution is controlled by the protonation of $>\text{CO}_3\text{H}^\circ$ surface complexes at $\text{pH}<6$ and by hydrolysis of $>\text{ZOH}_2^+$ groups at $\text{pH}>6$ (Provosky 1999⁷).

In the following research different salts and composition (CaCl_2 , NaCl , NaBr , $\text{Na}_2\text{B}_4\text{O}_7$, Na_2SO_4 , CsCl , MgCl_2 , GWB , ERDA-6) were used to make aqueous brines, which represent a wide range of ionic strength solutions expected in the Culebra dolomite

environment of the WIPP. The pH of these systems ranges from neutral to alkaline hydrolysis dominated systems. It is generally accepted that dolomite exhibits a two-step reaction due to its dependence on $MgCO_3$. Compared to calcite and magnesite, with four orders of magnitude difference in rate constants (Lei 1989⁸), dolomite dissolution can be based on successive reactions, with the first $CaCO_3$ component reaching equilibrium due to slow dissolution of $MgCO_3$.

Dolomite dissolution shown in Equation 1:

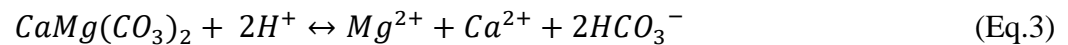


Second rate-limiting reaction in the dissolution of dolomite is illustrated in Equation 2:

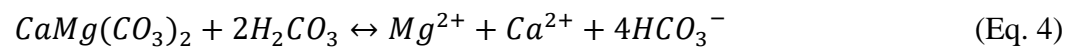


Also, according to (Plummer, Wigley, and Parkhurst 1978⁹; Chou, Garrels, and Wollast, 1989¹⁰; Stumm and Wollast, 1990¹¹) the dissolution of dolomite behaves just like calcite occurring via three parallel reactions shown in Equations 3-5:

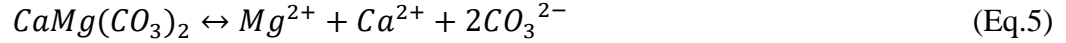
K₁



K₂



K₃



By assuming that dolomite crystallization is dominated by reaction 3 general dissolution rate (R) can be stated a (Provosky 2001¹²) as:

$$R = k_1 * a_{H^+}^n * k_2 * a_{H_2CO_3}^p + k_3 - k_{-3} * a_{Mg^{2+}} * a_{Ca^{2+}} * a_{CO_3^{2-}}^2$$

Here the k_i is used for each rate constant (1-3), a_i represents the specific aqueous species activity, n varies from 0.5 (Plummer 1982¹³) and 0.75 (Chou et al. 1986¹⁴), and p is equal to 1 (Plummer 1982). The first term is equal to the dolomite surface protonation, the second term is its carbonation, third term is its surface hydration, and the fourth term considers the precipitation reaction.

Previous studies have used K_d values ranging from 20 to 400 mL/g for Pu and Am in performance assessment (PA) for the WIPP. Moreover, reported K_d values for dolomite can vary from $10^{3.4}$ to 10^6 mL/g (Brady 1999¹⁵).

Although, actinides belong in the same row of the periodic table, they exhibit different chemistries affecting their behaviors and environmental mobility. Uranium IV and VI oxidation states are of key interest because it is the most abundant radionuclide in treated TRU waste. The chemistry of Am IV and V shows similarities to U in the same oxidation states. Am (IV, VI) has been shown to form strong complexes with EDTA, resulting in increased solubility (Chen et al. 1999¹⁶) Previous studies were performed under acidic conditions, highlighting the importance for studies with WIPP relevant alkaline conditions (Elesin and Zaitsev 1971¹⁷) U(IV) binds strongly to EDTA increasing its solubility up to 3 orders of magnitude in WIPP relevant alkaline conditions (Yalcintas 2003¹⁸). Since

reducing states are the dominating conditions in the WIPP site, previous studies showed that the organic ligands, including EDTA, enhanced the reductive dissolution of Pu (IV) and increased Pu (III) mobility in alkaline WIPP conditions (Schramke 2020¹⁹). Similar trends are expected for Th and Nd.

$$R_E(\%) = \frac{C_o - C_t}{C_o} \times 100 \quad (\text{Eq. 7})$$

$$Q_t = V \left(\frac{C_{initial} - C_{final}}{m} \right) \quad (\text{Eq. 8})$$

The WIPP subsurface environments typically consists of carbonate and hydroxide minerals that can increase tetravalent actinides solubility in alkaline conditions (pH>7) due to formation of carbonate and hydroxo-carbonate complexes.

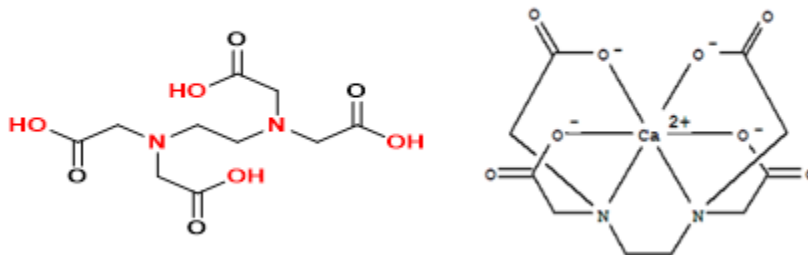
EDTA – Organic Chelating Ligand

EDTA is a polamino-carboxylate that consists of 4-four oxygen bonds as hard donor groups and two nitrogen bonds as soft donor groups. The EDTA is typically form as hexadentate complexes. As a TRU-waste sludge stabilizer, EDTA was used in decommissioning and is found as high as 3x10⁻⁴ M in sludge barrels following closure (Correspondence with Bill McInroy found in CRA-2014 technical report²⁰). The importance role of organic ligands, like EDTA in the speciation and mobility of actinides in the WIPP subsurface is becoming more apparent for PA modeling. EDTA’s chelating/complexation effect (Figure 4) has the potential to reduce and/or oxidize multivalent actinides, which can increase their behavior. Research has shown that in low ionic strength systems PuO₂²⁺ was reduced to Pu⁺⁴ creating

complexes or polymeric/hydrolytic precipitates. This study provided a relative rate in the order of EDTA>citrate>oxalate (Reed 1998²¹). This research was performed under a pH between 5-7 in simulated G-Seep brine and pH of 8-10 in EDRA-6 brine. The solubility of Thorium with EDTA has been observed as a 1:1 Th-EDTA complexes. EDTA concentrations ranged from 10^{-3} to 10^{-1} M under basic conditions (pH~11.8) and were not shown to absorb onto thorium hydroxide solid (Colas 2013²²).

Organic Ligand	Pre-2009 PABC Inventory (kg)	CRA-2014 Total Inventory (kg)	Maximum Concentration ^a (M)
Acetate	8.63×10^3	2.41×10^4	2.30×10^{-2}
Oxalate	4.77×10^4	1.85×10^4	1.18×10^{-2}
Citrate	1.59×10^3	7.78×10^3	2.33×10^{-3}
EDTA	2.56×10^1	3.76×10^2	7.40×10^{-5}
^a based on minimum brine volume for release			

Table 1: EDTA estimates on WIPP Site found in CRA-2014 report Source (Dittrich 2014²³)



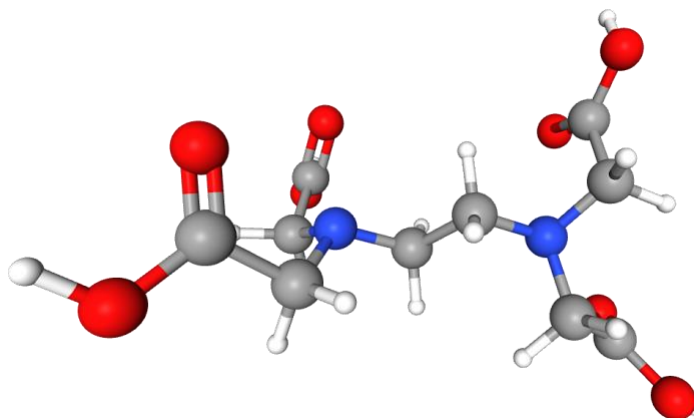


Figure 4 EDTA chemical structure showing the “Clawing Mechanism with Calcium – Chelating effect”

The environmental conditions like pH and variable ionic strength of solutions have been shown to greatly affect EDTA's chelating effect (Means and Alexander 1981²⁴). In a sediment remediation experiment where EDTA complexation was observed on how it impacts heavy metals dissolution from sediments proved that in more basic solutions (~pH=7) EDTA not only effectively binds to the heavy metals such as Zinc (Zn), Copper (Cu), and Pb (Lead) but also increase the dissolution of the sediments increasing their mobility. With Cu and Zn, the general dissolution trend was an initial rapid increase that achieved equilibrium at 72 hours. Due to pH dependency Pb affinity for carbonate ions increased its initially, leading to an increase in dissolution (Di Palma 2007²⁵). EDTA donor groups are heavily influenced by subsurface conditions and pH.. Figure 5 displays an example of complexation effect of EDTA on americium speciation as a function of pH (Griffiths et al. 2013²⁶).

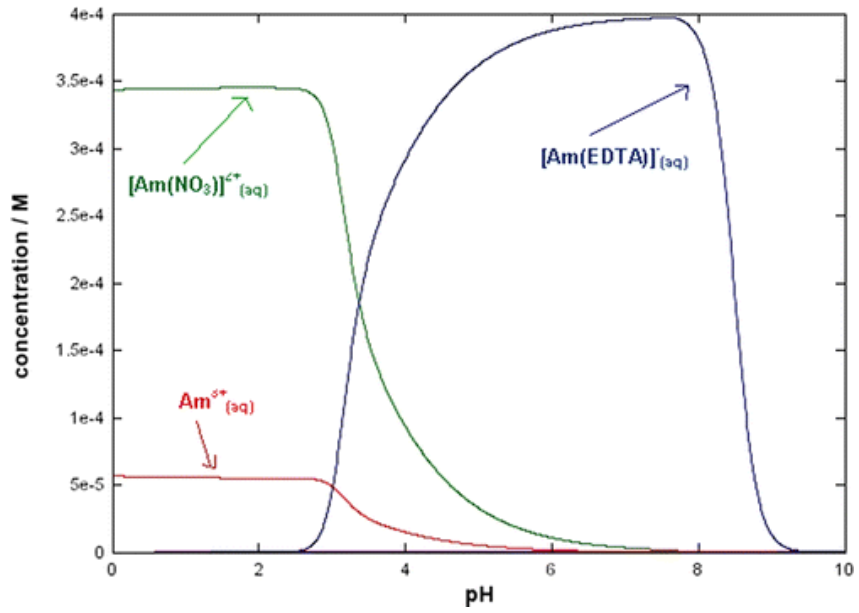


Figure 5: $Am^{III}/EDTA^{-4}$ speciation diagram showing how EDTA complexes and keeps contaminants in mobile in solution

Source from: Griffiths et al. 2013

Colloid formation in conditions relevant to the WIPP

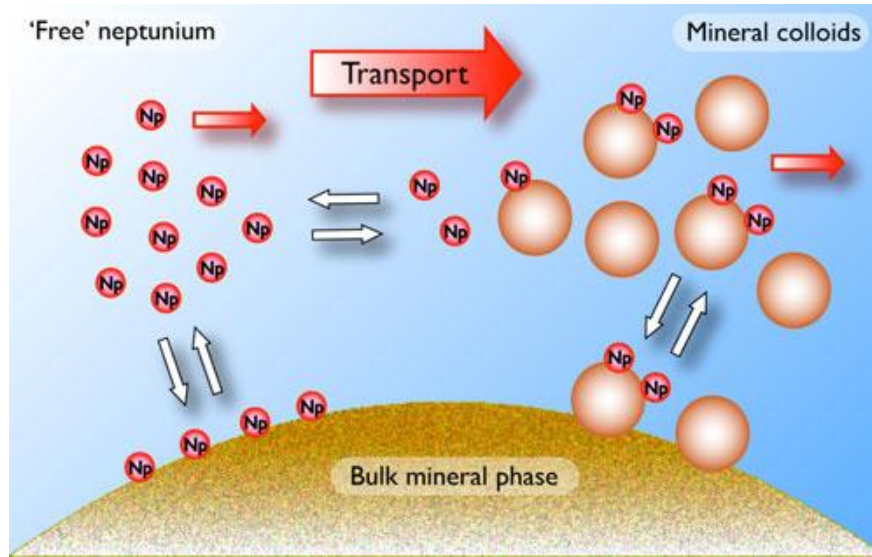


Figure 6: Radioactive contaminants adsorbing onto Colloids keeping contaminants in solution
Source from: Tinnacher 2011²⁷

Colloids are generally characterized as either intrinsic or associative/pseudo colloids. Intrinsic colloids are composed of oxides and hydroxides actinides (Utsunomiya et al., 2009²⁸) and are not important in nuclear waste disposal areas (Moulin and Ouzounian 1992²⁹), on the other hand associative colloids are formed from impurities or other foreign materials that have absorbed actinides (The Great Soviet Encyclopedia 1979³⁰). These are particles suspended in solution usually between 10^{-6} to 10^{-9} m (Figure 7) that tend to form aggregates due to the surface area charge and particle-particle interactions (Stumm 1977³¹). In fractures and conduits in the WIPP subsurface environment these colloidal particles can attract metals and possibly provide adsorption areas for contaminants. It is accepted that pseudo colloids are present in all groundwater systems such as clay, rock and mineral fragments, iron oxyhydroxide, alumina, “dissolved” organic carbon (DOC), and microemulsions from nonaqueous phase liquids which can typically be found at about 10^8 to 10^{14} particles L^{-1} (Degueldre et al. 1989, ³², Degueldre et al. 2000 ³³). In the case of

tetravalent actinides, when contaminant and colloid interaction occurs, the time for achieving equilibrium increases, resulting in increased distances for colloid-facilitated travel (Ryan and Elimelech 1996³⁴). In a column study of the impact of Suwannee River fulvic acid on Th mobility in the presence of hematite, an iron oxide mineral, Th adsorbed to hematite colloids was more than 90% at equilibrium with a k_d value of 230 L/kg (Emerson 2016³⁵).

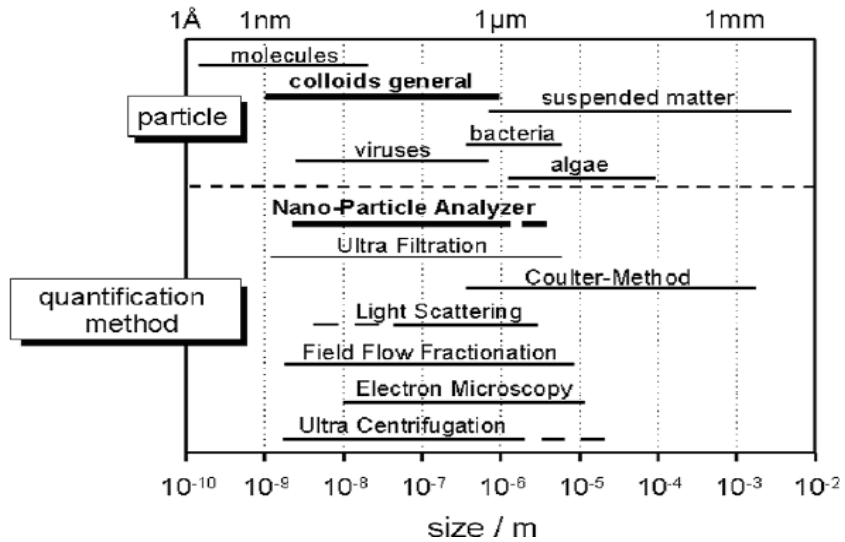


Figure 7 Size spectrum of natural colloids and selected particle detection methods Source from: (Bundschuh 2005³⁶).

Most of the waters on the Earth's crust is in oxidizing conditions due to superficial interface with the atmosphere (Aerobic), but deep, repository, sub-surface conditions are typically anoxic, resulting in reducing environments. The speciation of U, Pu, Am, Th and Nd are predominantly tetravalent under these reducing conditions greatly enhancing their mobility (Delecaut et al. 2002³⁷, Delecaut et al. 2004³⁸). When in their low valence states actinides remain immobile, but when they are reduced into tetravalent states, they become readily mobile. Once waterborne colloid-facilitated transport becomes a major pathway the classical two-phase transport model should be augmented with the third-phase model.

Originally the two-phase model considers most metals and radionuclides to readily sorb onto aquifer media making them immobile, resulting in minimal release. While the three phase models consider colloidal surface properties to readily adsorb like the surrounding aquifer media, thus increasing contaminant migration the aquifer surface matrix provides surfaces for the actinides to sorb to. The colloids moving through preferential pathways in the aquifer which themselves act as a sorbent, essentially pulling the actinides from the aquifer media and adsorbing onto the colloidal particle surface (McCarthy 1989³⁹).

Changes in ionic strength and pH are the major factors that account for the partitioning of colloid particles. These three main criteria need to meet for colloid-facilitated transport: 1. There needs to be a way for colloids to form; 2. Contaminant affinity for colloids; 3. Colloids must be mobilized through preferential pathway in aquifer (Ryan 1996⁴⁰). Our experiments justified these 3 criteria in considering the potential effect colloids have on the contaminants U, Th and Nd.

When comparing NaCl and CaCl₂ solutions the lower ionic strength, NaCl, generated more colloids overall, highlighting the intricate network of variables and environmental conditions. Understanding the possible interactions of colloids is critical to understanding colloidal interparticle interactions with actinides (Sen and Kartic 2006⁴¹).

Objective

The main objective of this research is to:

(1) evaluate the effect different ionic strength solutions have on dolomite dissolution in the presence and absence of EDTA and (2) and evaluate the effect of EDTA in various synthetic brine solutions relevant to WIPP have on actinide and lanthanide adsorption.

Under this main objective this research addresses the following questions:

- ❑ An updated literature review for WIPP-related dissolution and contaminant adsorption mechanisms pertaining to the WIPP subsurface environment, specifically within the Rustler, Salado, and Castille formation
- ❑ An analysis on the trends and correlations of the WIPP-specific data produced at ARC on the dolomite dissolution and contaminant adsorption for minimizing uncertainty and risk in WIPP performance assessment modeling.
 - ❑ Calcium and Magnesium aqueous phase concentrations
 - ❑ Uranium, Thorium, and Neodymium adsorption
- ❑ An assessment and comparison with the current WIPP literature and WIPP-specific results performed at ARC for updating and supporting WIPP PA position for the Compliance Recertification Application (CRA)

Research Challenges

1. WIPP subsurface environment contains interconnected network of fissures, conduits, and macro and micropores which contributes to a heterogenous, complex hydrogeology and geochemistry.
2. Insufficient scientific data on the WIPP subsurface environment, specifically water-mineral-contaminant dynamics.

3. Risk models for performance assessment need to be able to predict long-term fate and transport of contaminants.
4. Organic Ligands like EDTA further complicates geochemistry due to its chelating potential with metals.

Hypothesis

This research hypothesizes that dolomite dissolution rates will increase in neutral to high alkaline brine systems, that the presence of EDTA will promote the dissolution of Calcium and Magnesium from dolomite and keep U, Th, and Nd in solution, rather than letting it absorb onto the dolomite matrix. This is expected because of the high complexation affinity of EDTA for heavy metals as well as carbonate ions, especially in environments with ample hydrolysis.

Materials and Methods

Materials – Dolomite Dissolution

The target background ions for the synthetic brines were sodium chloride (NaCl), magnesium chloride (MgCl₂), cesium chloride (CsCl₂), calcium chloride (CaCl₂), (Fisher Scientific, Pittsburg, PA), sodium nitrate (NaNO₃), sodium sulfate (NaSO₄), and sodium borax (Na₂B₄O₇) (Acros Organics, Geel, Belgium). Salts were dissolved in ultrapure deionized water (>18mΩ -cm) to brine concentration 0.1, 1.0, and 5.0 M. These synthetic brines were made to simulate groundwater conditions at the WIPP. Dolomite mineral samples were collected from the Culebra bluff outcrop on the bank of the Pecos River near

the WIPP. The dolomite rock samples were crushed in an impact mortar and pestle (Chemplex, catalogue no. 850), washed with Milli-Q H₂O (> 18 MΩ·cm), and sieved to particle diameter size fraction (d_p) of ~0.250-0.50 nm. Bulk surface area measured for this dolomite samples via the Brunauer-Emmet-Teller (BET) method (Micromeritics TriSatr II 3030) was 1.70 m²/g (Emerson et al., 2018⁴²). The collected dolomite samples characterization via X-ray diffraction (XRD, Bruker D200) was >99% dolomite. Chemicals like hydrochloric acid (HCl), nitric acid (HNO₃), and sodium hydroxide (NaOH) were ACS reagent grade or better in purity and used as received. EDTA standard was made with Fisher Scientific brand with 99% or higher purity.

Batch reactor and sample preparation procedures – Dolomite Dissolution

Batch reactor experiments were conducted to examine the effect of various ionic strength solutions and EDTA on the dissolution of dolomite (CaMg(CO₃)₂) under aerobic conditions.

Synthetic brine stock solutions (NaCl, MgCl₂, CaCl₂, CsCl, NaNO₃, Na₂SO₄, Na₂B₄O₇) were in Deionized water (DIW) (Barnstead NANOpure® Diamond System with a >18mΩ·cm⁻¹) resistance day. Sodium bicarbonate (NaHCO₃) at 3 mM (~0.126 g) was added to each stock as a pH buffer and for equilibrating with atmospheric CO₂. The pH of groundwater around WIPP is found at neutral to alkaline conditions with a pH of 8 ± 0.5,

therefore, pH of brines was adjusted as needed by using a range of 0.01, 0.1, 1.0 M of either hydrochloric acid (HCl) or sodium hydroxide (NaOH). The batch experiments were conducted using 50 mL polypropylene centrifuge tubes (Corning Centristar) in triplicates: One triplicate contains dolomite and EDTA, while the other contains dolomite only. Additionally, an EDTA-only and dolomite-only samples were used as control for comparisons. Each tube is then weighed and recorded using a Mettler Toledo ME54TE Analytical Balance (0.0001 g).

Approximately 0.20 g of dolomite (5 g/L) was added to each tube. All batch reactors contained dolomite except controls (samples #7 and #8). Once added, the weight of the tubes with dolomite was recorded.

Ethylenediaminetetratic acid (EDTA) stock solution was made with a concentration of 5 mg/L and stored at 4 °C. An aliquot of 0.5 mL was pipetted into batch tubes. The batch tubes with EDTA were then weighed and recorded.

The batch reactors tubes were subsequently placed on a slow shaker for a time of up to 28 days. At the end of each time interval (1 hour, 24 hours, 48 hours, 7 days, and 28 days) batch reactor tube were sampled. Prior to sampling, the pH the pH for each sampling period using ThermoScientific Orion 9110DJWP electrode. Then using the equation below pH was converted to pcH values (Wall et al., 2002⁴³).

$$pcH = pH_R + (0.255 * m_{NaCl}) \quad (\text{Eq. 9})$$

Here m_{NaCl} is brine (NaCl) molality.

ICP-OES test tubes are labeled, weighed, and recorded for sample preparation to accurately calculate the dilution factor. 2% nitric acid (HNO₃, 68-70%, Trace Metal™ Grade) was used for samples preparation. The dilution factor was 10 times for lower ionic strength samples of 0.1 M and 20 - 100 times for the 1.0 and 5.0 M ionic strength brines, respectively. This was done to minimize the effect of salts on the sensitivity of the ICP-OES, as too saturated brines can provide excess carryover residuals between samples, clog up tubing, and/or extinguishing of the plasma. Acid is then pipetted into ICP tubes, then weighed and recorded.

Aqueous Phase Analysis

Inductively coupled plasma optical emission spectroscopy (ICP-OES) – Dolomite

Dissolution

Once all samples are ready, the inductively coupled plasma optical emission spectrometer (ICP-OES, Optima 7300 DV Perkin Elmer) is prepared for analysis. This instrument offers simultaneous measurement across the entire wavelength range (UV and Visible) of all 73 elements. This equipment can handle up to 30% high total dissolved solids (TDS) or suspended solids making it ideal for analyzing groundwater samples. Standards are made to generate calibration curves and for quality control measures throughout the analysis' run. Standard preparation included 2% HNO₃ and Ca²⁺ and Mg²⁺ 1000 µg/mL from High Purity Standards. The range for the standards includes: 0.1 µg/L, 0.5 µg/L, 1.0 µg/L, 5.0 µg/L, 10 µg/L, 25 µg/L, 50 µg/L, 100 µg/L, 250 µg/L, 500 µg/L, 1000 µg/L, 2500 µg/L, 5000 µg/L and 10000 µg/L. A sample list is created, standard concentrations entered, and samples are setup on ICP racks for analysis.

Once analysis is completed, data is exported into the master Excel spreadsheet where the values are used to calculate Ca and Mg $\mu\text{g/L}$ concentrations and fraction aqueous phase.

Materials – Adsorption Experiments

For the synthetic stock brines salts NaCl, NaSO₄, NaBr, KCl, LiCl, CaCl₂, MgCl₂, and Na₂B₄O₇ were used for preparing the Generic Weep Brine (GWB) and ERDA-6 (Energy Research and Development Administration Well 6). The GWB simulates intergranular (grain boundary) brines found in the Salado formation above the WIPP, and ERDA-6 consists of brines that can be typically found in the Castile Formation, below the WIPP. Various molar concentrations (0.1, 0.5, 1.0, 5.0 M) of NaCl synthetic brine stocks were also prepared. All salts used Fisher Chemical and Acros Organics brands. The contaminant chemical standards used for uranium, thorium, and neodymium (1000 $\mu\text{g/mL}$) are all from the brand High Purity Standards. EDTA standard was made with Fisher Scientific brand with 99% or higher purity. As stated earlier in dolomite dissolution materials section dolomitic minerals of ~0.250-0.50 μm was used and characterized using specific criteria.

Batch reactor and sample preparation procedures – Contaminant Adsorption

Batch reactor experiments were performed to measure the effect of various ionic strength solutions, in the presence and absence of EDTA, on the adsorption of actinides and lanthanides onto dolomitic minerals in aerobic conditions. Synthetic brine stocks were prepared using various molar concentrations of sodium chloride (0.1, 0.5, 1.0 and 5.0 M),

GWB, and ERDA-6. Strict recipe guidelines were sent from Los Alamos National Laboratories (Table 2) in preparing the GWB and ERDA-6 brines. Synthetic stock brines are prepared using 1 liter of deionized water (DIW) from a Barnstead NANOpure® Diamond System with a $>18\text{m}\Omega\text{-cm}^{-1}$ resistance. 3 mM ($\sim 0.126\text{ g}$) of sodium bicarbonate (NaHCO_3) is added to the stocks as a pH buffer and CO_2 atmospheric equilibrant. The stocks are then spiked with a uranium, neodymium, and thorium standard ($1000\text{ }\mu\text{g/mL}$). For these experiments consisting of $10\text{ }\mu\text{g/L}$ and $1000\text{ }\mu\text{g/L}$, $5\text{ }\mu\text{L}$ and $500\text{ }\mu\text{L}$ is pipette respectively into brine stocks. The spikes likely lowered the pH of the synthetic brines and because the pH of the WIPP groundwater is alkaline (pH environment of 8 ± 0.5) the pH of brines was adjusted to $\text{pH } 8 \pm 0.5$ using a range of 0.01, 0.1, 1.0 M of either hydrochloric acid (HCl) or sodium hydroxide (NaOH). The experiment setup is like the one described in the dolomite dissolution section above.

Component	ERDA-6 (M)	GWB (M)
NaCl	4.25	2.87
MgCl ₂	0.018	0.953
Na ₂ SO ₄	0.159	0.166
NaBr	0.010	0.025
Na ₂ B ₄ O ₇	0.015	0.037
KCl	0.092	0.437
CaCl ₂	0.011	0.013
LiCl	---	0.004
ionic strength (M)	4.97	6.84
pH correction factor (K)	0.94 ± 0.02	1.23 ± 0.01

Table 2 : Composition and ionic strength of ERDA-6 and GWB, two simulated WIPP brines (95% initial formation), pH correction factor for each brine. Source from Lucchini et al. 2012⁴⁴

Briefly, corresponding synthetic brine stocks were added (50 mL) to all eight batch tubes and then placed on a slow shaker at 80 rpm. Sampling was conducted at: 15 minutes, 1 hour, 3 hours, 24 hours, 48 hours, and 7 days. Preliminary experiments showed that adsorption rates are fast especially in first couple days, so samplings were performed to capture this rapid trend. ICP-MS test tubes are then labeled, weighed, and recorded in preparation for ICP-MS analysis. 2% nitric acid (HNO₃, 68-70% high purity) was prepared for sampling, typically 4.5 mL is pipetted into ICP tubes for 10 ppb experiments, but in some cases for higher concentrations (1.0 and 5.0M) acid volume was increased to 4.75 mL for a 20 times dilution factor. For the higher 1000 ppb contaminant concentrations it is necessary to dilute samples 100 times because of the ICP-MS limit of detection (Nd 0.0057 µg/L, Th 0.0053 µg/L, and U 0.0052 µg/L).

Three separation methods were used for each sampling period. In the settling method, the batch reactors are left to stand for 15 minutes. Depending on the dilution factor a 500 µL sample is taken from the top of the supernatant and pipetted into ICP tubes with acid. These are then weighed and recorded. For the centrifugation method, similarly, 1 mL sample is pipetted into 8 Eppendorf tube from batch reactors and centrifuged for 20 mins at 8000 rpm. Half the volume, 500 µL, is pipetted from the 8 Eppendorf tubes into ICP tubes with nitric acid which are then weighed and recorded. Lastly, after centrifugation the samples are further filtered using 10k MWCO to nanoparticles level. This step was added due to the literature and preliminary experiments showed the occurrence of actinide-colloid that could not be removed via centrifugation alone.

Separation method	Particle size (nm)
-------------------	--------------------

Settling (15 min)	<6 x 10 ⁴
Centrifugation (20 min, 8000 rpm)	<80
10k MWCO centrifugal filtration	<5

Table 3: Size-dependent particle separation methods and expected particle size remaining in solution after separation.

Aqueous Phase Analysis

Inductively coupled plasma mass spectroscopy (ICP-MS) – Contaminant adsorption

Once all samples are ready, the ICP-MS is prepared for analysis. The ICP-MS used is a ThermoFisher Scientific iCAP RQ inductively coupled plasma mass spectrometer (ICP-MS) with estimated quantification limits (EQL) for the target contaminants as Nd 0.0057 µg/L, Th 0.0053 µg/L, and U 0.0052 µg/L. Standards are made for the ICP-MS's calibration curves and for quality control measures throughout the analysis' run. The standards are made using 2% HNO₃ and Uranium, Thorium, and Neodymium 1000 µg/ml standard from High Purity Standards. The range for the standards includes: 0.01 µg/L, 0.05 µg/L, 0.1 µg/L, 0.5 µg/L, 1.0 µg/L, 5.0 µg/L, 10 µg/L, 25 µg/L, 50 µg/L, 100 µg/L, 250 µg/L, 500 µg/L, and 1000 µg/L. The range of 10 ppb and 1000 ppb of the contaminants covers expected solubility ranges for the studied contaminants. A sample list and standard concentrations are entered, and samples are setup on ICP racks for analysis. Finally, data is exported into the master Excel spreadsheet for ppb and % aqueous concentrations.

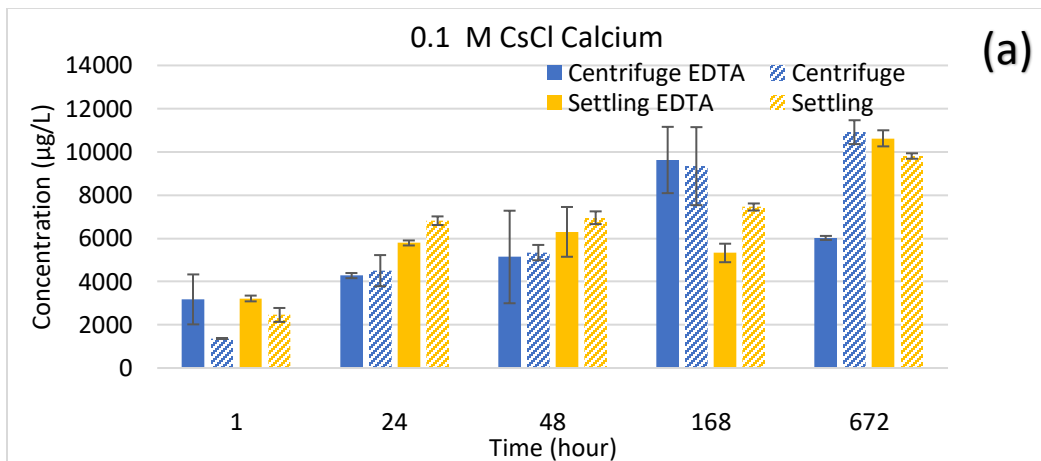
Results and Discussion

Rate of Dolomite Dissolution in various ionic strength solution in the absence and presence of EDTA

Dolomite dissolution kinetic rates were quantified in synthetic brine solutions (pH 8±0.5)

that simulate WIPP relevant conditions. Aqueous concentration of Calcium (Ca^{2+}) and Magnesium (Mg^{2+}) were monitored over 28-day period. Dolomite, a carbonate-based mineral, is known to dissolve and release under the right conditions, Ca^{2+} and Mg^{2+} ions (Eq 3, 4, and 5). Comparisons of samples in the presence and absence of EDTA was conducted with two separation steps: (1) Settling step and (2) Centrifugation step.

Study results showed similar dissolution trends for dolomite over time with an initial rapid increase within 3 days, then achieving a steady-state within 7- 28 days. Preliminary experiments with CaCl_2 and NaCl solutions showed dolomite dissolution reaching steady-state equilibrium within 28-days.



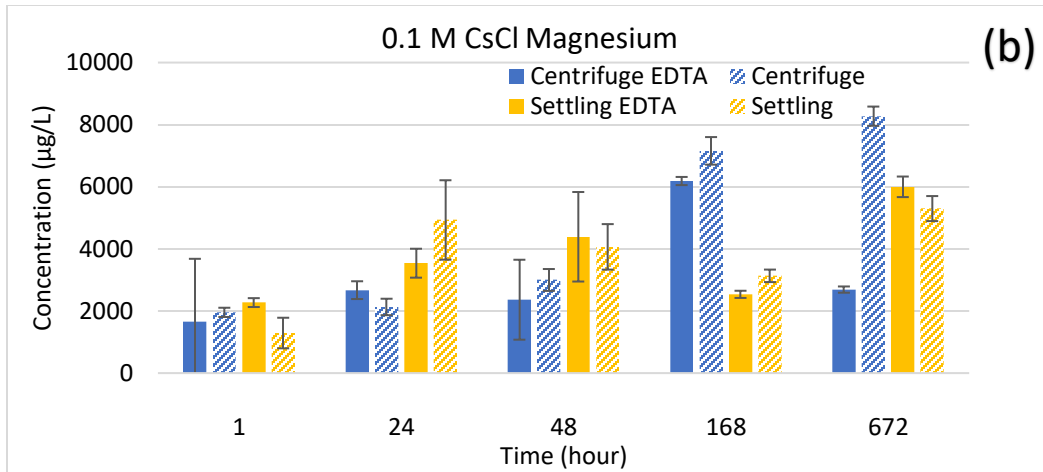
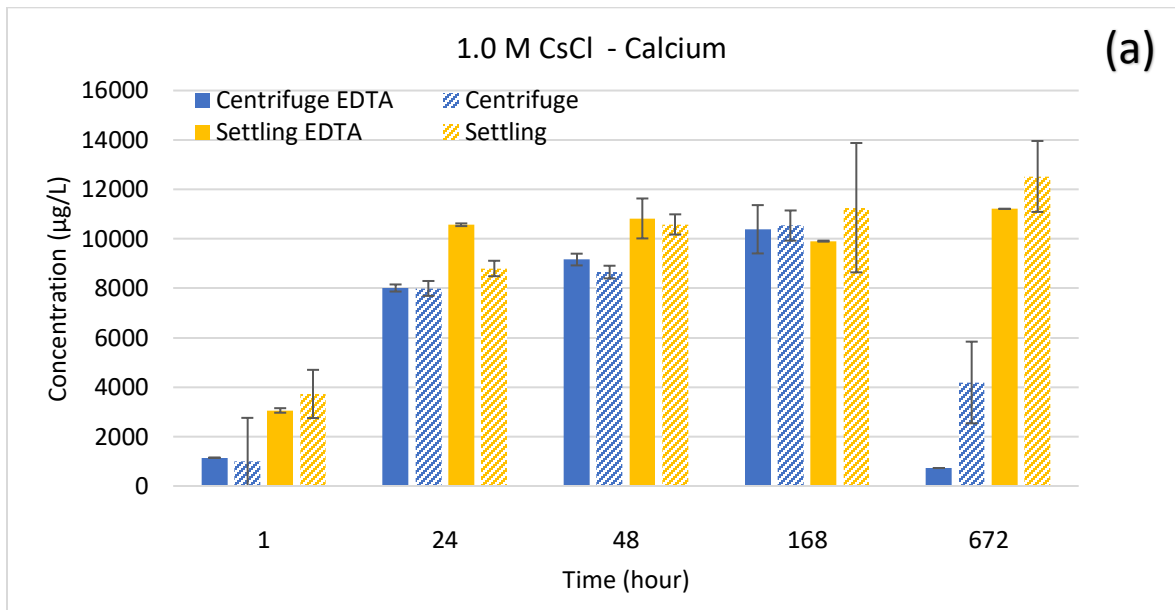


Figure 8 Dolomite dissolution as a function of time in a 0.1 M Cesium Chloride solution in basic condition ($\text{pH} = 8 \pm 0.5$) with constant 5.0 g/L of Dolomite and 5 mg/L EDTA. Error bars are a standard deviation of triplicate samples. (a) Aqueous Phase Calcium in solution. (b) Aqueous Phase Magnesium in solution. Increasing trend for Ca and Mg concentrations in solution throughout 28 days of the experiment.



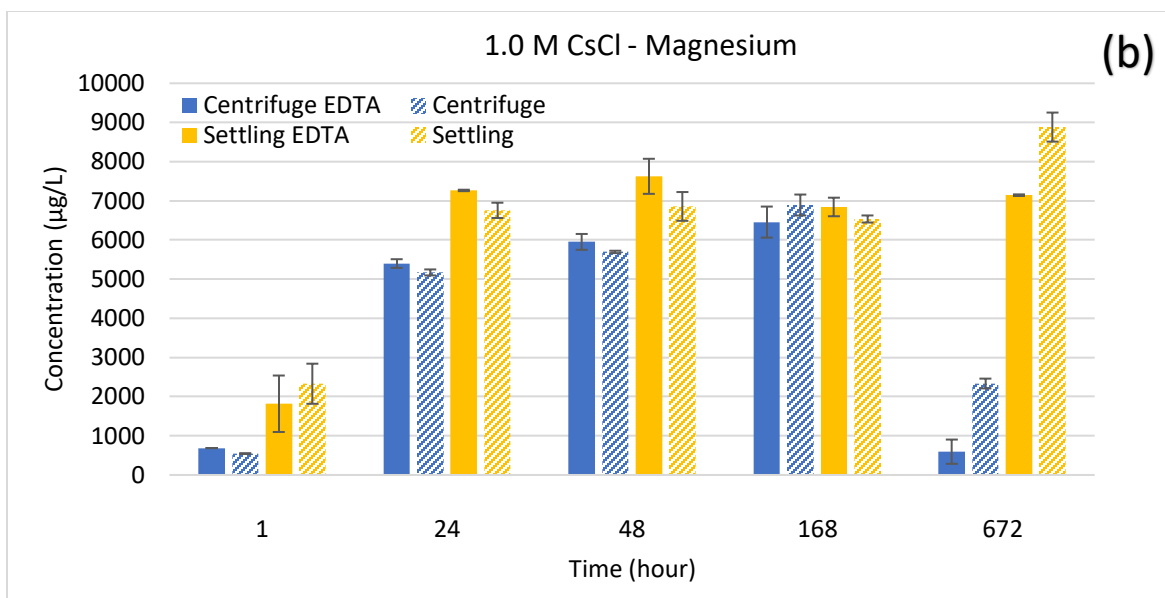
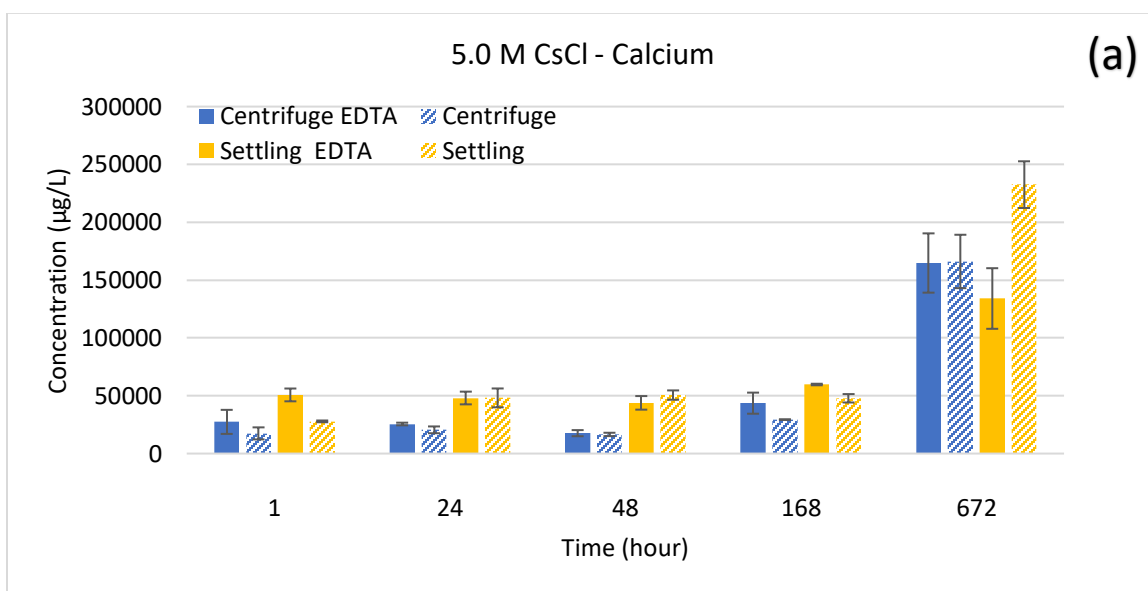


Figure 9: Dolomite dissolution as a function of time in a 1.0 M Cesium Chloride solution in basic condition ($\text{pH} = 8 \pm 0.5$) with constant 5.0 g/L of Dolomite and 5 mg/L EDTA. Error bars are a standard deviation of triplicate samples. (a) Aqueous Phase Calcium in solution. (b) Aqueous Phase Magnesium in solution. Increasing trend for Ca and Mg concentrations in solution throughout 28 days of the experiment.



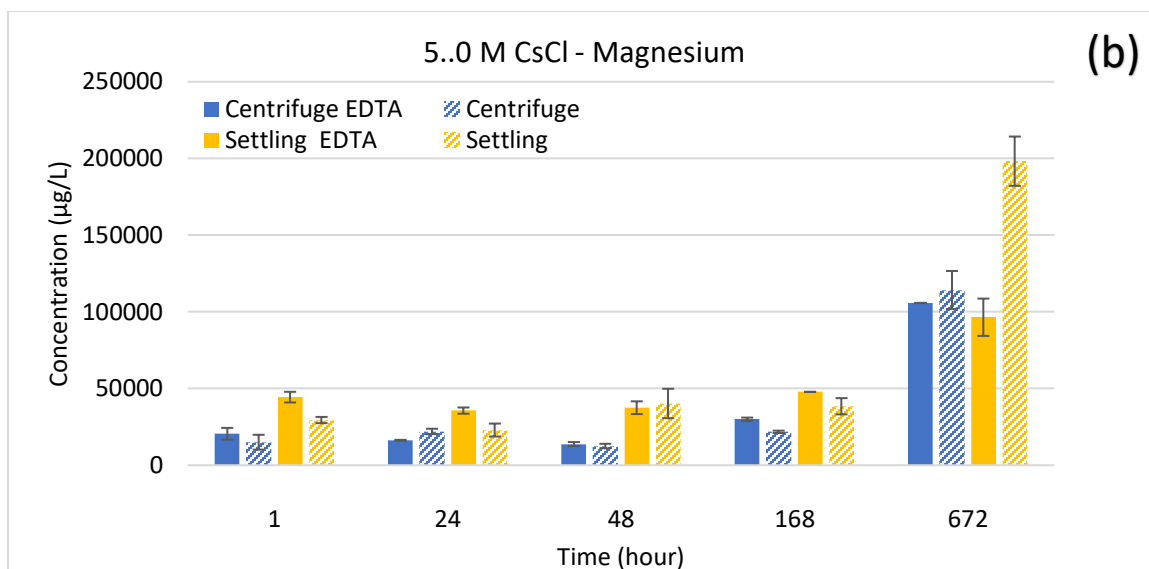


Figure 10: Dolomite dissolution as a function of time in a 5.0 M Cesium Chloride solution in basic condition (pH= 8±0.5) with constant 5.0 g/L of Dolomite and 5 mg/L EDTA. Error bars are a standard deviation of triplicate samples. (a) Calcium Concentration in Aqueous Phase (b) Magnesium Concentration in Aqueous Phase. An initial big increase for Ca and Mg concentrations, but plateaus until 28 days of the experiment where we see another big spike in concentration.

The Effect of Cesium Chloride Brine on Dolomite Dissolution:

In 0.1 M Cesium Chloride (

Figure 8), the dolomite dissolution is observed to follow a strong linear trend up to 28- days. An interesting observation that EDTA-free centrifuged samples exhibited higher Ca and Mg concentrations compared to other separation steps, especially the Mg, indicating that both EDTA and colloidal particles have negligible roles on the dissolution rate in this system.

In the 1.0 M CsCl solution Ca^{2+} concentration increased from 1000 µg/L to 10000 µg/L while Mg^{2+} increased from 500 µg/L to 7200 µg/L, showing higher dissolution of dolomite with time (

Figure 9).

On the other hand, 5.0 M CsCl CsCl solution exhibited a smaller increase in Ca^{2+} and Mg^{2+} concentrations at the start, reaching a steady state in 28 days with a significant

increase in dissolved Ca^{2+} and Mg^{2+} . Overall, dolomite dissolution rate in 5.0 M CsCl was higher than that in 1.0M CsCl (

Figure 10).

The dolomite dissolution in the CsCl solution does exhibit a distinct behavior when compared to all brine solutions employed in this study. The EDTA-free samples have relatively higher dissolved Ca^{2+} and Mg^{2+} compared to samples with EDTA. This is likely due to competing effect of cesium of larger ionic radius (0.167 nm) that weakened Ca^{2+} and Mg^{2+} affinity for EDTA complexation in the CsCl system. Moreover, the observed lower concentration of Ca^{2+} and Mg^{2+} in the centrifuged samples could be attributed to removal of suspended particle (colloid) from solution. It is noticeable the impact ionic strength has especially with the 5.0 M CsCl having significantly higher, two orders of magnitude, dissolved Ca^{2+} and Mg^{2+} when compared to 0.1 M and 1.0 M Na_2NO_3 .

Impact of Sodium Nitrate Brine on Dissolution of Dolomite

Dissolution of dolomite in 0.1 – 5.0M NaNO_3 solution follows similar trends as in cesium brine, increasing over time.

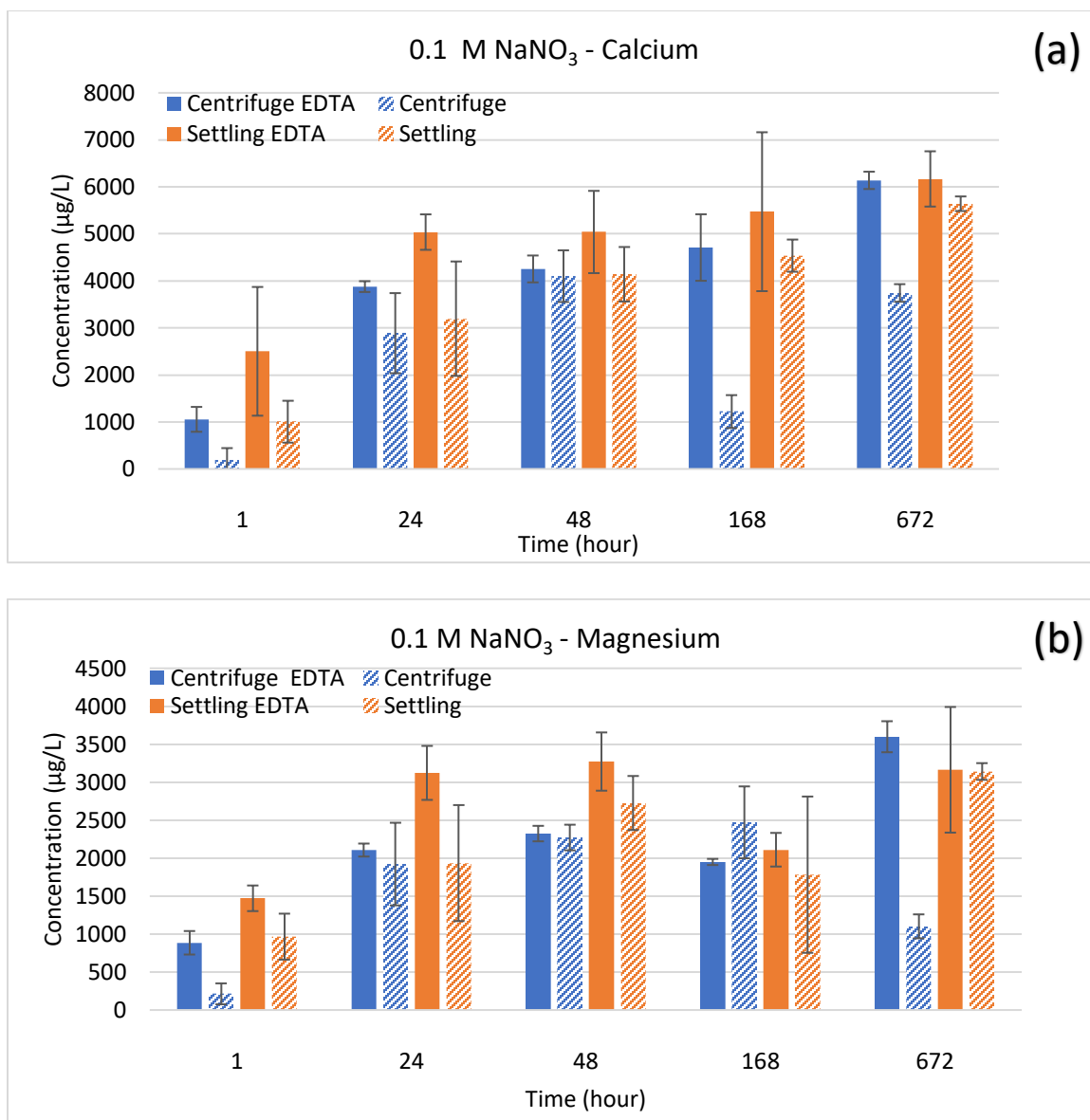


Figure 11 : Dolomite dissolution as a function of time in a 0.1 M Sodium Nitrate solution in basic condition (pH= 8±0.5) with constant 5.0 g/L of Dolomite and 5 mg/L EDTA. Error bars are a standard deviation of triplicate samples. (a) Calcium Concentration in Aqueous Phase (b) Magnesium Concentration in Aqueous Phase. A steady increase of Ca and Mg concentrations in solution overtime, indicating dolomite is dissolving.

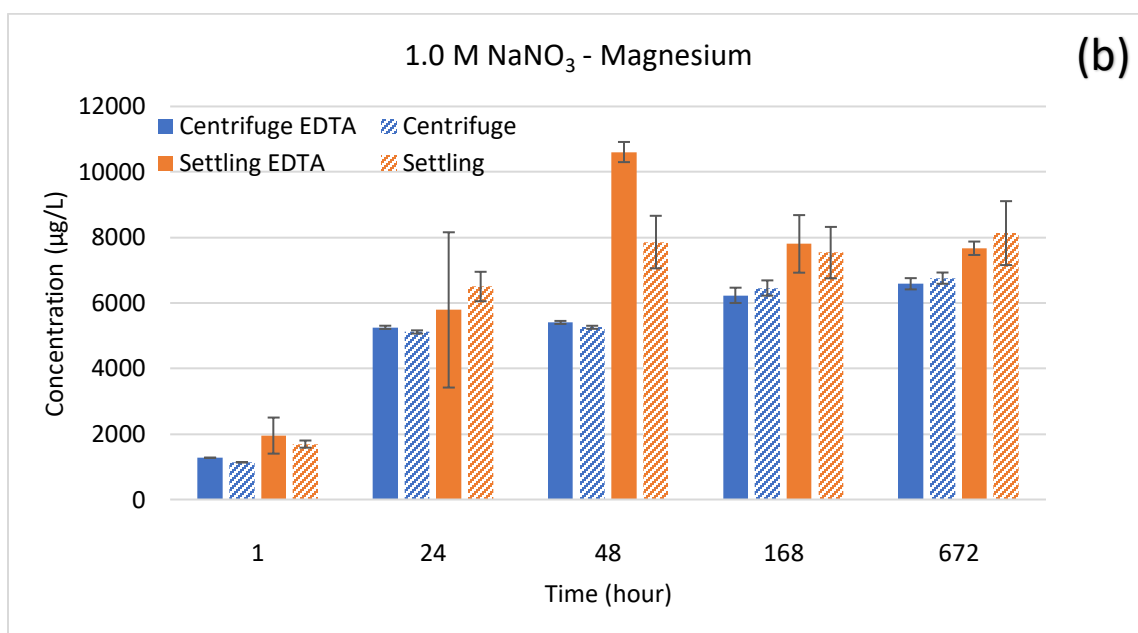
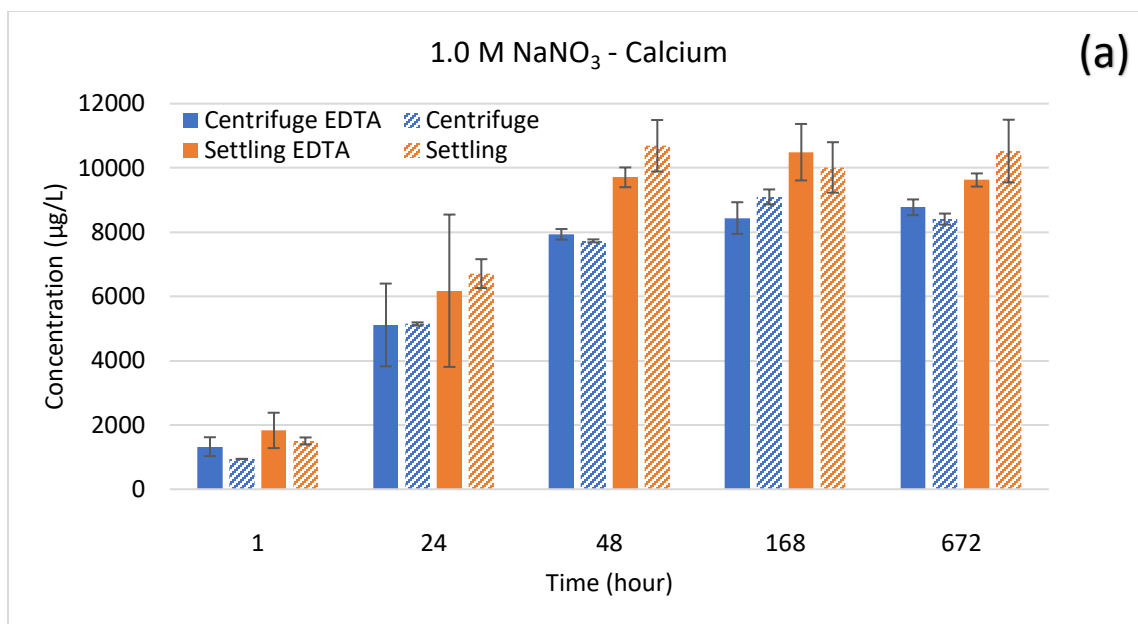


Figure 12: Dolomite dissolution as a function of time in a 1.0 M Sodium Nitrate solution in basic condition ($\text{pH} = 8 \pm 0.5$) with constant 5.0 g/L of Dolomite and 5 mg/L EDTA. Error bars are a standard deviation of triplicate samples. (a) Calcium Concentration in Aqueous Phase (b) Magnesium Concentration in Aqueous Phase. A steady increase of Ca and Mg concentrations in solution overtime, suggesting dolomite is dissolving.

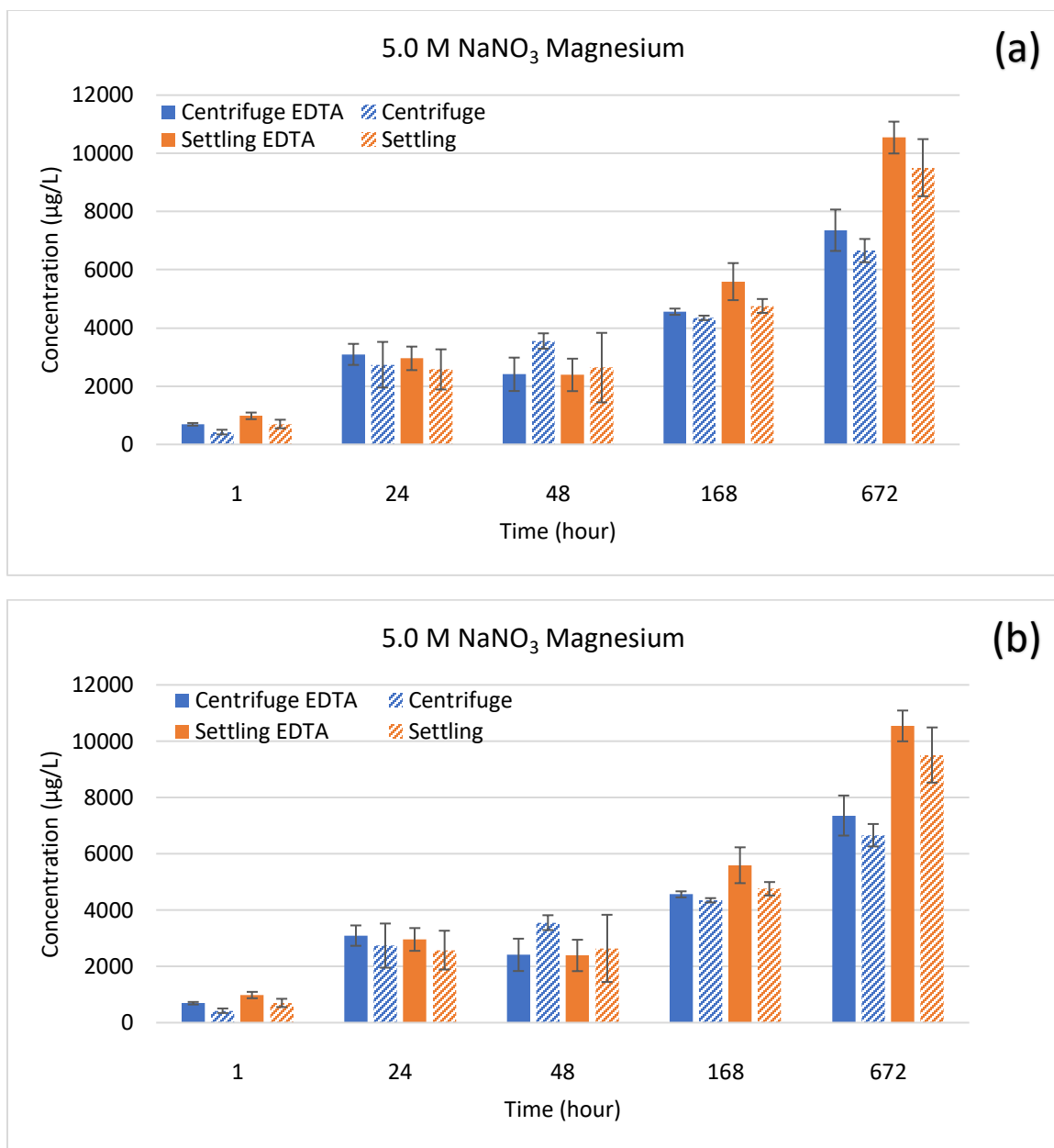


Figure 13 : Dolomite dissolution as a function of time in a 5.0 M Sodium Nitrate solution in basic condition (pH= 8±0.5) with constant 5.0 g/L of Dolomite and 5 mg/L EDTA. Error bars are a standard deviation of triplicate samples. (a) Calcium Concentration in Aqueous Phase (b) Magnesium Concentration in Aqueous Phase. A steady increase of Ca and Mg concentrations in solution overtime, implying dolomite is dissolving

The dissolution of dolomite in 0.1 M NaNO₃ increased significantly within first 24 hours, reaching steady state before trending upward to the last time interval (28 days) (Figure 11).

Dissolution of dolomite in the 1.0 M NaNO₃ was rapid initially, tapering off toward the 28-day period. The impact of EDTA on dolomite dissolution was insignificant as similar Ca and Mg concentration was observed for all studied samples (Figure 12). The dissolution of dolomite in 5.0 M NaNO₃ was slower at the initial time interval, reaching within 28 days a rate that was comparable to that observed in the 1.0 M NaNO₃ (Figure 13). Ionic strength is observed as having a greater impact when going from 0.1 M to 1.0 M NaNO₃, but not so much from 1.0 M to 5.0 M NaNO₃.

Impact of Sodium Chloride on Dissolution of Dolomite:

The dissolution of dolomite in 0.1 M NaCl solution followed predictable trends. Ca and Mg concentrations were consistent and increased with time, almost linearly.

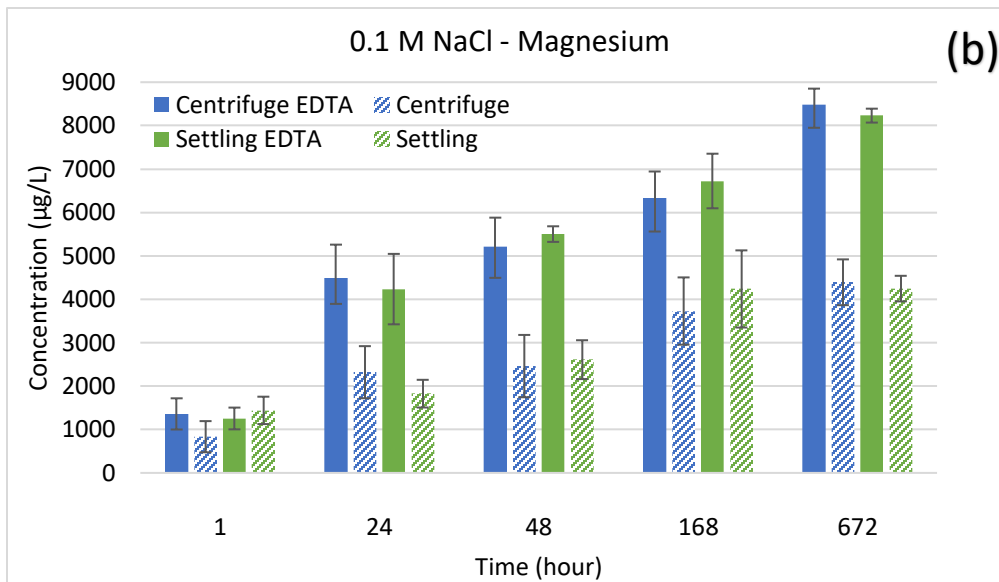
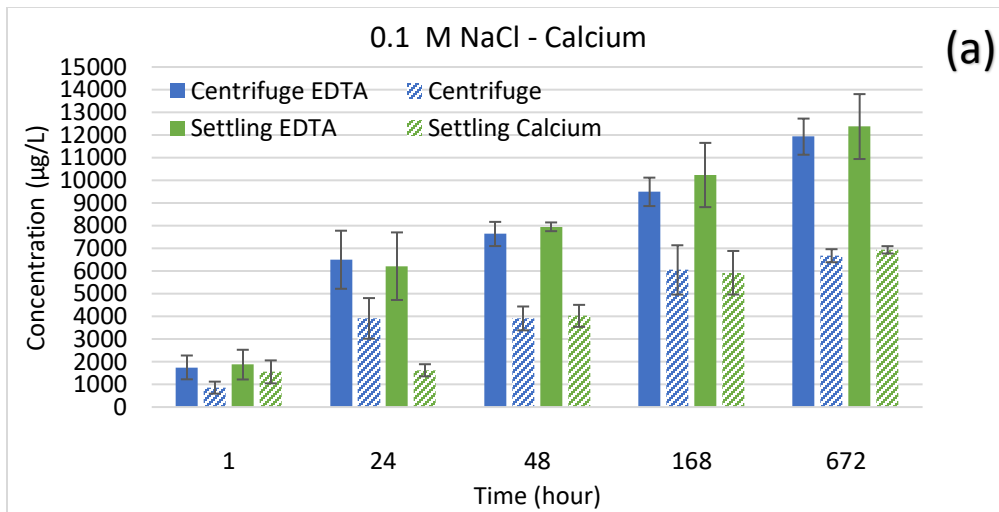


Figure 14: Dolomite dissolution as a function of time in a 0.1 M Sodium Chloride solution in basic condition ($\text{pH} = 8 \pm 0.5$) with constant 5.0 g/L of Dolomite and 5 mg/L EDTA. Error bars are a standard deviation of triplicate samples. (a) Calcium Concentration in Aqueous Phase (b) Magnesium Concentration in Aqueous Phase. NaCl brine solution has a consistent increase in Ca and Mg concentrations over time, thus depicting a more stable dissolution of dolomite.

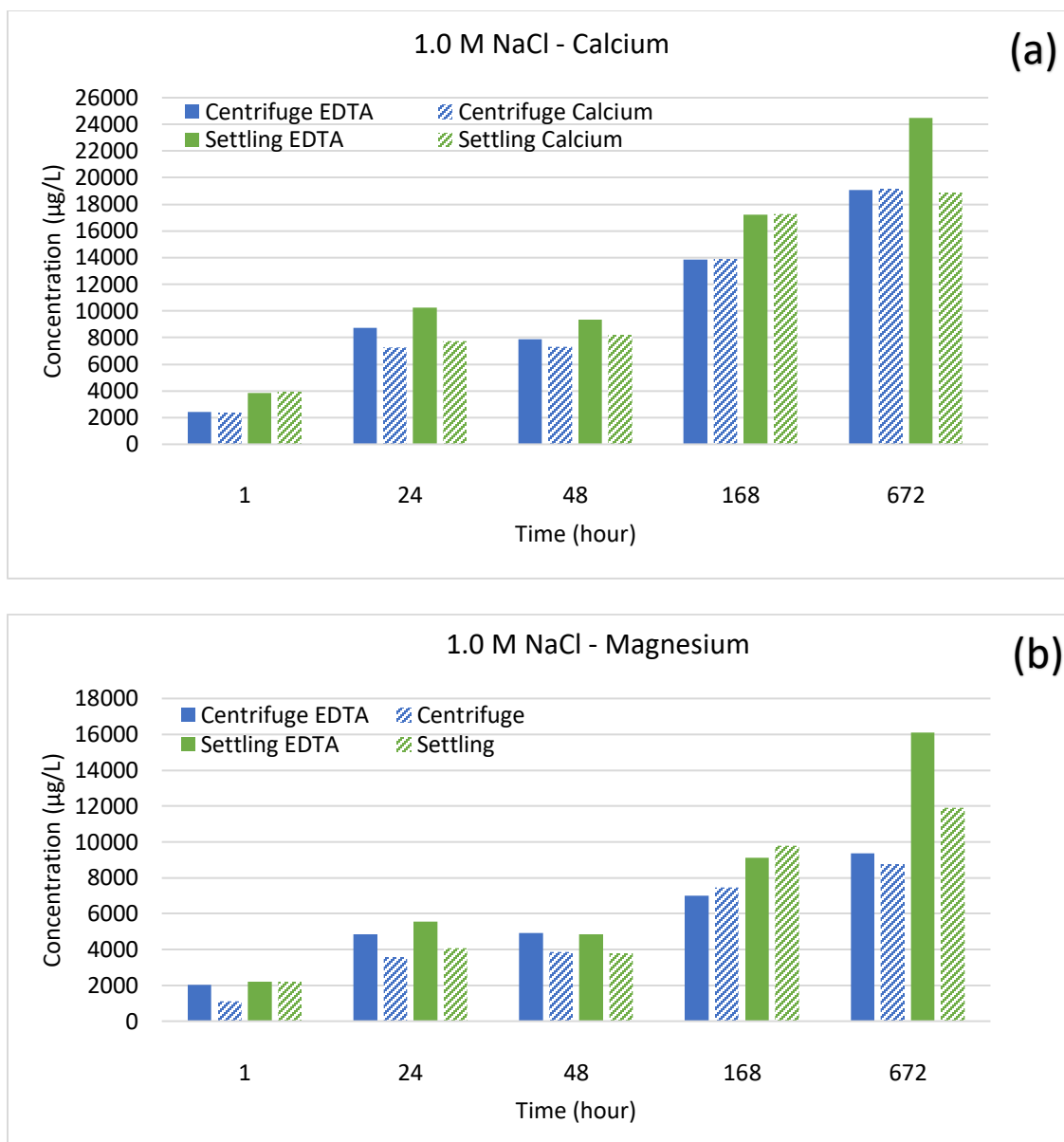


Figure 15: Dolomite dissolution as a function of time in a 1.0 M Sodium Chloride solution in basic condition ($\text{pH} = 8 \pm 0.5$) with constant 5.0 g/L of Dolomite and 5 mg/L EDTA. Error bars are a standard deviation of triplicate samples. (a) Calcium Concentration in Aqueous Phase (b) Magnesium Concentration in Aqueous Phase. NaCl brine solution has a consistent increase in Ca and Mg concentrations over time, thus depicting a more stable dissolution of dolomite.

In this brine EDTA favored dolomite dissolution due to higher formation constant with Ca^{2+} or Mg^{2+} in the presence of Na ions. Significant difference in Ca^{2+} and Mg^{2+} concentration between settling (unfiltered) and centrifuge (filtered) samples. In the 0.1 M NaCl solution the unfiltered samples contained aqueous Ca and Mg that was 30-

50% higher compared to the filtered samples (Figure 15). This is likely suggestive of the removal of suspended particle from solution during centrifugation.

Impact of Sodium Sulfate on Dissolution of Dolomite

Like the NaCl solutions, NaSO₄ increased consistently with time with somewhat of a linear trend.

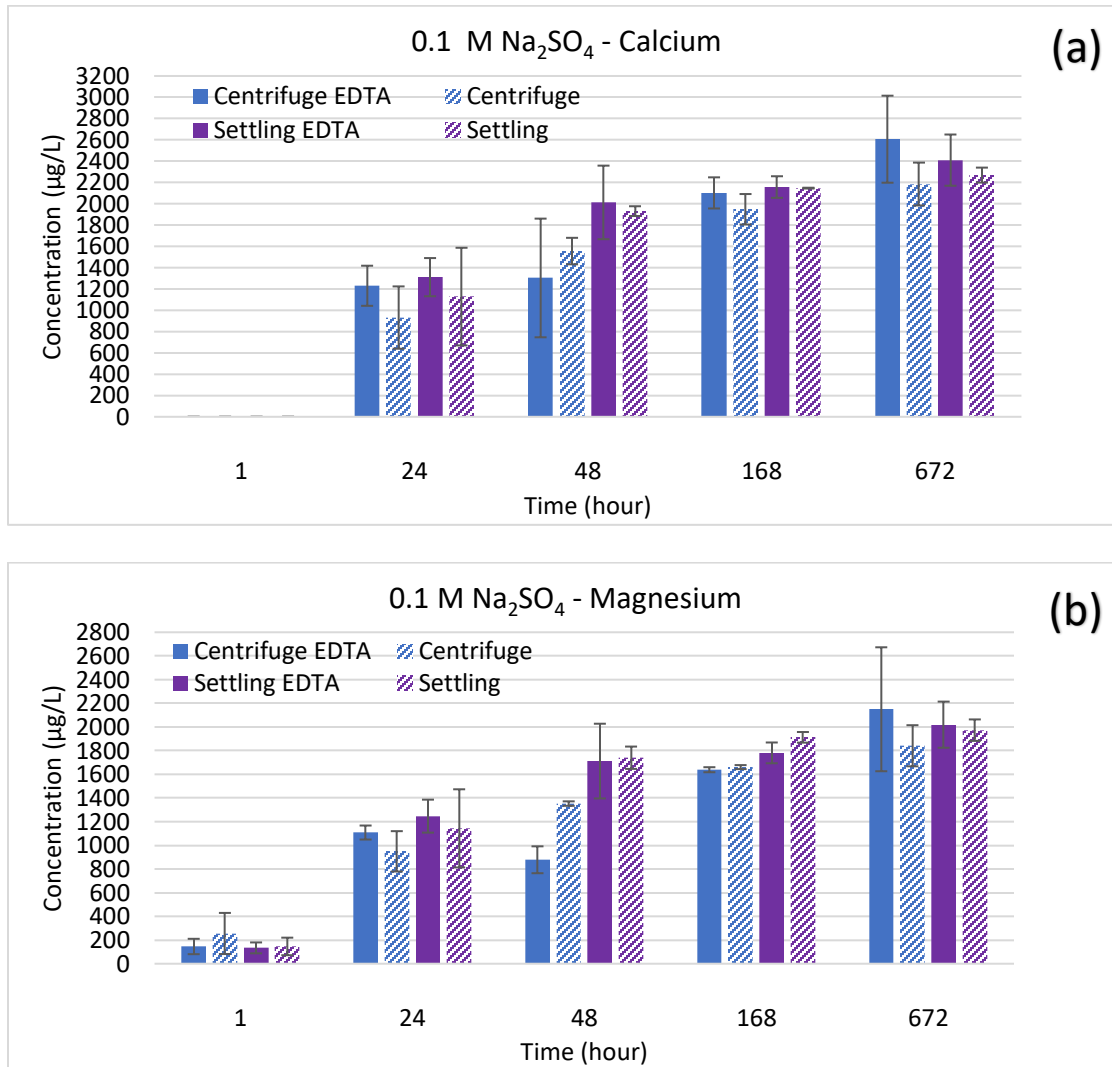


Figure 16 : Dolomite dissolution as a function of time in a 0.1 M Sodium Sulfate solution in basic condition (pH= 8±0.5) with constant 5.0 g/L of Dolomite and 5 mg/L EDTA. Error bars are a standard deviation of triplicate samples. (a) Calcium Concentration in Aqueous Phase (b) Magnesium Concentration in Aqueous Phase. Like NaCl brine solution, Na₂SO₄ has steady dolomite dissolution which is observed from the increasing Ca and Mg concentrations with time.

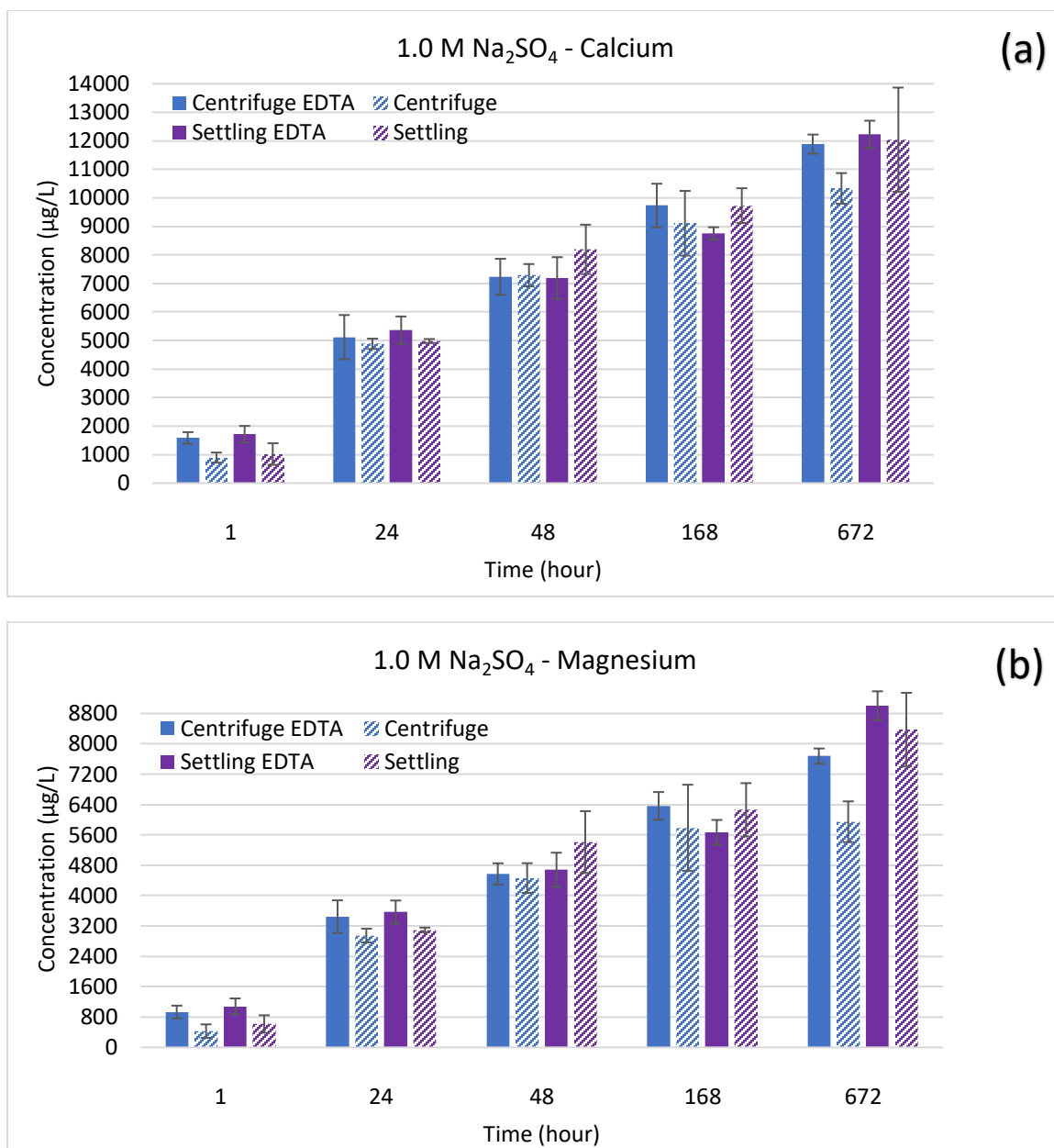


Figure 17: Dolomite dissolution as a function of time in a 1.0 M Sodium Sulfate solution in basic condition (pH= 8±0.5) with constant 5.0 g/L of Dolomite and 5 mg/L EDTA. Error bars are a standard deviation of triplicate samples. (a) Calcium Concentration in Aqueous Phase (b) Magnesium Concentration in Aqueous Phase. Na₂SO₄ brine solution has steady dolomite dissolution which is observed from the increasing Ca and Mg concentrations in solution with time.

In the sodium sulfate (Na₂SO₄) system, dolomite dissolution was consistent and trended upward with time, reaching an average of 30% increase in Ca²⁺. EDTA had a bigger impact on dolomite dissolution in filtered samples when compared to EDTA-free samples. The

filtered samples with EDTA had 2400 $\mu\text{g/L}$ Ca^{2+} compared to the EDTA-free samples that contained 2250 $\mu\text{g/L}$ Ca^{2+} (Figure 16). Overall, it was observed that dissolution of dolomite in low ionic strength system (0.1 M) was enhanced, and these results are similar to that observed in 0.1 M NaCl. The high ionic strength of Na_2SO_4 solutions favored dolomite dissolution and this is corroborated by previous studies that showed increase in dolomite dissolution in high ionic strength solutions when compared to low ionic strength solutions (Povorsky et al. 1999⁴⁵). The Ca^{2+} in 1.0 M is six times higher with 12000 $\mu\text{g/L}$ when compared to the 0.1 M with 2600 $\mu\text{g/L}$ (Figure 17).

Influence of Magnesium Brine on Dolomite Dissolution

The dissolution of dolomite in MgCl_2 brine solution showed very consistent increasing trend in both 0.1 M and 1.0 M concentrations. Only aqueous Ca^{2+} is monitored in the MgCl_2 solution. Also, 5.0 M MgCl_2 did not readily dissolve so it was excluded from this study.

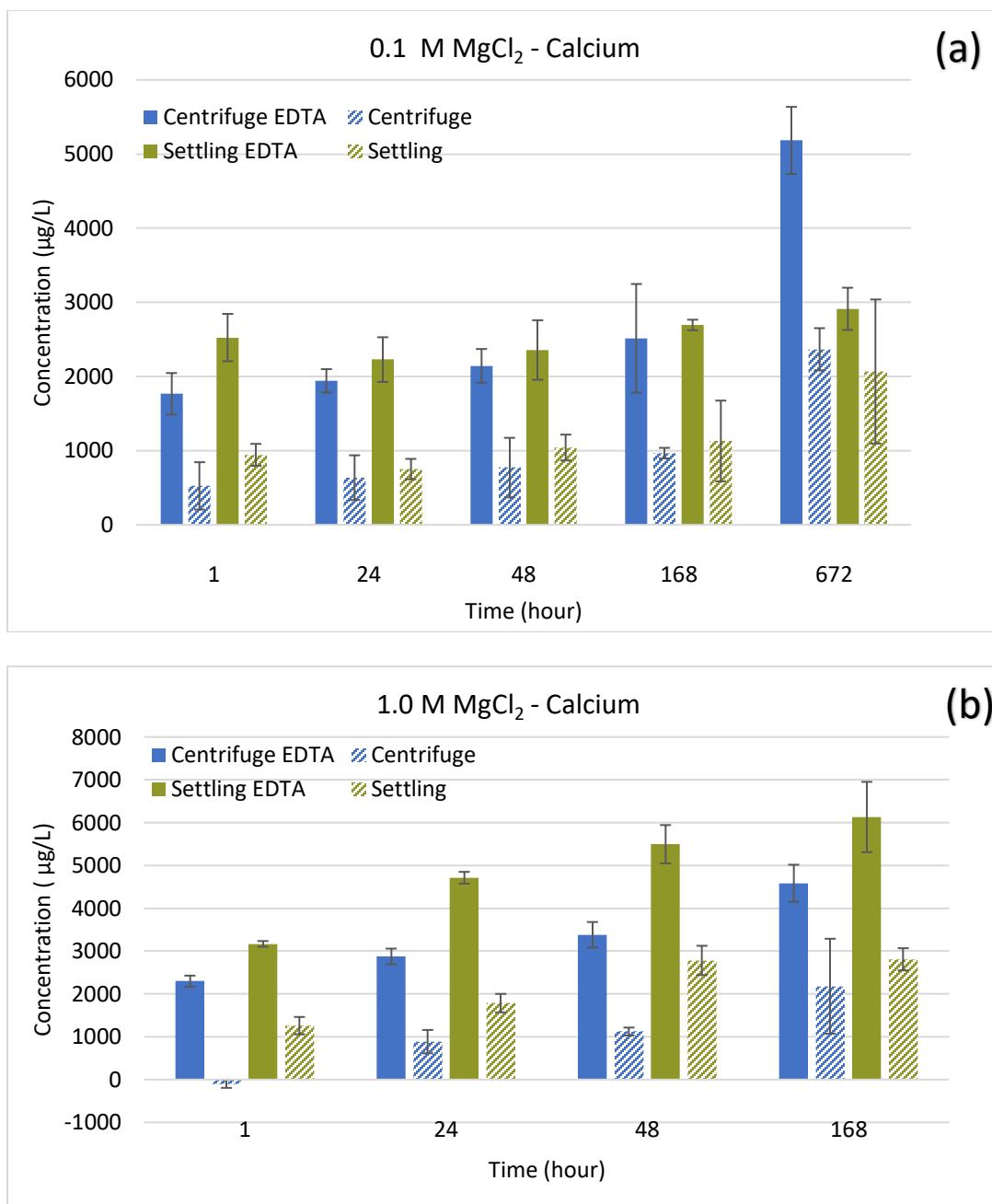


Figure 18: Dolomite dissolution as a function of time in a 0.1 M Magnesium Chloride solution (a) and 1.0 M Magnesium Chloride solution (b) in basic condition (pH= 8±0.5) with constant 5.0 g/L of Dolomite and 5 mg/L EDTA. Error bars are a standard deviation of triplicate samples. Calcium Concentration in Aqueous Phase. Ca and Mg concentrations in solution increase with time, but more aggressively in EDTA samples, thus showing the affinity EDTA has as a catalyst for increasing the dolomite dissolution rates.

The dissolution of dolomite in the EDTA-containing samples had higher Ca (50-60%) compared to EDTA-free counterparts, suggesting significant enhancement of EDTA

complexation in this system. It is worthy to note that dolomite dissolution in the 0.1 M MgCl_2 had not reached a steady state even after 28 days. (Figure 18 (a)). The dissolution of dolomite in the 1.0 M MgCl_2 brine with EDTA was significantly higher compared to that in the EDTA-free samples (Figure 18 (b)). Similar observation was noted in 0.1 M Na_2SO_4 , NaNO_3 , and NaCl solutions. This observation confirms that in lower ionic strength systems of 0.1 M, EDTA tends to dominate the complexation.

Control of Sodium Borate on Dolomite Dissolution

The $\text{Na}_2\text{B}_4\text{O}_7$ brine is a unique system due to complexation exhibited by the $\text{B}_4\text{O}_7^{2-}$ ions. The increase in aqueous phase Ca concentrations was immense when compared to all other synthetic brine solutions which is seen in Figure 21.

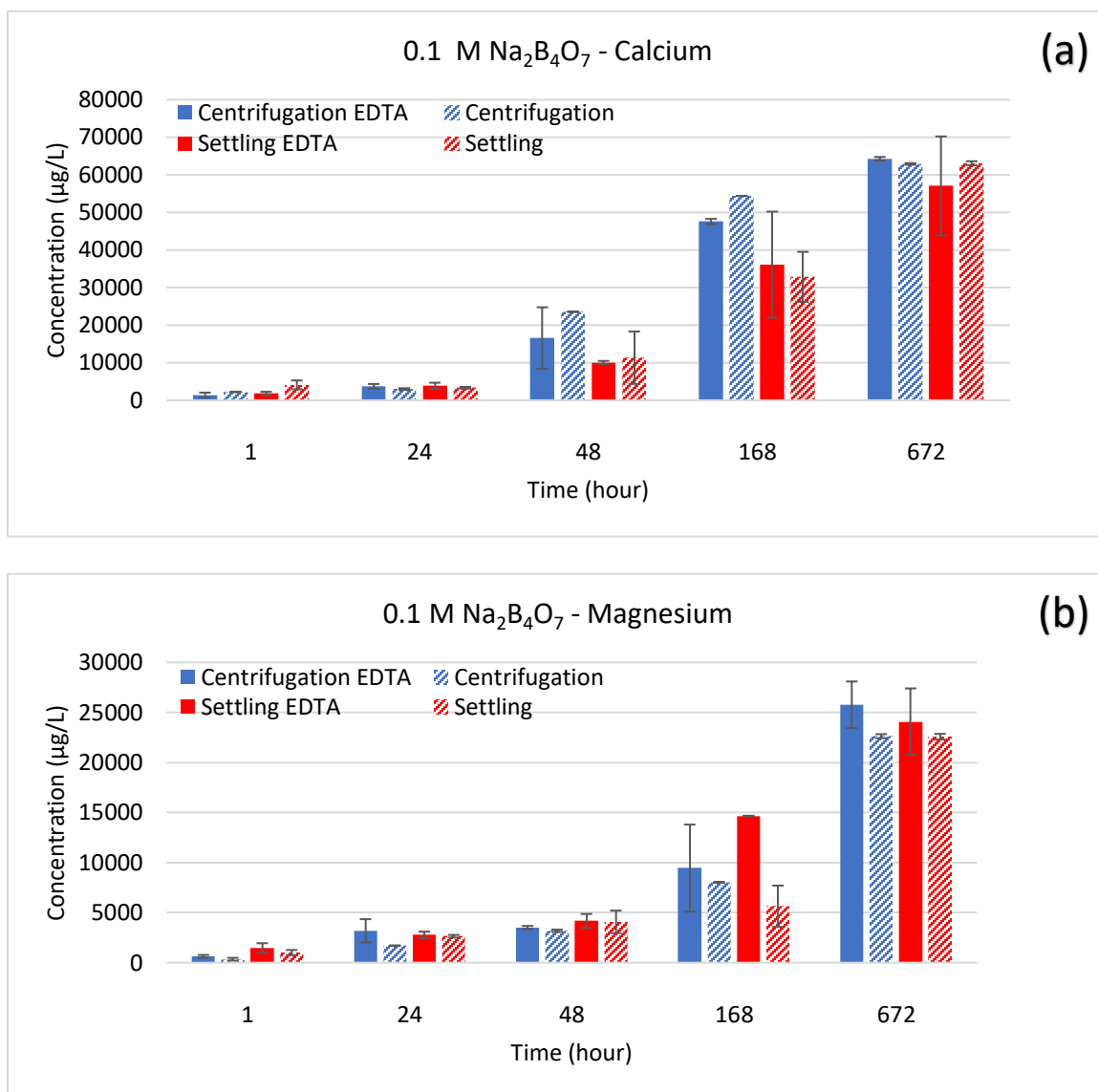


Figure 19: Dolomite dissolution as a function of time in a 0.1 M Sodium Tetraborate solution in basic condition (pH= 8±0.5) with constant 5.0 g/L of Dolomite and 5 mg/L EDTA. Error bars are a standard deviation of triplicate samples. (a) Calcium Concentration in Aqueous Phase (b) Magnesium Concentration in Aqueous Phase. With the initial concentrations of Ca and Mg in solution starting low and having a big spike towards the month-time we see boric acid's ability to create strong complexes and push the dissolution rate of dolomite.

Tetraborate (B₄O₇) is known to break down into boric acid, a weak acid and hydroxide ion.

Weak acids tend to form strong complexes with metal. This leads to an increase in hydrolysis, water-mineral interaction, resulting in significant increase in dissolution. No

difference is observed between EDTA amended and EDTA free samples with Ca and Mg concentrations around 60,000 $\mu\text{g/L}$ and 22,000 $\mu\text{g/L}$, respectively. This is the reason both our Ca and Mg aqueous concentration in this system dominate all the other background ion systems (Ruiz-Agudo et al. 2011⁴⁶). $\text{Na}_2\text{B}_4\text{O}_7$ speciation:

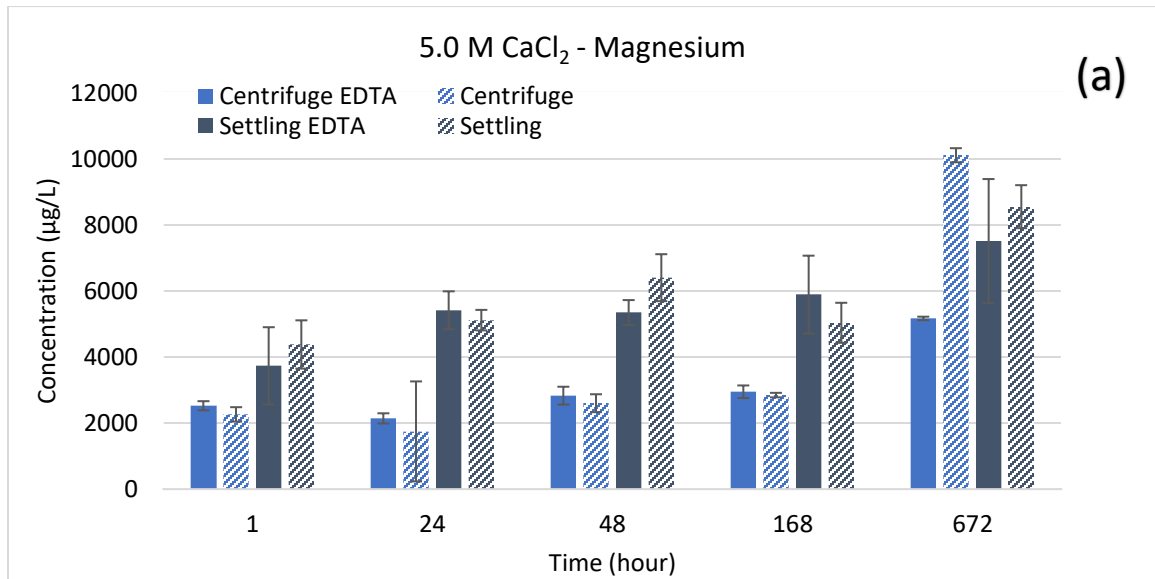
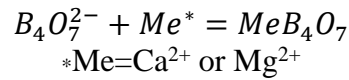
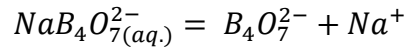
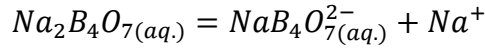


Figure 20: Dolomite dissolution as a function of time in a 5.0 M Calcium Chloride solution in basic condition (pH= 8±0.5) with constant 5.0 g/L of Dolomite and 5 mg/L EDTA. Error bars are a standard deviation of triplicate samples. Magnesium Concentration in Aqueous Phase. This CaCl_2 brine solution shows a slow increasing trend in both Ca and Mg, but the EDTA amended samples tend to show a slightly higher average increase in dissolution rates.

The concentration of magnesium in the 5.0 M CaCl_2 synthetic brine solution in samples amended with EDTA shows higher values with time compared to EDTA-free samples. At

the last sampling step (28 days), the settling samples and centrifuge EDTA-free samples have higher aqueous phase Mg when compared to samples amended with EDTA. This is an interesting characteristic that is also shared by CsCl brine solutions (Figure 21). Due to the high ionic strength ($I = 20 \text{ M}$) of CaCl_2 solution, stabilization in the molecular structure in this system, increasing electrostatic repulsion between ions and hydration potential, causing an increase in solvent-ion interaction. This results in increasing dissolution rates even at 28 days sampling period (Ruiz-Agudo et al. 2011⁴⁷).

Dolomite Dissolution trend lines for 0.1 M Synthetic Brines

Both Figure 21 and Figure 22 shows a side by side comparison of the aqueous phase Ca concentrations of 0.1 and 1.0 M brine solutions.

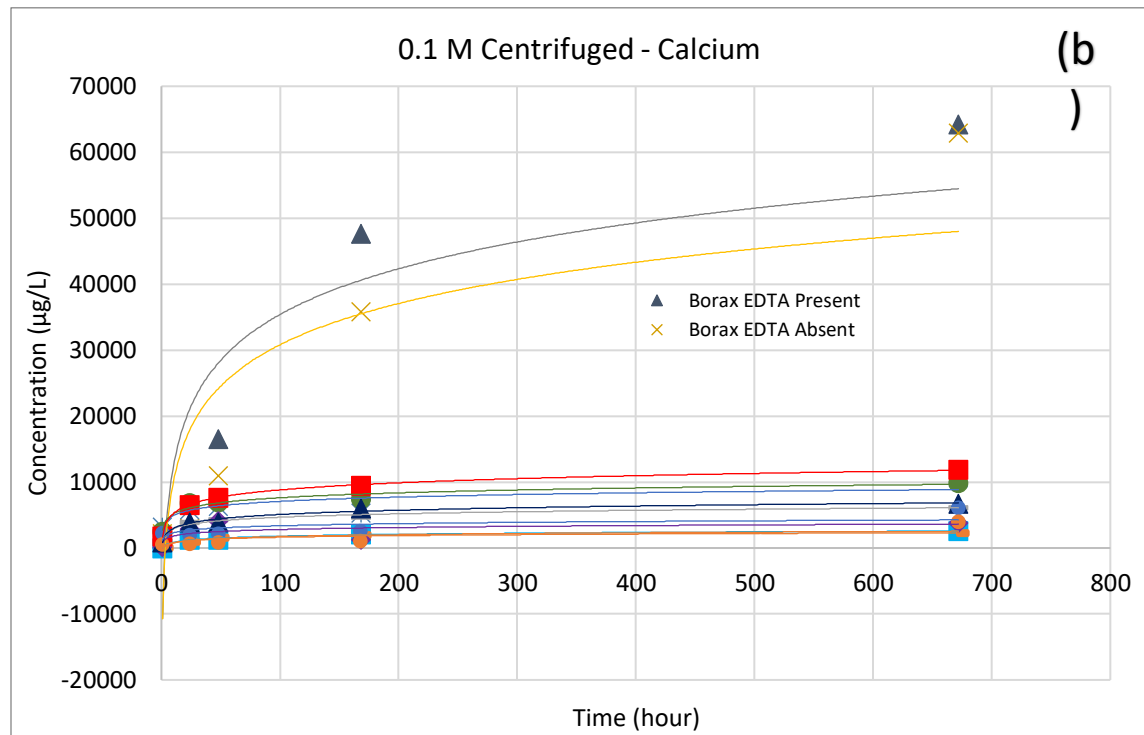
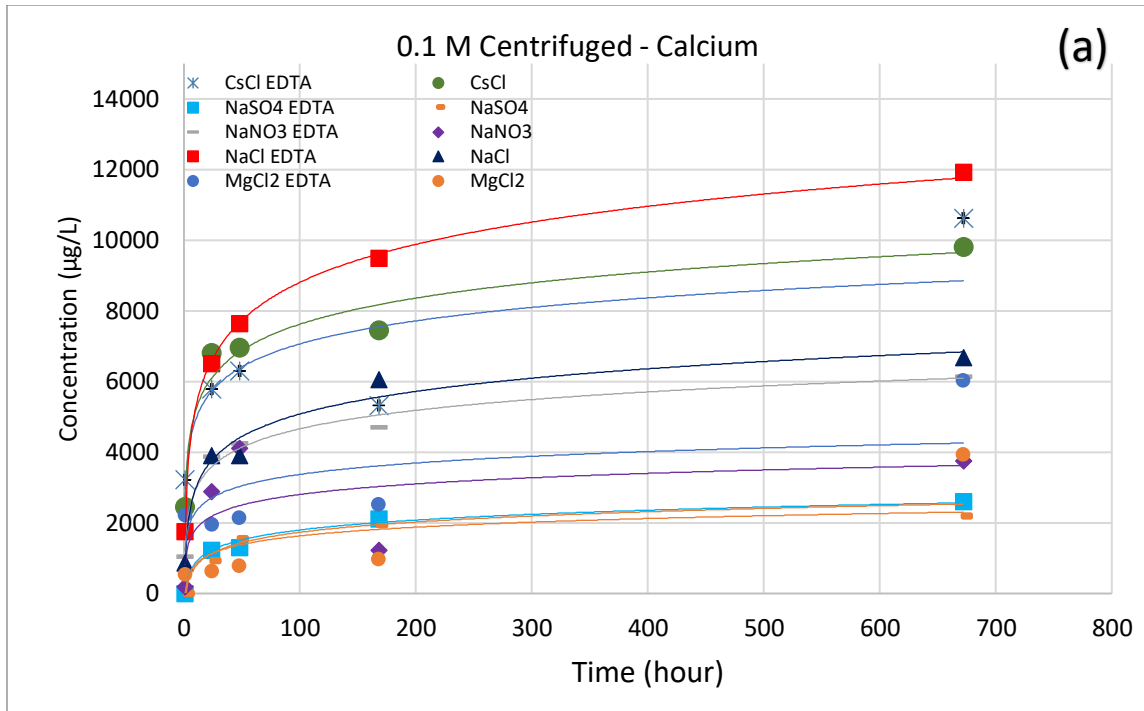


Figure 21: Dissolution trend lines of 0.1 M of studied synthetic brines for centrifuged samples with regards to Aqueous Phase Calcium concentration ($\mu\text{g/L}$) as a function of time in the presence and absence of EDTA. (a) Borax excluded (b) Borax included. Borax is seen to dominate due to the complexing nature of boric acid, which like EDTA, serves as a catalyst for increasing dolomite dissolution. The chart compares all Ca concentration trends with all brines. This gives an idea what brines are preferred for dolomite dissolution.

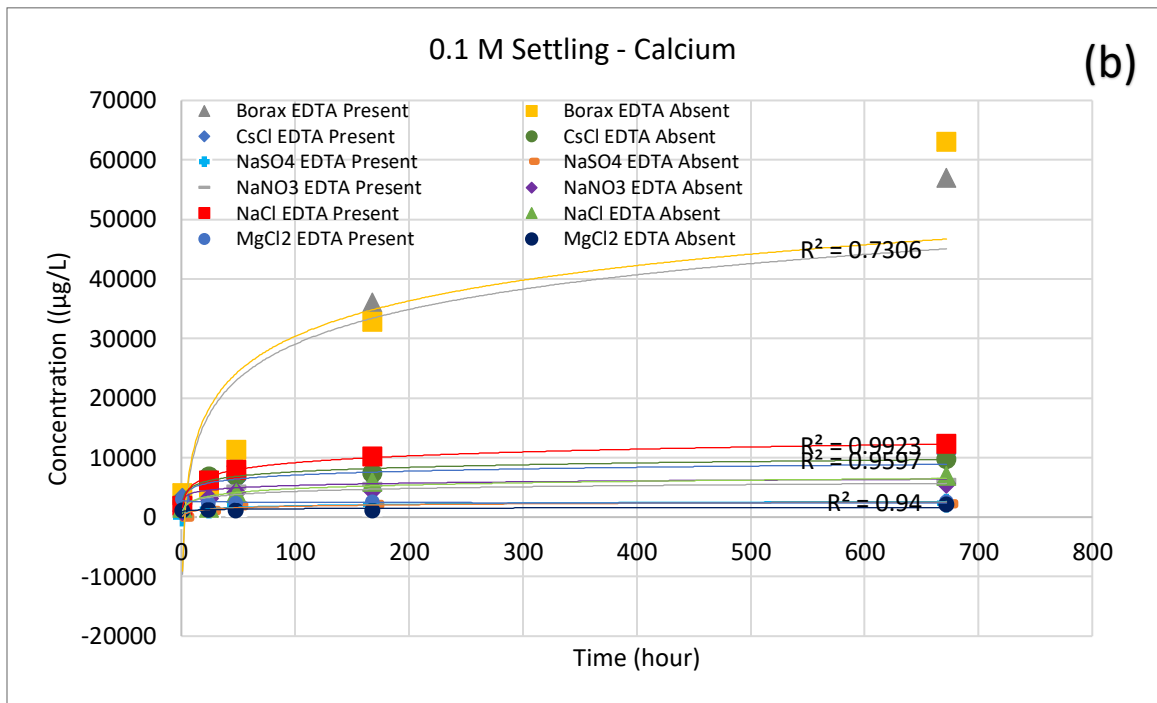
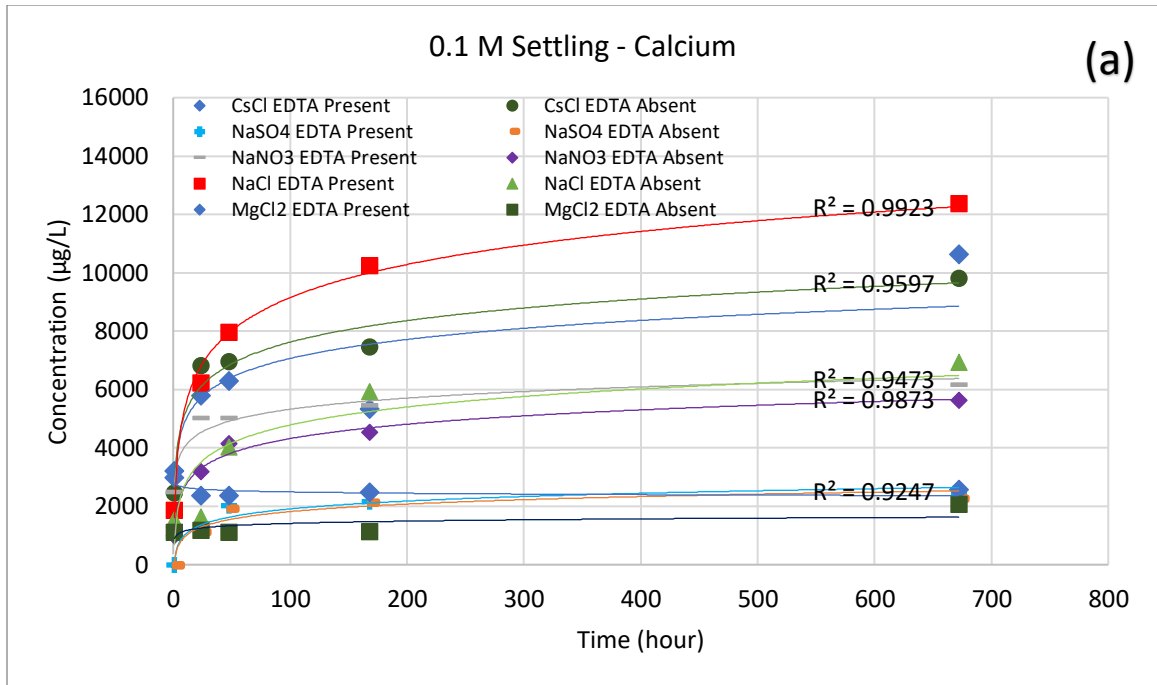


Figure 22 : Dissolution trend lines of 0.1 M of studied synthetic brines for Settling samples with regards to Aqueous Phase Calcium concentration ($\mu\text{g/L}$) as a function of time in the presence and absence of EDTA. (a) Borax excluded (b) Borax included. Like the previous figure, the settling (unfiltered) samples practically have the same order in Ca concentrations in solution.

The charts show how aqueous phase Ca concentrations in each brine solution can differ in regard mineral- water dynamics. The dolomite surface interacts with water and ions molecules in solution and with time begins to dissolve through hydrolysis releasing calcium and then magnesium into solution (equation 3, 4, and 5). The release of Ca from dolomite in most synthetic brines increased within first 3 days and then equilibrate after 7 days until the end of 28 days sampling. Some of the synthetic brine solutions like NaCl, CsCl, and Na₂NO₃ with consistent increases of aqueous phase Ca showed good R² values.

The release of Ca in a few salts, CsCl, NaCl and Na₂B₄O₇, revealed slower equilibration increasing beyond the 28 days. Borax in solution has an incredibly high complexing potential for metals (Lucchini et al. ⁴⁸). This is shown here for both settling and centrifugation samples in Figure 21 and Figure 22 above. Borax trend lines dwarfs Ca Concentrations released to aqueous phase by one to two orders of magnitude.

Dolomite Dissolution trend lines for 1.0 M Synthetic Brines

Figure 23 shows that Ca has the highest dissolution in NaCl brine compared to all the other salts with both EDTA amended and EDTA-free having 24000 µg/L and 19000 µg/L of aqueous phase Ca concentrations for settling samples. This is also the case in centrifuged samples where we find a similar tier order. MgCl₂ scores low in both 0.1 M and 1.0 M charts due to saturation of Mg in solution, therefore inhibiting the dolomite dissolution rate.

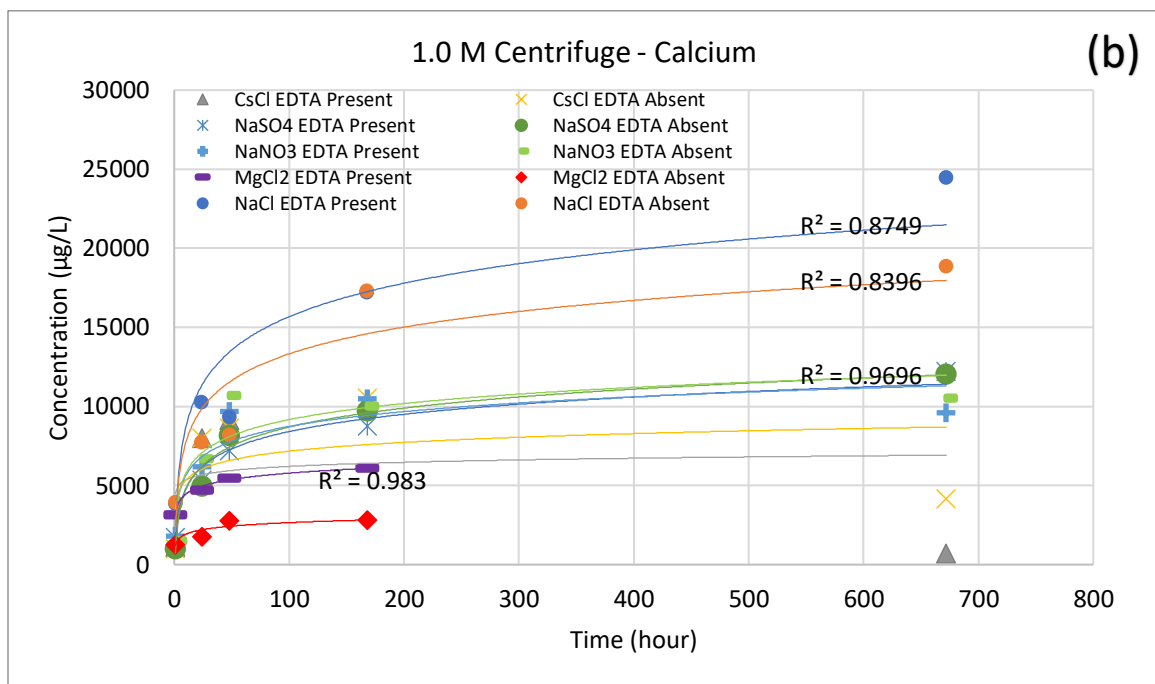
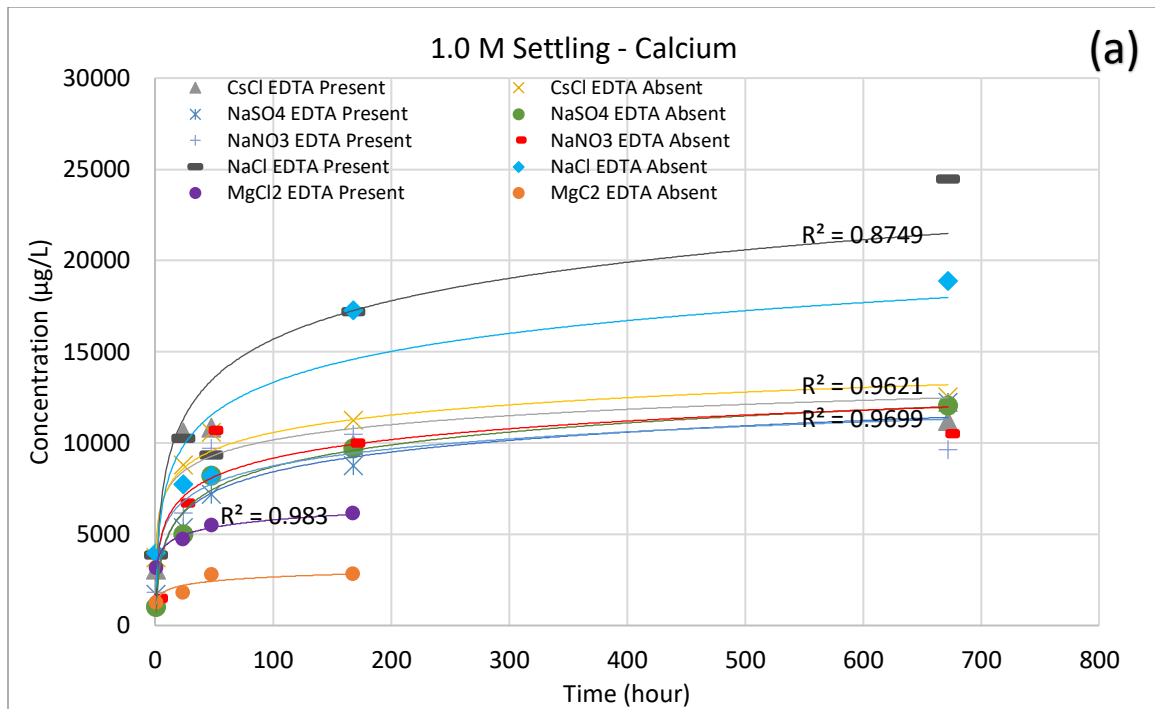


Figure 23: Dissolution trend lines of 1.0 M of studied synthetic brines with regards to Aqueous Phase Calcium concentration ($\mu\text{g/L}$) as a function of time in the presence and absence of EDTA. (a) Settling samples (b) Centrifuged samples. This chart reflects a different order for some of the solutions like NaCl and CsCl, this can be contributed to the different ionic strengths with the 1.0 M concentration.

It is observed that R^2 values tend to be better with brines with lower overall aqueous phase Ca concentrations.

Dolomite Dissolution trend lines for 5.0 M Synthetic Brines

The release of Ca from dolomite in 5.0 M CsCl salt solutions are 2 orders of magnitude higher compared to the 0.1 M and 1.0 M CsCl (Figure 24). Cs has shown to complex and absorb readily with ligands and colloids. As Cs^{1+} and Cl^{-1} ions dissociate, from, Cs can complex with carbonate ions released from dolomite, resulting in Cl^{-1} ion increase that further enables dissolution by pulling the Ca and Mg from the dolomite (Tran et al. 20018⁴⁹). This results in higher Ca content in higher IS solutions.

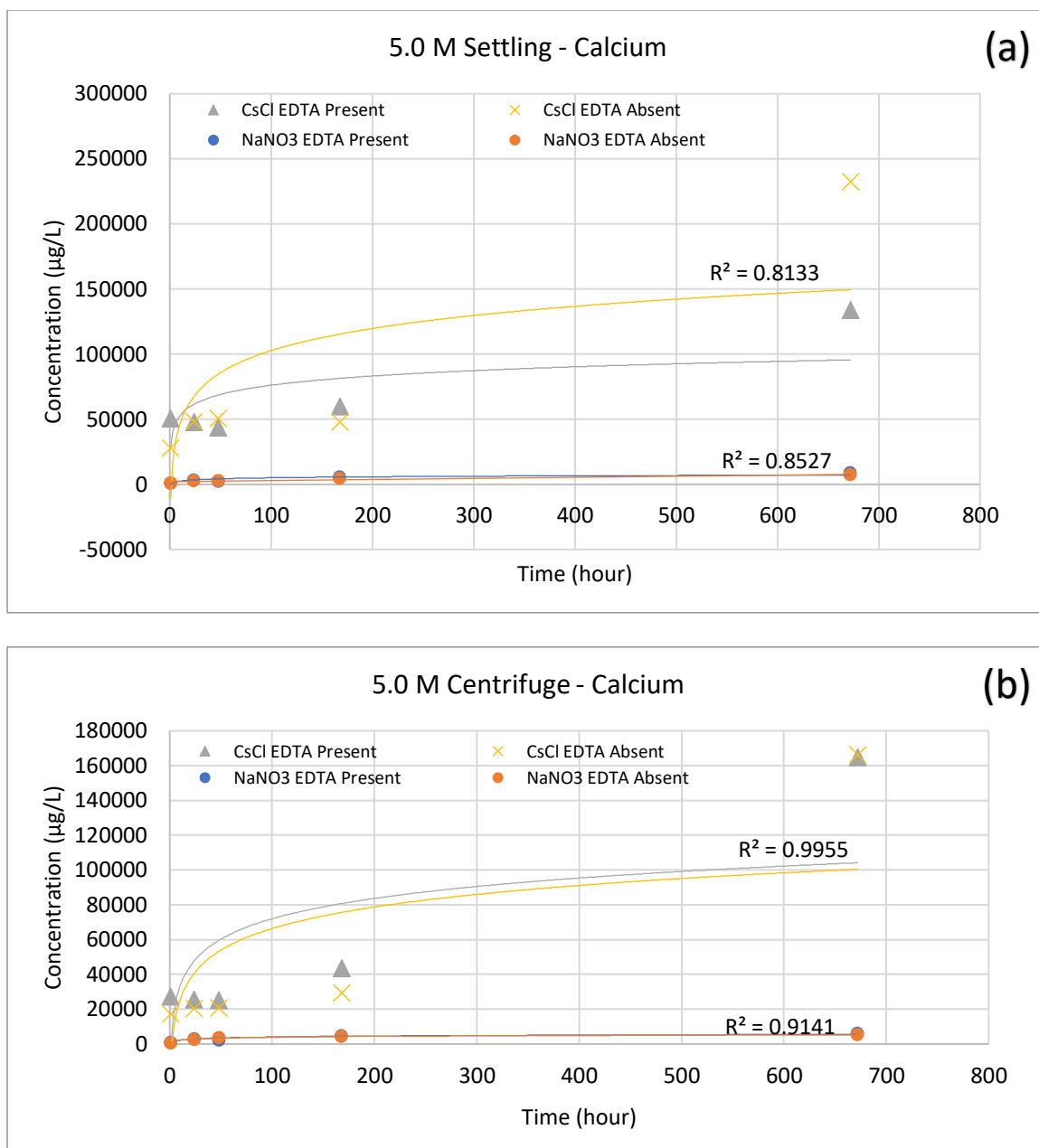


Figure 24: Dissolution trend lines of 5.0 M of studied synthetic brines with regards to Aqueous Phase Calcium concentration ($\mu\text{g/L}$) as a function of time in the presence and absence of EDTA. (a) Settling samples (b) Centrifuged samples. CsCl dominates over NaNO_3 due to its higher ionic strength.

Actinide and Lanthanide Adsorption onto Dolomitic Surface under Various Ionic Strength Solution in the Presence and Absence of EDTA

Adsorption was quantified in synthetic brine solutions (8 ± 0.5) that simulate WIPP relevant conditions. The design of this experiment is to gain a deeper understanding of EDTA (Table 1) complexation effect on radionuclides adsorption in alkaline conditions ((pH 8 ± 0.5) in the presence of dolomite. Aqueous concentrations of U, Th, and Nd was monitored over 7-days and analyzed via ICP-MS. Comparisons of samples in the presence and absence of EDTA was conducted with two parallel separation steps conducted at the same time (1) Settling step and (2) Centrifugation step for $10\ \mu\text{g/L}$ initial concentrations of each contaminant. Another batch was evaluated via three parallel separation steps conducted at the same time 3 separation steps (1) Settling step, (2) Centrifugation step, and (3) 10k MWCO for $1000\ \mu\text{g/L}$ experiments initial concentrations of each contaminant.

From previous experiments described in literature, the majority of adsorption is shown to happen within the first few days (Schnurr et al. 2013⁵⁰), thus sampling periods were chosen at: 15minutes, 1 hour, 3 hours, 24 hours, 48 hours, and 7 days. A range of NaCl synthetic brine concentrations (0.1, 1.0, 5.0 M) were used to compare the effect of ionic strength and saturation on the contaminant-water-mineral dynamics in these systems. Two complex brines, the GWB and ERDA, encompass of a mixture of many salts (Table 2). These two brines were also considered in the case of the potential brine release scenario. Also, salts used in the previous dissolution experiments are also present in GWB and ERDA-6 brines which can help support the conclusions deduced in these adsorption experiments.

The effect of 0.1 M Sodium Chloride brine on Contaminants Adsorption at concentration of 10 µg/L

Monitoring of U, Th, and Nd aqueous phase concentrations in 0.1 M NaCl brine solutions shows adsorption of Th and Nd concentrations, but no removal in U concentrations is observed.

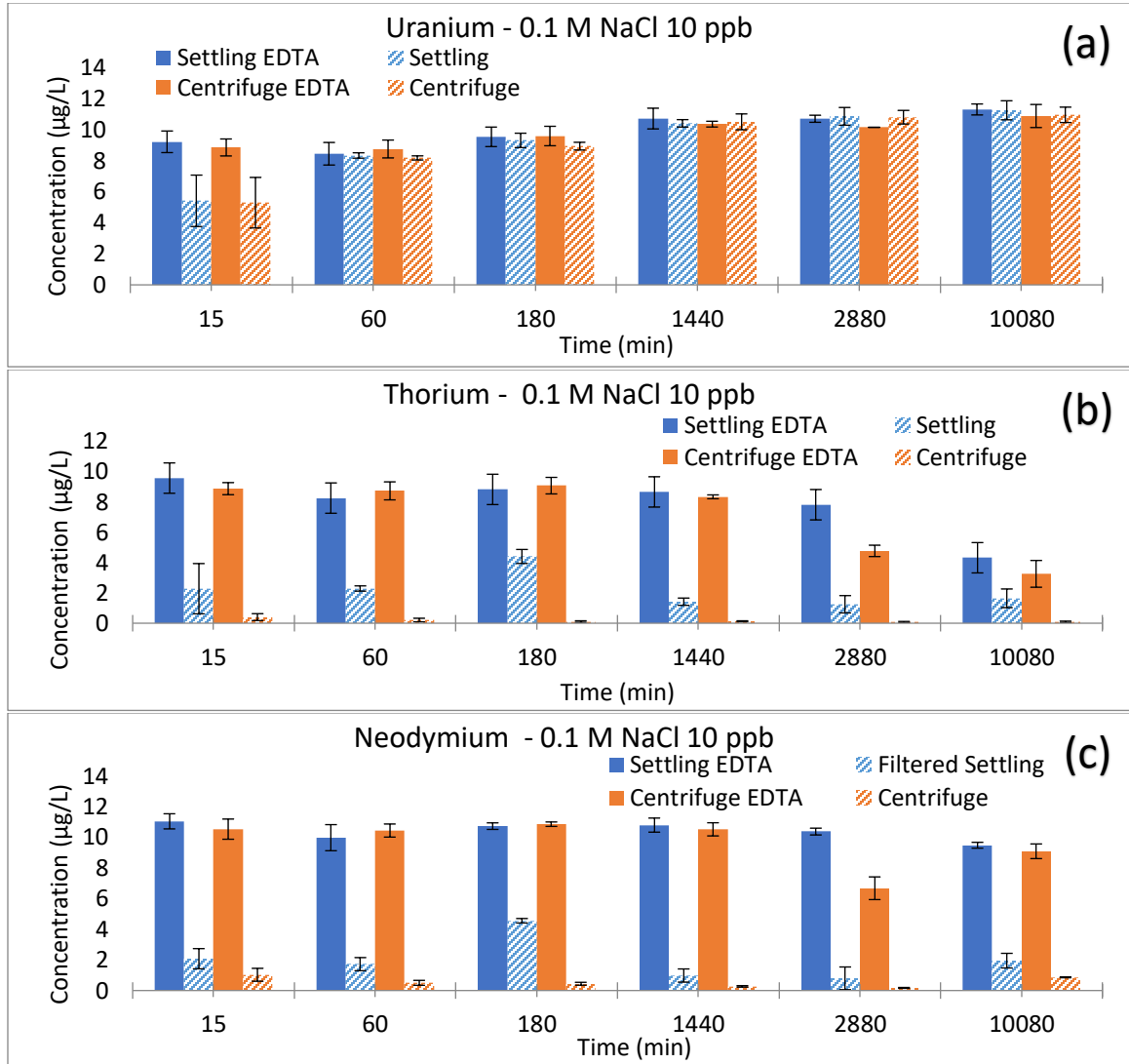


Figure 25: Actinide and Lanthanide concentrations (µg/L) as a function of time in a 0.1 M NaCl solution in basic conditions (pH= 8±0.5) with constant 5.0 g/L of Dolomite, 5 mg/L EDTA and 10 µg/L (undersaturated) of contaminants. Error bars are a standard deviation of triplicate samples. (a) Aqueous Phase Uranium Concentrations (b) Aqueous Phase Thorium Concentrations (c) Aqueous Phase Neodymium Concentrations. U concentrations are steady, showing it to be unaffected, whereas Th and Nd concentration without EDTA are reduced almost immediately. This shows the ability EDTA has with complexing these metals.

At low ionic strength of 0.1 M NaCl, aqueous phase U concentrations remained constant throughout all samples. There was a decrease to 5 µg/L in the first 15 min in aqueous phase U concentration in both settling and centrifugation EDTA-free samples (Figure 25 (a)). Since both aqueous phase U concentrations are similar in this small-time frame, it can be assumed that U is adsorbing on particle lower 80 nm that represent colloidal particles (Figure 7, Table 3). Uranium in the presence of carbonate ion forms uranyl- carbonate-U(VI) complexes, which are very stable in solution (Blake 1956⁵¹). This complexation outcompetes any possible adsorption by dolomite or small colloidal particles. An increase in CO₃²⁻ ions is expected because (1) it is an open system due to increased CO₂ solubility and (2) the dolomite dissolution releases its carbonate anions. The dissolution of dolomite releases aqueous phase Ca up to 12000 µg/L in 28 days (Figure 14). In addition, uranyl complexation with EDTA is forming [U(VI)/EDTA] keeping U in solution.

After the 1-hour sampling, there is no sign of colloid-contaminant adsorption because all aqueous phase U concentrations remained the same for both EDTA-amended and EDTA-free samples due to the strong complexation uranyl ion with carbonate (Figure 25 (a)). Previous study on similar batch sorption experiments with bentonite colloids, which have a high surface loading and cation exchange capacity of 102 meq/100g, suggested very little adsorption of U in two different solutions amended by carbonate and low and high colloid concentrations U (Tran et al. 2018⁵²). This ties back to what is mentioned earlier in that the uranyl carbonate complexes outcompete any possible colloid interaction and effect of EDTA.

On the other hand, aqueous phase Th and Nd both showed an appreciable decrease in concentration across all samples, especially in samples free of EDTA. The immense drop

in aqueous phase Th and Nd concentration for EDTA- free samples is the result of contaminants adsorption onto dolomite and onto a small fraction of colloids reflected in the centrifugation samples. It does seem that the particle size (Table 3) has an impact of contaminant adsorption (Figure 25 (b) & (c)).

Another distinguishable observation is that EDTA is playing a major role in keeping aqueous phase Th and Nd in solution and not the carbonate ions like in the case of U. All samples contain similar carbonate ion concentrations, therefore the difference of Th and Nd concentrations between EDTA- amended and EDTA- free samples is attributed to the EDTA effect.

A major difference between aqueous phase Th and Nd is seen with the EDTA- amended samples at 28 days. Here Th concentrations decrease substantially, while Nd not as much. This shows that with enough time adsorption of Th and Nd in EDTA- amended samples, Th has a less affinity towards EDTA, outcompeting Nd for adsorption spots. Th is seen to adsorbed from the initial 10 $\mu\text{g/L}$ to 4 and 3 $\mu\text{g/L}$ in settling and centrifuge EDTA samples, respectively, and Nd was removed from 11 $\mu\text{g/L}$ to 9 $\mu\text{g/L}$ in 28 days.

The effect of 0.1 M Sodium Chloride brine on Contaminants Adsorption at concentration of 1000 $\mu\text{g/L}$

Aqueous phase U concentrations remained consistent in the 0.1 M NaCl synthetic brine solution throughout the experiment. In contrast, aqueous phase Th and Nd concentrations were considerably removed.

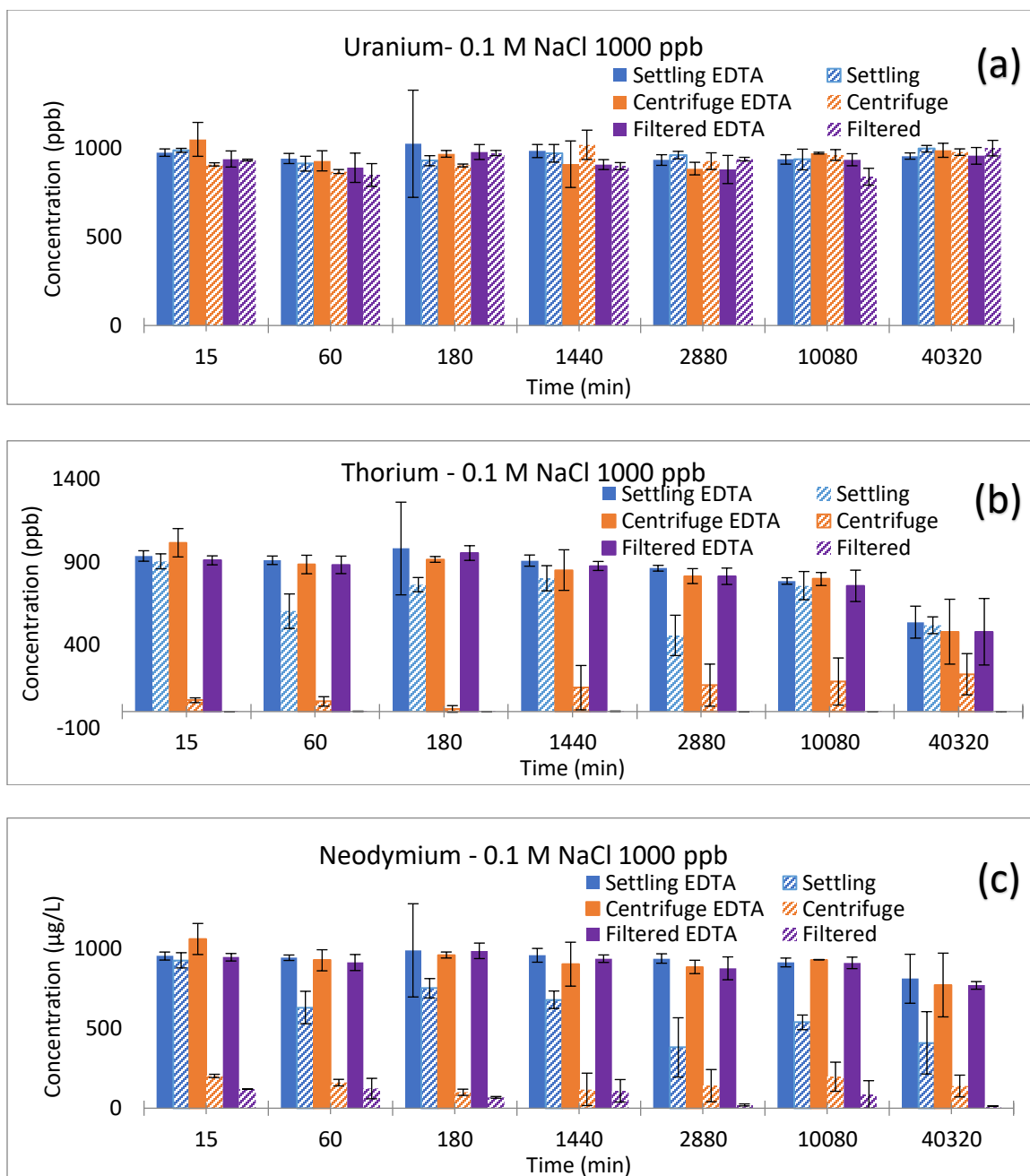
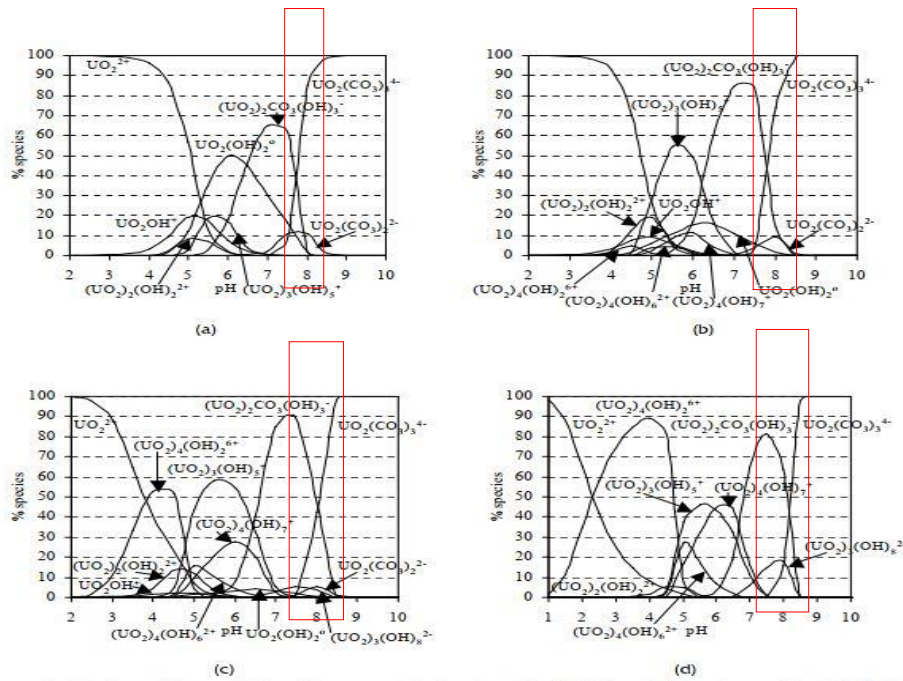
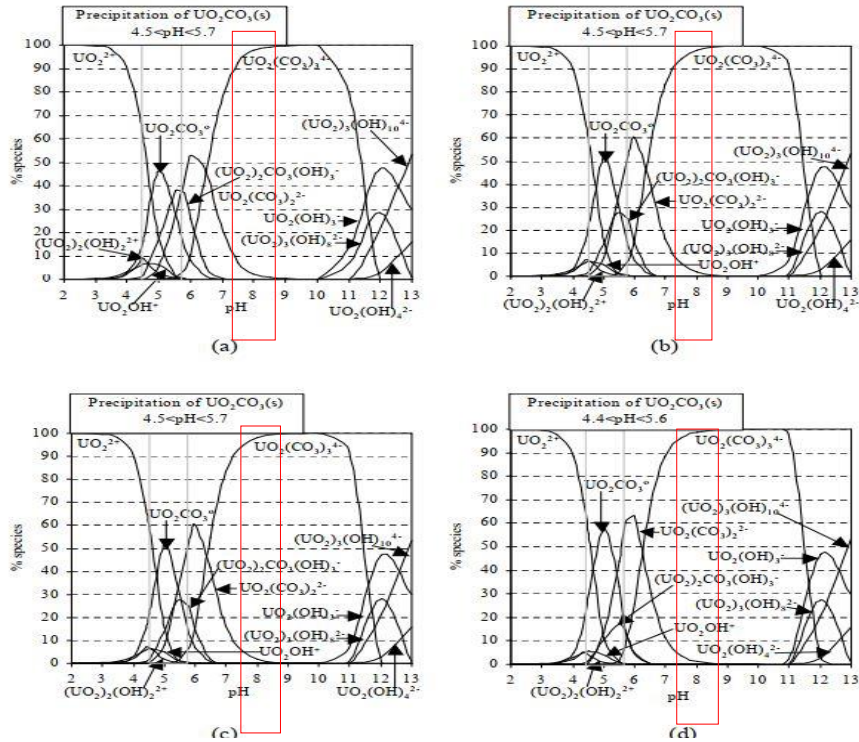


Figure 26: Actinide and Lanthanide concentrations ($\mu\text{g/L}$) as a function of time in a 0.1 M NaCl solution in basic conditions ($\text{pH} = 8 \pm 0.5$) with constant 5.0 g/L of Dolomite, 5 mg/L EDTA and 1000 $\mu\text{g/L}$ (over-saturated) of contaminants. Error bars are a standard deviation of triplicate samples. (a) Aqueous Phase Uranium (b) Aqueous Phase Thorium (c) Aqueous Phase Neodymium. U concentrations are unaffected showing its preference to stay in solution, but Th and Nd concentration without EDTA are reduced almost immediately except the unfiltered (settling) samples. This can be due to the larger colloids present in these samples which absorb small concentrations keeping them in solution.

Aqueous phase U concentration remains relatively consistent and unaffected by either separation step (Figure 26). The carbonate ion's complexation with U(VI) is shown to be

the limiting adsorption onto the dolomite matrix in this high contaminant saturation, which is similar to the 10 µg/L data shown previously. It is acknowledged that uranyl sorption is considered a long-term process; thus, 1 week and 28-day sampling might not simply be enough time to reach equilibrium. A study measuring Uranium adsorption exhibited a plateau in adsorption until 3.5 months (Tran et al. 2018⁵³). Studies done by Krestou 2000⁴⁵⁴ on open and closed ternary systems of $\text{UO}_2^{2+}/\text{CO}_3^{2-}/\text{H}_2\text{O}$, show that uranyl ions (UO_2^{2+}) in the presence of carbonate ions in both open and closed system at a pH of 8 ± 0.5 will be carbonato-U(VI) complexes (Figure 27).





Source from: Krestou 20004

Figure 27: Ternary Systems of $\text{UO}_2^{2+}/\text{CO}_3^{2-}/\text{H}_2\text{O}$ with open system (left) and closed system (right). This depicts the carbonate ions that exist in systems of pH 7.5-8.5 which are the conditions in which the experiments on this thesis operated under.

Both concentrations of aqueous phase Th and Nd were reduced, though Th more than Nd. Th and Nd both immediately decrease to 68 and 1 $\mu\text{g/L}$ and 202 and 120 $\mu\text{g/L}$ with the centrifuge and filtered samples free of EDTA, respectively. When comparing aqueous phase Th and Nd concentrations in centrifuge and filtered samples free of EDTA with the settling samples free of EDTA there is an enormous difference in concentration (903 and 926 $\mu\text{g/L}$). This difference is attributed to the fast adsorption taking place especially on colloidal particles with smaller particle sizes of $<5\text{nm}$. Similar, all samples amended with EDTA maintain both Th and Nd in solution until around the 24-hours and 48-hours mark where adsorption becomes more noticeable. (Figure 26 (b) and (c)).

The effect of 1.0 M Sodium Chloride brine on Contaminants Adsorption at concentration of 10 µg/L

Here 1.0 M NaCl synthetic brine solutions show data that is similar to previous data shown but with subtle differences. Due to increase in IS changes in subtle differences in concentration are noticed.

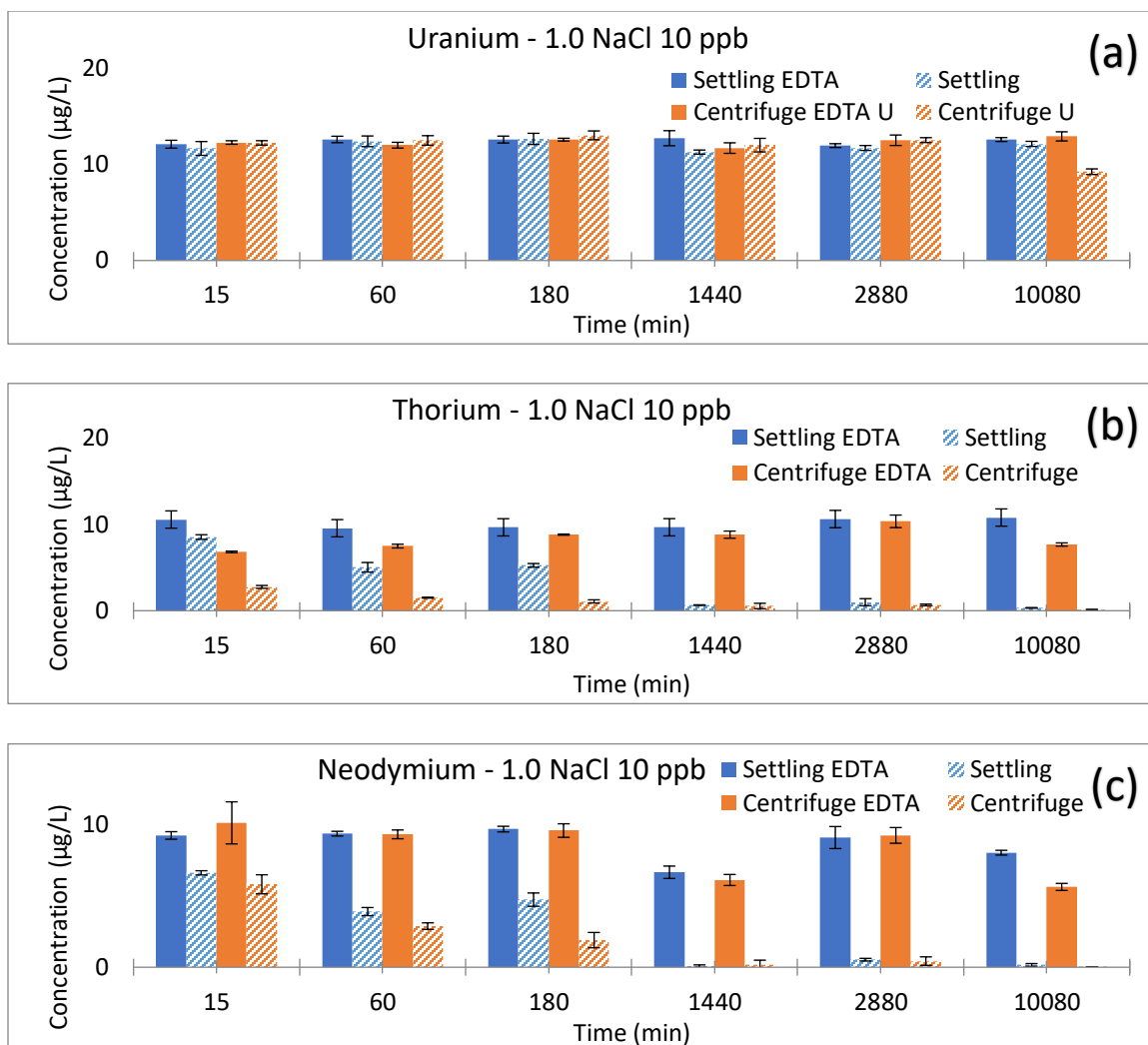


Figure 28: Actinide and Lanthanide concentrations ($\mu\text{g/L}$) as a function of time in a 1.0 M NaCl solution in basic conditions ($\text{pH} = 8 \pm 0.5$) with constant 5.0 g/L of Dolomite, 5 mg/L EDTA and 10 $\mu\text{g/L}$ (undersaturated) of contaminants. Error bars are a standard deviation of triplicate samples. (a) Aqueous Phase Uranium (b) Aqueous Phase Thorium (c) Aqueous Phase Neodymium. U preference to stay in solution shows consistent concentration throughout the weeklong experiment, but Th and Nd concentration are more easily absorbed in samples without EDTA which is observed from the steady decreasing trend in concentration.

As ionic strength increases, like with this 1.0 M NaCl synthetic brine solution, there is yet any decreases in aqueous phase U. When looking at the 1.0 M NaCl dissolution data (Figure 15) it can be understood this system will have high concentrations of aqueous phase Ca^{2+} and CO_3^{2-} in solution, therefore uranyl ions are complexed by carbonate ions and EDTA, thus keeping them soluble.

In contrast, aqueous phase Th and Nd both have significant decreases in concentration in both the settling and centrifugation samples free of EDTA. One notable difference between this 1.0 NaCl data and the previous 0.1 M NaCl is the concentrations in aqueous phase Th and Nd are averagely higher for EDTA amended samples. This could be that at a higher ionic strength the background ions are limiting contaminant adsorption, thus creating a more gradual decrease in aqueous phase Th and Nd. Recent research has shown that an increase in ionic strength creates stabilization in the water-mineral dynamics which does not favor adsorption and colloid-mineral interaction (Ruiz-Agudo et al. 2011).

The effect of 1.0 M Sodium Chloride brine on Contaminants Adsorption at concentration of 1000 $\mu\text{g/L}$

In this 1.0 M NaCl synthetic brine solution U, Th, and Nd aqueous phase concentrations are affected very similar to the previous 10 $\mu\text{g/L}$ data with concentrations scaled up to 1000 $\mu\text{g/L}$.

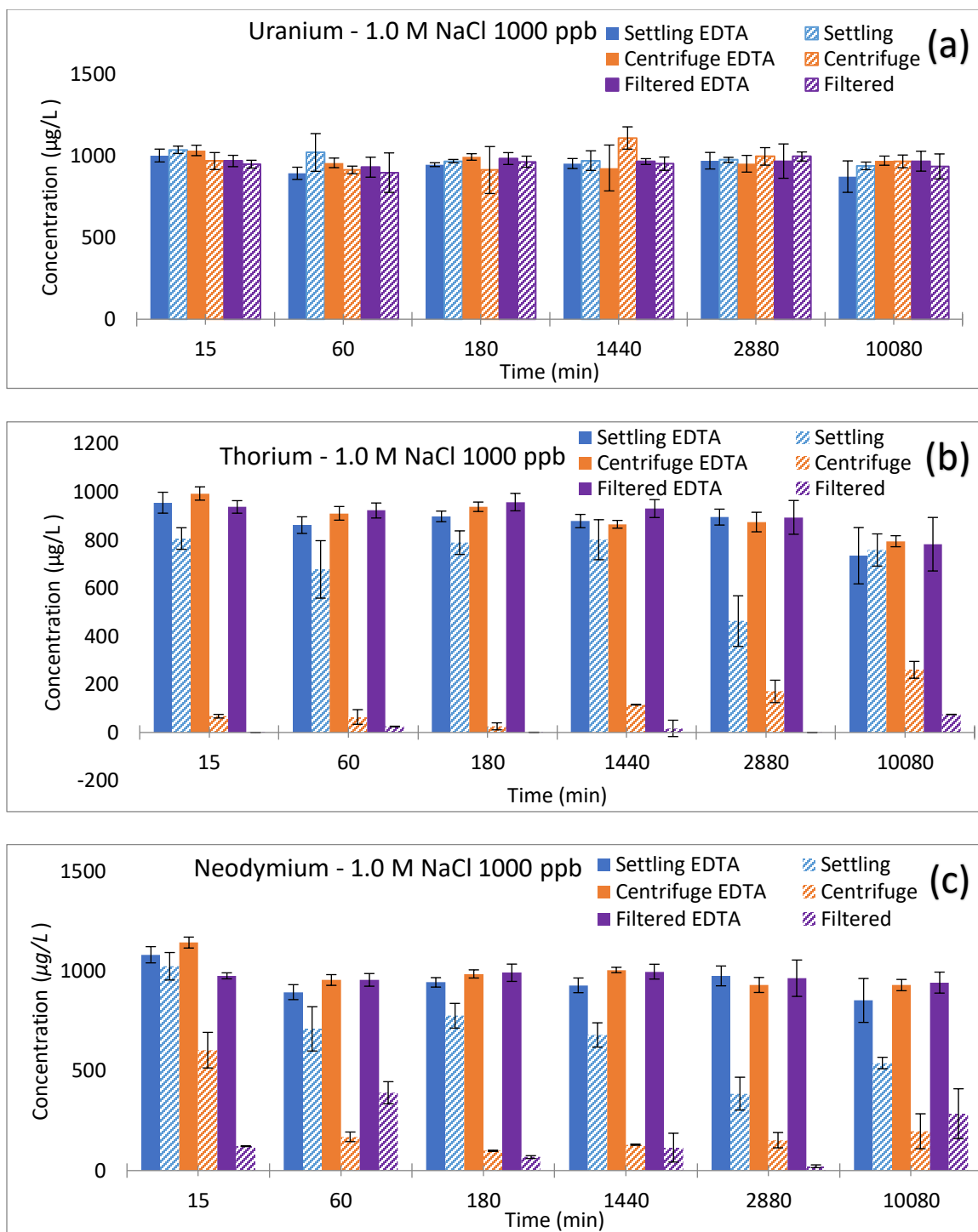


Figure 29: Actinide and Lanthanide concentrations ($\mu\text{g/L}$) as a function of time in a 1.0 M NaCl solution in basic conditions ($\text{pH} = 8 \pm 0.5$) with constant 5.0 g/L of Dolomite, 5 mg/L EDTA and 1000 $\mu\text{g/L}$ (undersaturated) of contaminants. Error bars are a standard deviation of triplicate samples. (a) Aqueous Phase Uranium (b) Aqueous Phase Thorium (c) Aqueous Phase Neodymium. U concentrations don't show any sign of reducing in solution. Th and Nd concentrations both show minimal decrease showing EDTA complexing ability keeping the contaminants in solution longer. Samples without EDTA are not bound therefore, are readily absorbed by the dolomite.

It is observed that aqueous phase U is kept in solution due to carbonate ions and EDTA increasing its solubility in 1.0 M NaCl 1000 $\mu\text{g/L}$ solution.

It does seem that the adsorption of Th and Nd becomes even more gradual in this system when compared to the previous systems, but this is attributed to the higher contaminant concentration making differences seem more subtle. What is starting to become more apparent with 1000 $\mu\text{g/L}$ systems and increasing is the difference between settling samples free of EDTA and the centrifugation and filtered samples free of EDTA. This could mean two things (1) an over-saturated system with both background ions and contaminants (1000 $\mu\text{g/L}$) creates a more organized solution, therefore limiting the ability for larger colloid aggregates to fall out and (2) the higher ionic strength stabilizes the system, thus slowing down adsorption.

The effect of 5.0 M Sodium Chloride Brine Contaminants Adsorption at concentration of 10 $\mu\text{g/L}$

At high ionic strength like this 5.0 M NaCl synthetic brine solution it is shown that aqueous phase U, Th, and Nd in the presence of EDTA are all consistently staying in solution.

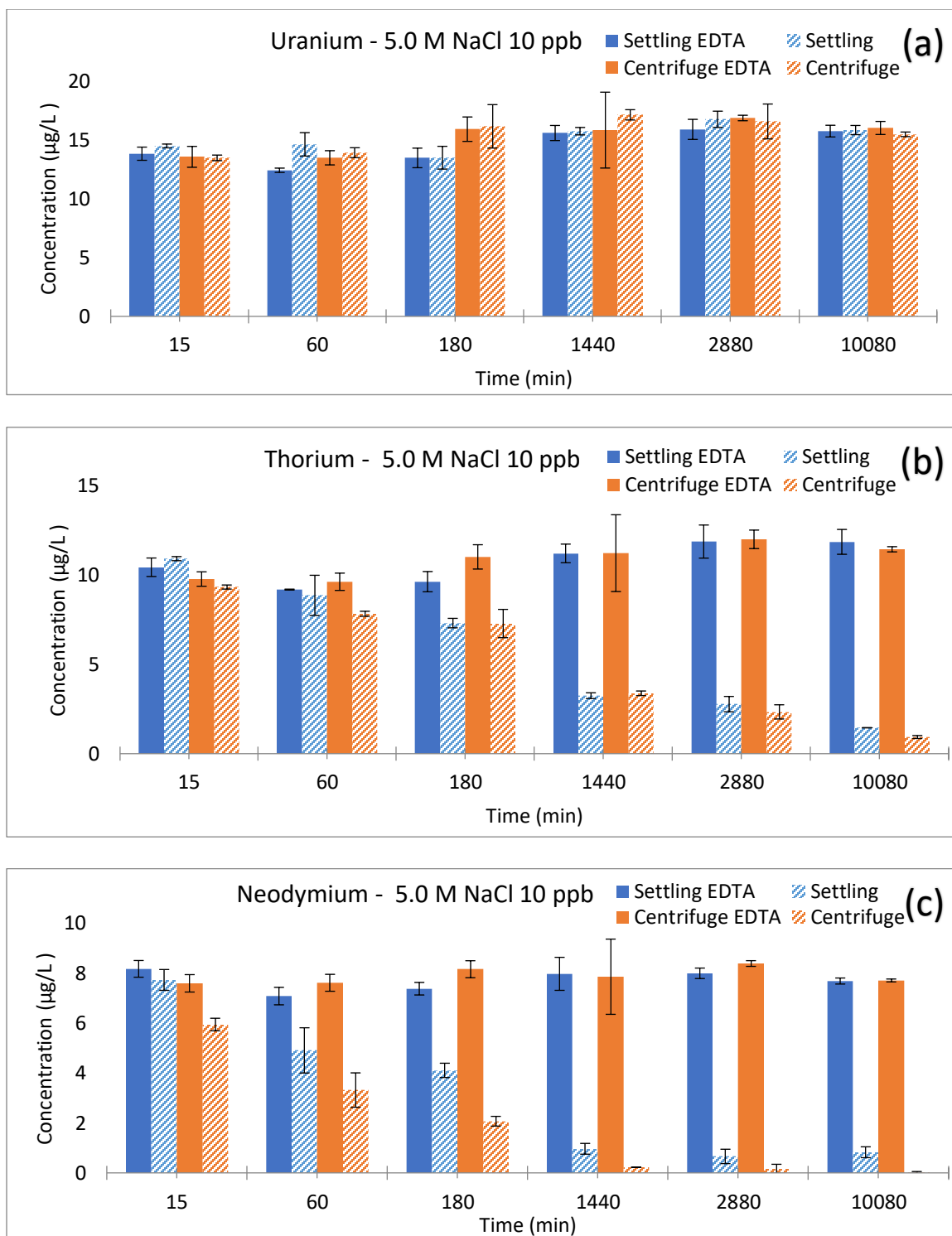


Figure 30: Actinide and Lanthanide concentrations ($\mu\text{g/L}$) as a function of time in a 5.0 M NaCl solution in basic conditions ($\text{pH} = 8 \pm 0.5$) with constant 5.0 g/L of Dolomite, 5 mg/L EDTA and 10 $\mu\text{g/L}$ (undersaturated) of contaminants. Error bars are a standard deviation of triplicate samples. (a) Aqueous Phase Uranium (b) Aqueous Phase Thorium (c) Aqueous Phase Neodymium. Th and Nd concentration are absorbed readily in samples without EDTA. This shows how the affinity EDTA for these contaminants keeps them in solution. U affinity for carbonate ions and EDTA keeps it solution throughout the experiment.

Uranium initially had a slightly higher concentration in this experiment at 13 $\mu\text{g/L}$. We see a decrease in aqueous phase U concentration within the first 15 minutes, but soon after it reaches back to its original concentration and stays consistent throughout the end of the experiment (Figure 30(a)).

With the increase in concentration and ionic strength ($I= 10 \text{ M}$) in this 5.0 M NaCl solution the water-mineral structure dynamics, will move towards a more stable system, therefore minimum decreases in both aqueous phase Th and Nd concentrations within EDTA amended samples are observed. This is quite the opposite of what was seen in the lower IS system of 0.1 M and 1.0 M NaCl. Samples free of EDTA also exhibited even more gradual decreases in aqueous phase Th and Nd concentrations when compared to lower IS of 0.1 M and 1.0 M NaCl data. With the increase in ionic strength, the immediate decreases in Th and Nd concentrations in EDTA free samples concentrations witnessed earlier in the 0.1 and 1.0 M NaCl solutions are not present (Figure 25 and Figure 26 (b) & (c)). This means adsorption is being inhibited in the presence of EDTA and high ionic strength solutions, resulting in the contaminant adsorption becoming a long-term process. Nevertheless, adsorption is observed with EDTA free samples as time increases (Figure 30(b) and (c)).

The effect of 5.0 M Sodium Chloride brine on Contaminants Adsorption at concentration of 1000 $\mu\text{g/L}$

This 5.0 M NaCl synthetic brine solution with 1000 $\mu\text{g/L}$ of U, Th, and Nd is a unique system because of the over-saturation from both NaCl brine and contaminant

concentration. It is seen that aqueous phase U concentrations decrease with time for all samples.

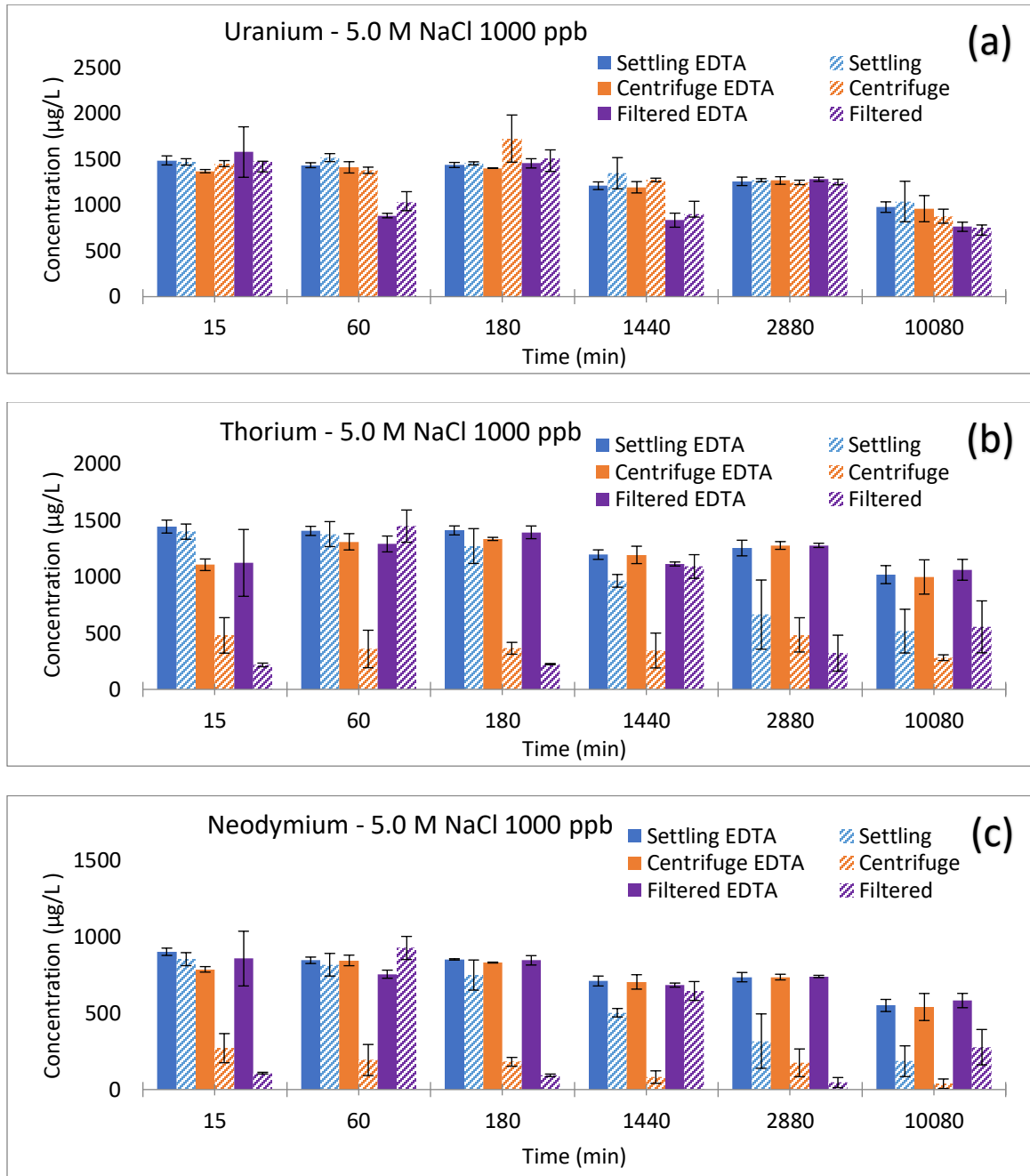


Figure 31: Actinide and Lanthanide concentrations ($\mu\text{g/L}$) as a function of time in a 5.0 M NaCl solution in basic conditions ($\text{pH} = 8 \pm 0.5$) with constant 5.0 g/L of Dolomite, 5 mg/L EDTA and 1000 $\mu\text{g/L}$ (undersaturated) of contaminants. Error bars are a standard deviation of triplicate samples. (a) Aqueous Phase Uranium (b) Aqueous Phase Thorium (c) Aqueous Phase Neodymium. It is observed with both Th and Nd concentrations that both are absorbed in samples without EDTA, except the settling samples. These samples contain larger particle sized colloid which tend to attract metals, therefore keeping them in solution.

For the first time a significant decrease in aqueous phase U concentration is observed in the Figure 31 (a). With the increase ionic strength (I=10M), contaminant over-saturation (1000 $\mu\text{g/L}$) and an increase in aqueous phase Ca^{2+} , Mg^{2+} and CO_3^{2-} concentrations from dolomite dissolution (Dolomite Dissolution data) seems to be what U needed to tilt equilibration favoring adsorption.

It is seen that in high ionic strength solutions, larger colloidal particles ($<6 \times 10^4 \text{nm}$) in the settling samples free of EDTA have their colloid-contaminant interaction limited. This decrease is still observed with centrifuge and filtered samples absent of EDTA showing that smaller colloid particles ($<80 \text{nm}$, $<5 \text{nm}$) are still seem effective in absorbing aqueous phase Th and Nd and do not seem to be affected by the higher ionic strength solution. It may seem these smaller particles are not as affected by the stabilization in the water-mineral dynamics provided by this 5.0 M NaCl synthetic brine solution.

EDTA is still shown to complex contaminants quickly as even in this 5.0 NaCl synthetic brine solution we see a gradual (30-40%) decrease of all three contaminants.

The effect of GWB brine on Contaminants Adsorption at concentration of 10 $\mu\text{g/L}$

This GWB synthetic brine presents a unique situation because of the myriad of salts present in it. The recipe is presented in Table 2

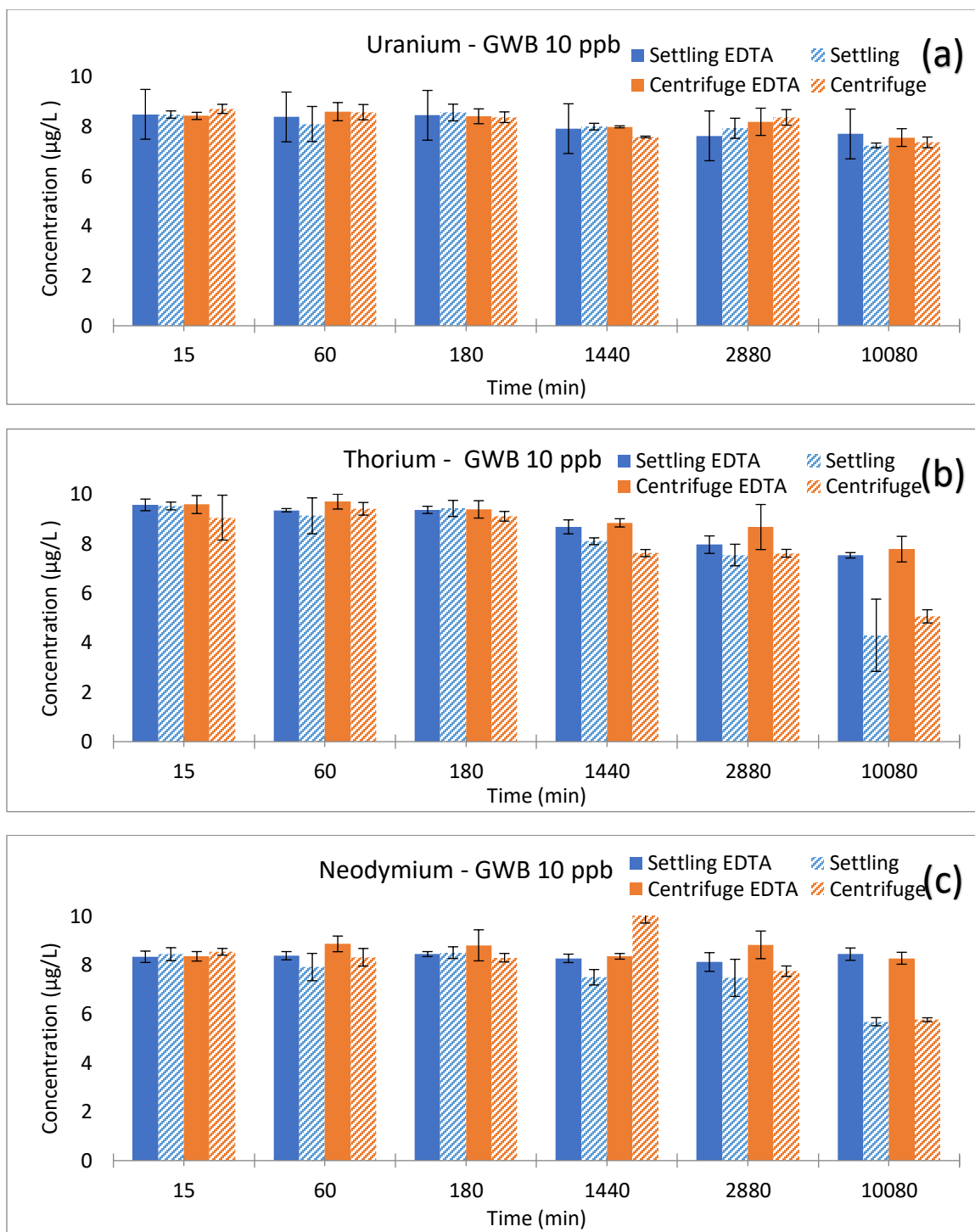


Figure 32 : Actinide and Lanthanide concentrations ($\mu\text{g/L}$) as a function of time in a GWB (Generic Weep Brine) in basic conditions ($\text{pH} = 8 \pm 0.5$) with constant 5.0 g/L of Dolomite, 5 mg/L EDTA and 10 $\mu\text{g/L}$ (undersaturated) of contaminants. Error bars are a standard deviation of triplicate samples. (a) Aqueous Phase Uranium (b) Aqueous Phase Thorium (c) Aqueous Phase Neodymium. In this GWB brine we see all three contaminants concentration staying in solution. This can be contributed to the high levels of Borax which has similar complexing effects to EDTA.

In this 10 ppb GWB synthetic brine solution aqueous phase U behaves similarly to most the data presented previously with aqueous phase U staying in solution.

Something different in this data is that aqueous phase Th and Nd does not decrease. Interestingly, tetraborate concentration is found to be more than double in GWB (0.037 M) when compared to the ERDA-6 (0.015 M). The complexation from borate ions is highly likely in neutral to alkaline conditions (8 ± 0.5 pH). As dolomite dissolute releasing carbonate ions pH becomes more alkaline where boric acid is shown to dominate, thus complexing U and increasing its solubility. According to Lucchini et al. 2012⁵⁵ U solubility in GWB brine was increased most likely due to ligand activity of tetraborate, when compared to ERDA-6 which was not affected as much. It also showed that carbonate containing experiments in a pH region of 8-10 had two orders of magnitudes greater in U concentration when compared to non-carbonate experiments.

Aqueous phase Th and Nd concentrations in EDTA-free samples decreased by 30-50%, but EDTA amended samples exhibited a gradual decrease only in Th. With the GWB brine having a high ionic strength of 6.84 M and other ligands present in solution adsorption is greatly limited, which is like the 5.0 M NaCl system.

The effect of GWB Brine on Contaminants Adsorption at concentration of 1000 µg/L

The effect on 1000 µg/L contaminant in this GWB solution is similar to the previous 10 µg/L data. All three contaminants U and Nd shows no removal in concentration, while Th show a decrease at 7 days.

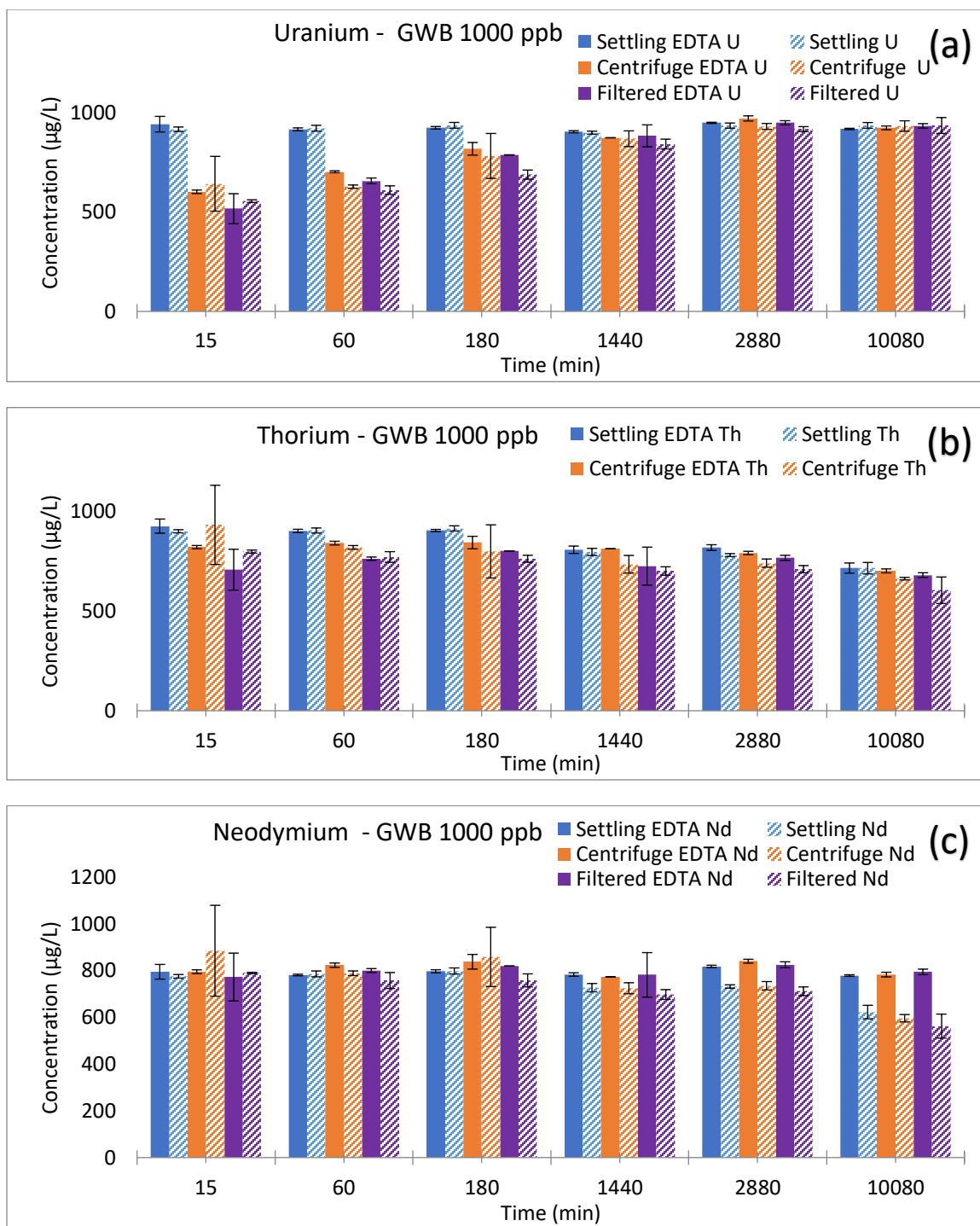


Figure 33: Actinide and Lanthanide concentrations ($\mu\text{g/L}$) as a function of time in a GWB (Generic Weep Brine) solution in basic conditions ($\text{pH} = 8 \pm 0.5$) with constant 5.0 g/L of Dolomite, 5 mg/L EDTA and $1000 \mu\text{g/L}$ (under-saturated) of contaminants. Error bars are a standard deviation of triplicate samples. (a) Aqueous Phase Uranium (b) Aqueous Phase Thorium (c) Aqueous Phase Neodymium. Due to the high levels of Borax, its ability to complex with the contaminants keeping them in solution. Th and Nd only begin to decrease at the 1-week sampling period, entailing that these reactions might need more time to break the bonds.

In this over-saturation (1000 $\mu\text{g/L}$) GWB solution contaminant adsorption is minimal in aqueous phase Th. Decreases are seen in aqueous phase Th concentration at 7-days, but there is no decrease in aqueous phase U concentrations.

Aqueous phase Nd samples amended with EDTA do not decrease. A decrease in aqueous phase Nd with samples free of EDTA is only seen at 7-days. It is also considered that the combined complexation from the many background ions like borate ions, sulfate ions, and carbonate ions, in the GWB synthetic brine solution, is limiting adsorption capacity in all three contaminants. The GWB synthetic brine solution with both 10 $\mu\text{g/L}$ and 1000 $\mu\text{g/L}$ of contaminants points to adsorption being a long-term process in these systems because adsorption is only beginning to be seen at 7 days.

The effect of ERDA-6 brines on Contaminants Adsorption at concentration of 10 $\mu\text{g/L}$

The ERDA-6 brine is a different compared to the GWB because it has double NaCl concentration, half as much $\text{Na}_2\text{B}_4\text{O}_7$ concentrations, fifty times less MgCl_2 and a lower IS of 4.97 M (Table 2).

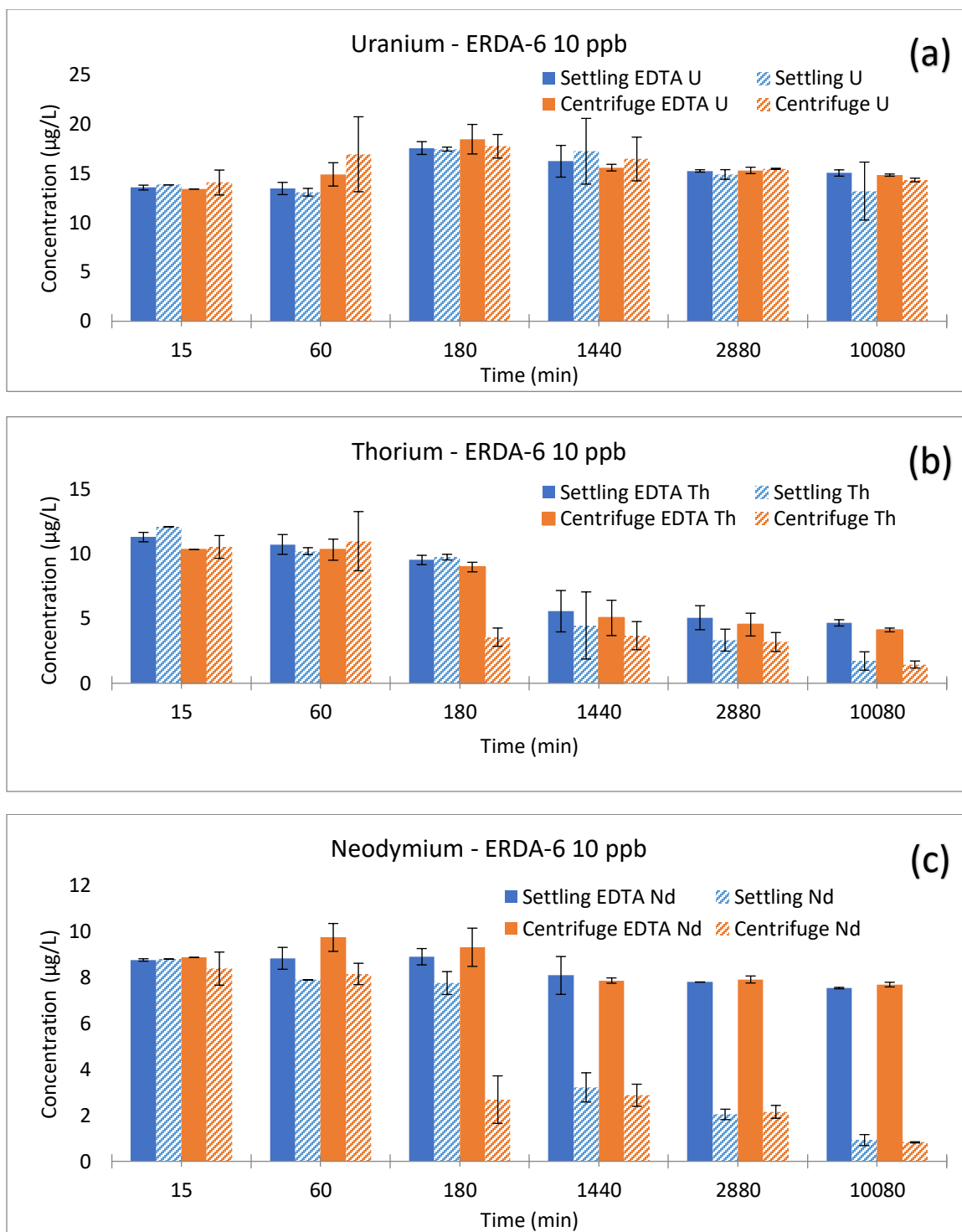


Figure 34: Actinide and Lanthanide concentrations ($\mu\text{g/L}$) as a function of time in a ERDA -6 (Energy Research and Development Administration Well 6) in basic conditions ($\text{pH} = 8 \pm 0.5$) with constant 5.0 g/L of Dolomite, 5 mg/L EDTA and $10 \mu\text{g/L}$ (under-saturated) of contaminants. Error bars are a standard deviation of triplicate samples. (a) Aqueous Phase Uranium (b) Aqueous Phase Thorium (c) Aqueous Phase Neodymium. In this ERDA brine we see both Th and Nd decrease in concentrations over time, with a bigger impact on Th concentrations. Only Nd samples without EDTA show it to readily absorb, whereas U concentrations remain constant throughout the experiment.

The ERDA-6 synthetic brine solutions have higher amount of NaCl, less borax and a weaker ionic strength ($I = 4.97$) when compared to GWB ($I=6.84$). Like the 0.1 M and 1.0 M NaCl synthetic brine solutions, ERDA-6 synthetic brine solution is seen to share similar decreasing trends in aqueous phase Th and Nd concentrations. Th adsorbs readily after 24-hours and continues to decrease in concentration having over a 50% decrease by the 7-days. Aqueous phase Nd concentrations in EDTA amended samples gradually decrease with time, while on the other hand the EDTA free samples see a plunge in concentration after 24 hours. Aqueous phase U concentrations follow a consistent concentration throughout the experiment mirroring the effect in 0.1M and 1.0 M NaCl solutions.

The effect of ERDA-6 brines on Contaminants Adsorption at Concentration of 10 µg/L

In Figure 35 the (a) ERDA-6 synthetic brine solution shows no sign in U adsorption. There is an immediate decrease in aqueous phase U concentration with both centrifugation and filtered samples showing colloid adsorption, but as the system approaches equilibration uranyl ions become complexed by EDTA and other ligands like carbonate ion, borate ions, and sulfate ions increasing its solubility indefinitely.

Aqueous phase Th concentrations are observed to drastically reduce to $<100 \mu\text{g/L}$ for centrifugation and filtered samples with and without EDTA. Here EDTA is keeping Th soluble in the settling sample, but not in the centrifugation and filtered samples. This exhibits colloids adsorption capacity of Th, specifically in the smaller sizes particles ($<80\text{nm}$, $<5\text{nm}$). As time increases both settling samples gradually reduce in concentration due to adsorption. Aqueous phase Nd concentrations, on the other hand, remain in solution with all EDTA amended samples demonstrating that Nd has a high affinity for EDTA

complexation. With both aqueous phase Th and Nd centrifugation and filtered samples we see the same immediate drop, as well as the settling samples gradually reducing in concentrations. It shows reflects that the size of the colloids has an impact on adsorption (Figure 35 (b) and(c)).

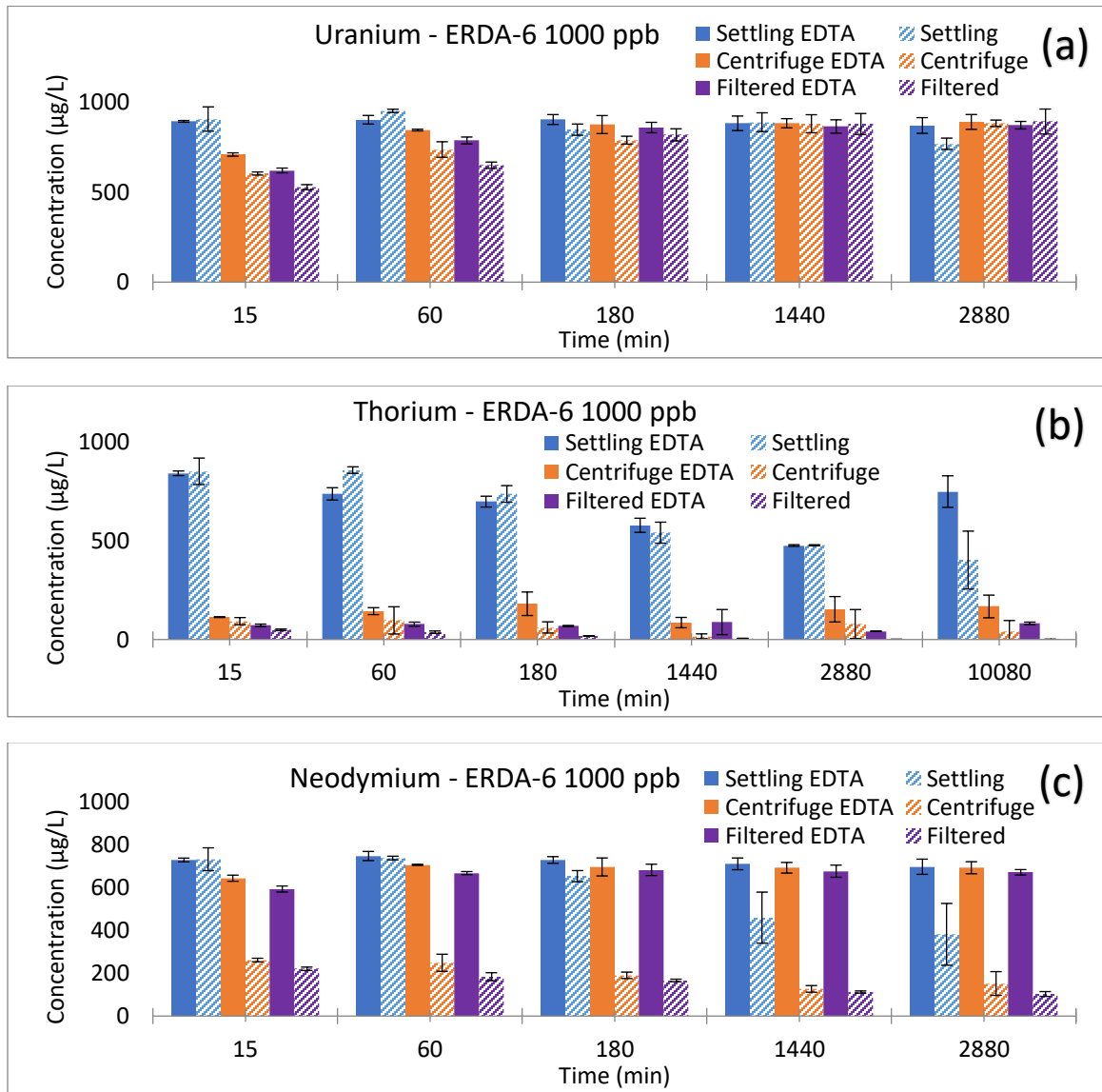


Figure 35: Actinide and Lanthanide concentrations ($\mu\text{g/L}$) as a function of time in a ERDA -6 (Energy Research and Development Administration Well 6) in basic conditions ($\text{pH} = 8 \pm 0.5$) with constant 5.0 g/L of Dolomite, 5 mg/L EDTA and $1000 \mu\text{g/L}$ (under-saturated) of contaminants. Error bars are a standard deviation of triplicate samples. (a) Aqueous Phase Uranium in solution. (b) Aqueous Phase Thorium in solution. (c) Aqueous Phase Neodymium in solution. Th shows significant affinity in absorbing as well as how much it is affected by larger colloids (settling samples) keeping it in solution. Nd concentrations.

without EDTA show immediate decrease in concentrations, but none in the samples with EDTA which implies EDTA ability to keep contaminants in solution and not letting them absorb onto dolomite.

Conclusion

The long-term management of TRU waste is at the core of the WIPP Performance assessment. Even though the WIPP has been established as the one of the most “ideal” locations for storage and disposal of radioactive waste there are still many uncertainties when it comes to understating the behavior of U, Th, and Nd in these subsurface environments. The complications posed by the Culebra member are critical priorities to address, therefore this research has extended the existing body of knowledge on what little is known around the dolomite mineral, the effect EDTA, and contaminant fate in these systems. The Culebra represents a network for groundwater flow, thus presenting a significant amount of uncertainty for risk model assessment of the WIPP site. The various ionic strength solutions in these experiments provides critical information in understating the dolomite dissolution and contaminant adsorption and best simulates subsurface environmental conditions at the WIPP.

Increases of aqueous phase Ca and Mg concentrations are seen across all the synthetic brines, with some like NaCl, Na₂NO₃, and Na₂SO₄ more consistent than others having around 5000-12000 µg/L and 3000-8000 µg/L, respectively. These significant findings show how the powerful chelating ligand, EDTA, has a major impact on dolomite dissolution by increasing aqueous phase Ca and Mg between 20-50% in most cases. According to 0.1 M synthetic brine solutions aqueous phase Ca increased in the order of: MgCl₂(I=0.3M) <NaNO₃(I=0.1M) <NaCl(I=0.1M) <CsCl(I=0.1M) <Na₂SO₄(I=0.15M) <Na₂B₄O₇ (I=0.15M) in the presence of EDTA. As ionic strength increases, dolomite dissolution increases because an increase in aqueous phase Ca and Mg concentrations is

observed with time. Increasing ionic strength is also shown to inhibit contaminant adsorption due to the conflict between ligand complexation, high ionic activity, and solution stabilization limits (contaminant-mineral-colloid interaction). U is only seen to be minimally absorbed in the 5.0 M NaCl synthetic brine solution with 1000 $\mu\text{g/L}$ after 7 days. U metal has an affinity for carbonate ion complexes as well as EDTA keeping it solution, thus U is seen to remain in its original concentration throughout the life of almost all the experiments except the one mentioned previously. This may well mean that U requires a much longer residence time and different environmental conditions (pH, ionization, media, etc.) for it to readily absorb. Due to EDTA's strong affinity for complexing U, Th, and Nd, it is observed to inhibit the adsorption of the contaminants onto dolomite mineral. This is especially true when a 60-80% decrease in concentration is observed in Th and Nd aqueous phase concentrations when comparing EDTA amended samples to samples absent of EDTA, mainly in lower ionic strength solutions of 0.1 and 1.0 M. This exhibits how EDTA complexation works best in lower ionic strength solutions in both the dolomite dissolution and adsorption experiments partly due to the absence of the hindering affects of high ionic activity found in high ionic strength solutions. It also renders a clear picture of how involved colloids are in these systems, as settling (unfiltered samples) without EDTA have a higher Th and Nd aqueous phase concentration when compared to the EDTA free centrifugation and filtered samples in the higher ionic strength solutions. This shows larger colloids have a role in keeping U, Th, and Nd mobile in solution. As ionic strength increases less adsorption by colloids of larger sizes is observed, thus inhibiting colloid-contaminant interaction. On the other hand, when considering lower ionic strength, all samples without EDTA show Th and Nd immensely decreased with some instances of up

to decrease of >98% in concentration, displaying how quickly they absorb in 0.1 NaCl synthetic brine solutions. This reveals how readily Th and Nd absorb onto dolomite and colloid particles in systems devoid of EDTA and proves how critical the understanding of the behavior of EDTA and its interactions with contaminants in these environmental conditions are for the WIPP.

References

- ¹ Hess, Harry H., Adkins, John N., Benson, William E., Frye John C., Heroy, William B., Hubbert, Kinh M., Russel, Richard J., Theis, Charles V., The Disposal of Radioactive Waste on Land. 2015. Report of the Committee on Waste Disposal of the Division of Earth Sciences, Washington, D.C.: National Academy of Sciences-National Research Council.
- ² Tracy, Cameron L., Feasibility and Risks of Human Intrusion in WIPP. 2019, Belfer Center for Science and International Affairs, Kennedy School of Government, Harvard University, USA
- ³ Stumm, Werner. Chapter 8 Carbonates and their Reactivities. Chemistry of Solid-Water Interface, 1992. Pages 289-307.
- ⁴ Leigh, Christi D. The Current State of the Safety Case for WIPP. No. SAND2016-9965C. Sandia National Lab.(SNL-NM), Albuquerque, NM (United States), 2016.
- ⁵ Cappellen, Philippe Van., Charlet, Laurent. Stumm, Werner, Wersin, Paul. A Surface Complexation Model of the Carbonate Mineral-Aqueous Solution Interface, 1992. School of Earth and Atmospheric Sciences, Georgia Institute of Technology, Atlanta, GA. Institute of Inorganic Chemistry, University of Bern, CH-3000 Bern 9, Switzerland. Institute for Aquatic Sciences (EAWAG), Swiss Federal Institute of Technology, CH-8600 Dübendorf, Switzerland. Department of Geology, Stanford University, Stanford, CA 94305, USA.
- ⁶ Povorsky, Oleg S., Schott, Jacques. Thomas, Fabien. Dolomite Surface Speciation and Reactivity in Aquatic Systems, 1999. Laboratoire de Géochimie, Toulouse, France. Laboratoire Environnement et Métallurgie, Vandoeuvre les Nancy Cedex, France.
- ⁷ Povorsky, Oleg S., Schott, Jacques. Thomas, Fabien. Dolomite Surface Speciation and Reactivity in Aquatic Systems, 1999. Laboratoire de Géochimie, Toulouse, France. Laboratoire Environnement et Métallurgie, Vandoeuvre les Nancy Cedex, France.
- ⁸ Lei, Chou. Garrels, Robert M., Wollast, Roland. Comparative Study of the kinetics and mechanisms of Dissolution of Carbonate Minerals, 1989. Department of Marine Science, University of South Florida, St. Petersburg. Laboratoire d'Océanographie, Université Libre de Bruxelles, Brussels Belgium
- ⁹ Plummer, L. N., T. M. L. Wigley, and D. L. Parkhurst. "The kinetics of calcite dissolution in CO₂-water systems at 5 degrees to 60 degrees C and 0.0 to 1.0 atm CO₂." American journal of science 278.2 (1978): 179-216.

-
- ¹⁰ Chou, L. E. I., Robert M. Garrels, and Roland Wollast. "Comparative study of the kinetics and mechanisms of dissolution of carbonate minerals." *Chemical geology* 78.3-4 (1989): 269-282.
- ¹¹ Stumm, Werner, and Roland Wollast. "Coordination chemistry of weathering: Kinetics of the surface-controlled dissolution of oxide minerals." *Reviews of Geophysics* 28.1 (1990): 53-69.
- ¹² Provosky, Oleg S., Kinetics and Mechanism of Dolomite Dissolution in Neutral to Alkaline Solutions Revisited, 2001. N. Laverov FCIAR RAS, and Tomsk State University
- ¹³ Plummer, L. Niel, and Eurybiades Busenberg. "The solubilities of calcite, aragonite and vaterite in CO₂-H₂O solutions between 0 and 90 C, and an evaluation of the aqueous model for the system CaCO₃-CO₂-H₂O." *Geochimica et cosmochimica acta* 46.6 (1982): 1011-1040.
- ¹⁴ Chou, L. E. I., Robert M. Garrels, and Roland Wollast. "Comparative study of the kinetics and mechanisms of dissolution of carbonate minerals." *Chemical geology* 78.3-4 (1989): 269-282.
- ¹⁵ Brady, V. Patrick, Papenguth, Hans W., Kelly, John W., Metal Sorption to Dolomite Surfaces, 1997. Geochemistry Research. Sandia National Laboratories, Albuquerque, New Mexico.
- ¹⁶ Chen, Jian-Feng, Gregory R. Choppin, and Robert C. Moore. "Complexation and ion interactions in Am (III)/EDTA/NaCl ternary system." *Actinide Speciation in High Ionic Strength Media*. Springer, Boston, MA, 1999. 187-197.
- ¹⁷ Elesin, A. A., and A. A. Zaitsev. "ION-EXCHANGE BEHAVIOR OF TRIVALENT AMERICIUM, CURIUM, AND PROMETHIUM IONS IN THE PRESENCE OF EDTA." *Sov. Radiochem.(Engl. Transl.)* 13: No. 5, 798-801 (Sep-Oct 1971). (1971).
- ¹⁸ Yalcintas, E., Reed, D. T., Gaona, X., Altmaier, M., Impact of EDTA on the Solubility and Redox Behavior of Uranium in Dilute to Concentrated NaCl Solutions, 2003. Karlsruhe Institute of Technology, Karlsruhe, Germany. Institute for Nuclear Waste Disposal, Los Alamos National Laboratory, USA
- ¹⁹ Schramke, J. A., Santillan, E. F. U., Peake, R. T., Plutonium Oxidation States in the Waste Isolation Plant Repository, 2020. U.S. Environmental Protection Agency, Office of air and Radiation. Arlington, Virginia.
- ²⁰ Brush, Laurence H., and P. S. Domski. "Uncertainty Analysis of Actinide Solubilities for the WIPP CRA-2014 PA." Analysis report, February 22 (2013): 2013.

-
- ²¹ Reed, D. T., et al. Reduction of Np (VI) and Pu (VI) by organic chelating agents. No. SAND-97-2845C; CONF-971090-. Sandia National Labs., Albuquerque, NM (United States); Argonne National Lab., IL (United States), 1998.
- ²² Colàs, Elisenda, et al. "The effect of gluconate and EDTA on thorium solubility under simulated cement porewater conditions." *Journal of Solution Chemistry* 42.8 (2013): 1680-1690.
- ²³ Dittrich, Timothy M. Actinide Sorption Under WIPP-Relevant Conditions. No. LA-UR-17-22353. Los Alamos National Lab.(LANL), Los Alamos, NM (United States), 2017.
- ²⁴ Means, Jeffrey L., and Carl A. Alexander. "The environmental biogeochemistry of chelating agents and recommendations for the disposal of chelated radioactive wastes." *Nuclear and Chemical Waste Management* 2.3 (1981): 183-196.
- ²⁵ Di Palma, L., and R. Mecozi. "Heavy metals mobilization from harbour sediments using EDTA and citric acid as chelating agents." *Journal of hazardous materials* 147.3 (2007): 768-775.
- ²⁶ Griffiths, Tamara L., et al. "Understanding the Solution Behavior of Minor Actinides in the Presence of EDTA⁴⁻, Carbonate, and Hydroxide Ligands." *Inorganic chemistry* 52.7 (2013): 3728-3737.
- ²⁷ Tinnacher, R.M., M. Zavarin, B.A. Powell, and A.B. Kersting (2011), Kinetics of neptunium(V) sorption and desorption on goethite: An experimental and modeling study. *Geochimica et Cosmochimica Acta*, 75 (21), 6584–6599; published online, DOI: 10.1016/j.gca.2011.08.014.
- ²⁸ Utsunomiya, Satoshi, et al. "Application of Electron Microscopy to Understanding Colloid-Facilitated Transport of Radionuclides at the Mayak Production Association Facility, Near Lake Karachai, Russia." *Behavior of Radionuclides in the Environment I*. Springer, Singapore, 2020. 177-200.
- ²⁹ Moulin, V., and G. Ouzounian. "Role of colloids and humic substances in the transport of radio-elements through the geosphere." *Applied geochemistry* 7 (1992): 179-186.
- ³⁰ "Association Colloid." *The Great Soviet Encyclopedia*, 3rd Edition. 1970-1979. The Gale Group, Inc. 10 May. 2021
- ³¹ Stumm, Werner. "Chemical interaction in particle separation." *Environmental Science & Technology* 11.12 (1977): 1066-1070.
- ³² Degueldre, C., et al. "Colloids in water from a subsurface fracture in granitic rock, Grimsel Test Site, Switzerland." *Geochimica et Cosmochimica Acta* 53.3 (1989): 603-610.

-
- ³³ Degueldre, C., et al. "Colloid properties in granitic groundwater systems. II: Stability and
- ³³ Reed, D. T., et al. Reduction of Np (VI) and Pu (VI) by organic chelating agents. No. SAND-97-2845C; CONF-971090-. Sandia National Labs., Albuquerque, NM (United States); Argonne National Lab., IL (United States), 1998.
- ³³ Colàs, Elisenda, et al. "The effect of gluconate and EDTA on thorium solubility under simulated cement porewater conditions." *Journal of Solution Chemistry* 42.8 (2013): 1680-1690.
- ³³ Di Palma, L., and R. Mecozzi. "Heavy metals mobilization from harbour sediments using EDTA and citric acid as chelating agents." *Journal of hazardous materials* 147.3 (2007): 768-775.
- ³³ Utsunomiya, Satoshi, et al. "Application of Electron Microscopy to Understanding Colloid-Facilitated Transport of Radionuclides at the Mayak Production Association Facility, Near Lake Karachai, Russia." *Behavior of Radionuclides in the Environment I*. Springer, Singapore, 2020. 177-200.
- ³³ Moulin, V., and G. Ouzounian. "Role of colloids and humic substances in the transport of radio-elements through the geosphere." *Applied geochemistry* 7 (1992): 179-186.
- ³³ "Association Colloid." *The Great Soviet Encyclopedia*, 3rd Edition. 1970-1979. The Gale Group, Inc. 10 May. 2021
- transport study." *Applied Geochemistry* 11.5 (1996): 697-710.
- ³⁴ Ryan, Joseph N., and Menachem Elimelech. "Colloid mobilization and transport in groundwater." *Colloids and surfaces A: Physicochemical and engineering aspects* 107 (1996): 1-56.
- ³⁵ Emerson, Hilary P., Katherine A. Hickok, and Brian A. Powell. "Experimental evidence for ternary colloid-facilitated transport of Th (IV) with hematite (α -Fe₂O₃) colloids and Suwannee River fulvic acid." *Journal of environmental radioactivity* 165 (2016): 168-181.
- ³⁶ Bundschuh, T., et al. "Detection of biocolloids in aquatic media by Nano-Particle Analyzer." *Spectroscopy* 19.1 (2005): 69-78.
- ³⁷ Delécaut, Grégory, et al. "Solubility of an uranium (IV) amorphous phase under geochemical conditions representative for the direct disposal of spent nuclear fuel in Boom Clay." *Uranium in the Aquatic Environment*. Springer, Berlin, Heidelberg, 2002. 197-206.

-
- ³⁸ Delécaut, Grégory, et al. "Effect of reducing agents on the uranium concentration above uranium (IV) amorphous precipitate in Boom Clay pore water." *Radiochimica Acta* 92.9-11 (2004): 545-550.
- ³⁹ McCarthy, John, and John Zachara. "ES&T Features: Subsurface transport of contaminants." *Environmental science & technology* 23.5 (1989): 496-502.
- ⁴⁰ Ryan, Joseph N., and Menachem Elimelech. "Colloid mobilization and transport in groundwater." *Colloids and surfaces A: Physicochemical and engineering aspects* 107 (1996): 1-56.
- ⁴¹ Sen, Tushar Kanti, and Kartic C. Khilar. "Review on subsurface colloids and colloid-associated contaminant transport in saturated porous media." *Advances in colloid and interface science* 119.2-3 (2006): 71-96.
- ⁴² Emerson, H. P., Zengotita, F., Richmann, M., Katsenovich, Y., Reed, D. T., & Dittrich, T. M. (2018). Retention of neodymium by dolomite at variable ionic strength as probed by batch and column experiments. *Journal of Environmental Radioactivity*, 190-191, 89-96.
<https://dx.doi.org/10.1016/j.jenvrad.2018.05.007>
- ⁴³ Wall, N. A., Borkowski, M., Chen, J., & Choppin, G. R. (2002). Complexation of americium with humic, fulvic and citric acids at high ionic strength. *Radiochimica Acta*, 90(9-11), 563-568.
- ⁴⁴ Lucchini, Jean-Francois, Sally Ballard, and Hnin Khaing. "Influence of Carbonate on Uranium Solubility in the WIPP." *MRS Online Proceedings Library* 1444.1 (2012): 217-222.
- ⁴⁵ Povorsky, Oleg S., Schott, Jacques, Thomas, Fabien. *Dolomite Surface Speciation and Reactivity in Aquatic Systems*, 1999. Laboratoire de Géochimie, Toulouse, France. Laboratoire Environnement et Mineralurgie, Vandoeuvre les Nancy Cedex, France.
- ⁴⁶ Ruiz-Agudo, Encarnación, et al. "Ion-specific effects on the kinetics of mineral dissolution." *Chemical geology* 281.3-4 (2011): 364-371.
- ⁴⁷ Ruiz-Agudo, Encarnación, et al. "Ion-specific effects on the kinetics of mineral dissolution." *Chemical geology* 281.3-4 (2011): 364-371.
- ⁴⁸ Lucchini, Jean-Francois, Sally Ballard, and Hnin Khaing. "Influence of Carbonate on Uranium Solubility in the WIPP." *MRS Online Proceedings Library* 1444.1 (2012): 217-222.
- ⁴⁹ Tran, Emily L., et al. "Uranium and cesium sorption to bentonite colloids under carbonate-rich environments: implications for radionuclide transport." *Science of the Total Environment* 643 (2018): 260-269.
- ⁵⁰ Schnurr, A., et al. "Investigation of actinide and lanthanide sorption on clay minerals under saline conditions." *Migration Conference*, Brighton, United Kingdom. 2013.

⁵¹ Blake, C. A., et al. "Studies in the carbonate-uranium system." *Journal of the American Chemical Society* 78.23 (1956): 5978-5983.

⁵² Tran, Emily L., et al. "Uranium and cesium sorption to bentonite colloids under carbonate-rich environments: implications for radionuclide transport." *Science of the Total Environment* 643 (2018): 260-269.

⁵³ Tran, Emily L., et al. "Uranium and cesium sorption to bentonite colloids under carbonate-rich environments: implications for radionuclide transport." *Science of the Total Environment* 643 (2018): 260-269.

⁵⁴ Krestou, A., and D. Panias. "Uranium (VI) speciation diagrams in the $\text{UO}_2^{2+}/\text{CO}_3^{2-}/\text{H}_2\text{O}$ system at 25° C." *European Journal of Mineral Processing & Environmental Protection* 4.2 (2004).

⁵⁵ Lucchini, Jean-Francois, Sally Ballard, and Hnin Khaing. "Influence of Carbonate on Uranium Solubility in the WIPP." *MRS Online Proceedings Library* 1444.1 (2012): 217-222.